



TECHNICAL UNIVERSITY OF SOFIA
English Language Faculty of Engineering

FINAL YEAR PROJECT

BEng Degree

VIBRATION PIEZOELECTRIC ENERGY HARVESTING

STUDENT: Asier Zazpe Delgado

SUPERVISOR: Assoc. Prof. K. Nedelchev, PhD

Academic Year 2015-2016
Sofia, Bulgaria

CONTENTS

ACKNOWLEDGEMENTS.....	3
1. INTRODUCTION.....	4
2. LITERATURE REVIEW	5
2.1. ENERGY HARVESTING	5
2.2. KINETIC ENERGY HARVESTING.....	7
2.2.1. Basis.....	7
2.2.2. Transduction mechanisms	10
2.3. PIEZOELECTRICITY	16
2.3.1. Basis.....	16
2.3.2. Classification of piezoelectric materials.....	16
2.3.3. Piezoelectric mathematical parameters.....	18
2.3.4. Methods to change the response characteristics	22
2.3.5. Piezoelectric materials applications for energy harvesting	27
2.3.6. Piezoelectric energy harvesters patents	32
3. DEVICE FOR THE VIBRATION ENERGY HARVERSTING	45
3.1. CONSTRUCTION.....	45
3.2. INPUT DATA.....	45
4. EXPERIMENTAL STUDY.....	46
4.1. MEASURING SISTEM.....	46
4.1.1. Equipment used	46
4.1.2. Scheme of measurement system	47
4.1.3. Program measurement and visualization	48
4.2. METHODS OF MEASUREMENT.....	51
4.3. EXPERIMENTAL RESULTS.....	52

5. MODELLING THE STRUCTURE IN ANSYS	56
5.1. DIAGRAM OF MODELING AND SIMULATION	56
5.2. BASE MODEL.....	57
5.2.1. Construction	57
5.2.2. Drawing of the model	58
5.2.3. Model of the construction.....	58
5.2.4. Boundary conditions.....	60
5.2.5. Mesh	61
5.2.6. Material.....	62
5.2.7. Simulation.....	63
5.2.8. Solution analysis.....	63
5.3. MODEL WITH SPRING	65
5.3.1. Model of the construction.....	65
5.3.2. Boundary conditions.....	66
5.3.3. Mesh	67
5.3.4. Material.....	68
5.3.5. Simulation.....	71
5.3.6. Solution analysis.....	72
5.4. STUDY THE EFFECTS OF AMPLITUDE OF VIBRATIONS OR OF THE SPRING CONSTANT ON VOLTAGE GENERATED	73
5.4.1. Base model	73
5.4.2. Model with spring	74
6. ANALYSIS OF THE RESULTS.....	79
6.1. EXPERIMENTAL RESULTS.....	79
6.2. ANSYS RESULTS.....	79
6.2.1. Base model	79
6.2.2. Model with spring	80
7. CONCLUSIONS.....	81
8. REFERENCES.....	82

ACKNOWLEDGEMENTS

This research was supported by the English Language Faculty of Engineering at Technical University of Sofia in Bulgaria.

First of all, I would like to thank my main supervisor, Professor Krasimir Nedelchev, for his support during all the process. Thank you for sharing your knowledge. I would also like to thank Vice Rector, Professor Ivan Kralov, as he helped me to find the topic for my project.

Besides, I wish to thank my coordinator, Professor Vladislav Slavov, and the English Language Faculty of Engineering Dean, Tasho Tashev, for their help with the paperwork and their interest on how my Erasmus program was going.

Last but not least, I would like to express my gratitude to my family and friends for their support during the whole degree.

My entirely gratefulness.

1. INTRODUCTION

As it will be explained on the following chapters, piezoelectric devices are really important for vibration energy harvesting. For this reason, this research is focused on them.

The aim of this bachelor project is to analyse one piezoelectric vibrational harvester and how the change on its configuration will affect to its behaviour. In order to reach this, the first step will consist on doing experimental measurements. After that, the model will be reproduced by computer software (in this case ANSYS), with which it will also be compared with another different configuration. Finally, the results will be discussed.

2. LITERATURE REVIEW

2.1. ENERGY HARVESTING

Energy harvesting is the conversion of ambient energy present in the environment into electrical energy, which is accumulated and stored for later use. It has the same principle as large-scale renewable energy generation (such as wind or solar power) but it is very different in scale. It is usually referred to micro- or milliwatts, while large-scale power generation is concerned with megawatts of power.

Research and development on energy harvesting technologies started in the early 21st century and since then, they have evolved, advanced and even been successfully developed into hardware prototypes.

This development has been driven by the proliferation of autonomous wireless electronic systems. As this systems are wireless by definition, they cannot be plugged into a mains supply and the energy has to be provided by a local supply which it usually is a battery. Although batteries are low cost and convenient for these systems, they must be periodically replaced or recharged. Moreover, this means that the wireless system has to be accessible. Finally, there are some environmental concerns about the use of batteries, mainly because of the chemical waste produced by replacing them. Taking all of this into account, energy harvesting was developed for replacing or augmenting batteries, as the conversion of ambient energy from the environment provides the electrical power that the wireless system requires for its lifetime.

In spite of the fact that energy harvesters provide a small amount of power, current advanced technical developments have increased the efficiency of devices in capturing the energy and transforming it into electrical energy.

This energy comes from natural source and therefore it is clean, virtually unlimited and essentially free. It is available in different ways so that it could be used in different applications, as the main energy supplementing primary power in the systems or to enhance the reliability of the overall system and prevent power interruptions.

There are many energy harvesting sources. Some of them are:

- Mechanical energy – from sources such as vibration, mechanical stress and strain
- Thermal energy – from furnaces, heaters and friction sources
- Light energy – captured from sunlight or room light via photo sensors, photo diodes or solar panels
- Electromagnetic energy – from inductors, coils and transformers
- Natural energy – from the environment such as wind, water flow, ocean currents and solar

- Human body – using the thermal energy or human's movements as walking
- Other energy – from chemical and biological sources

An energy harvesting system requires an energy source (like the previously mentioned) and three other electronic components. These key components are the following:

- Energy conversion device to transform the energy into electrical form
- Energy harvesting module that captures, stores and manages power for the device
- Devices where the energy will be used

In addition to these three components, some applications might need additional components in order to guarantee the right performance of the energy harvesting system:

- An electronic interface device or module to condition the energy captured from a low voltage source (less than 500 mV) and power the energy harvesting module
- A supplementary energy storage device, such as thin-film batteries, ultracapacitors, and supercapacitors
- An energy or power management module that will further regulate and condition the power output from the supplementary energy storage devices

All these optional components require energy to work, so they reduce the overall efficiency of the energy harvesting system and increase the bulk and cost. For this reason, it is important to evaluate the cost vs. benefit trade-off.

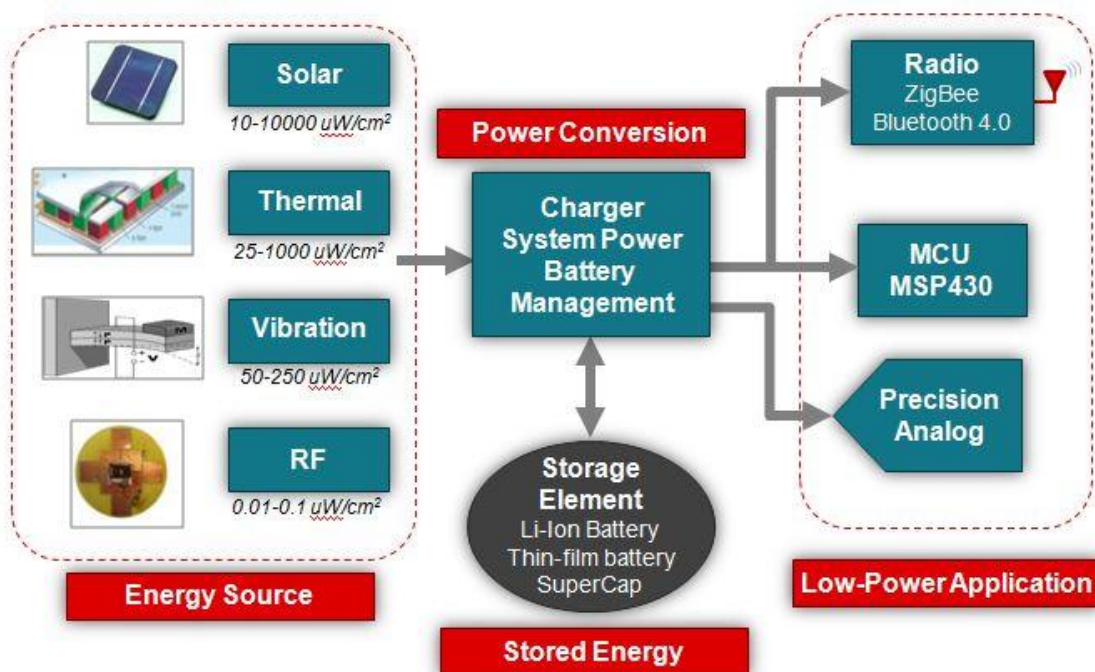


Figure 1 - Components of an energy harvesting system [4]

Energy source	Example	Energy level	Conversion mechanism
Ambient radiation	RF signal	$<1 \mu\text{W}/\text{cm}^2$	Electromagnetic
Ambient light	Sunlight Illumination	100 mW/cm ² (bright sunlight) 100 $\mu\text{W}/\text{cm}^2$ (office illumination)	Photovoltaic
Vibration	Machine vibration Human motion	4-800 $\mu\text{W}/\text{cm}^3$	Piezoelectric Electromagnetic Electrostatic
Fluid flow	Wind Ventilation Piping Current Wave	Air: 200-800 $\mu\text{W}/\text{cm}^3$	Turbine (electromagnetic) Piezoelectric
		Water: 500 mW/cm ³	
Thermal	Temperature differential	60 $\mu\text{W}/\text{cm}^2$ at 5°C difference	Thermoelectric Thermionic Thermotunnelling
Pressure variation	Daily atmosphere pressure change	$<10 \mu\text{W}/\text{cm}^3$	Unclear

Table 1 - Energy sources and characteristics [1]

2.2. KINETIC ENERGY HARVESTING

2.2.1. BASIS

Vibrations can be found in many different environments such as industrial machines, structures, roads, stairs or human bodies. They constitute an important kind of mechanical source of energy.

Kinetic energy harvesting consists in extracting electrical energy from vibration motion by a particular transduction mechanism such as electromagnetic, electrostatic and piezoelectric. The generator also requires a mechanical system to couple environmental displacements to the transduction mechanism. This mechanical system has to be designed to maximize the coupling between the mechanical energy source and the transduction mechanism.

Most kinetic energy harvesters (also known as vibration power generators) are usually single degree of freedom second-order spring-mass-damping system consisting of an inertial frame that transmits the vibration to a suspended inertial mass to produce a relative displacement or cause mechanical strain. The transduction mechanism can then generate electrical energy by exploiting the relative displacement or strain. The strain

effect utilizes the deformation within the mechanical system and typically employs active materials (e.g. piezoelectric). In the case of relative displacement, either the velocity or position can be coupled to a transduction mechanism. Velocity is typically associated with electromagnetic transduction while relative position is associated with electrostatic transduction. Each transduction mechanism exhibits different damping characteristics and this should be taken into consideration while modelling the generators.

The generic model of kinetic energy harvesters was first developed by Williams and Yates in 1996 as shown in the following figure:

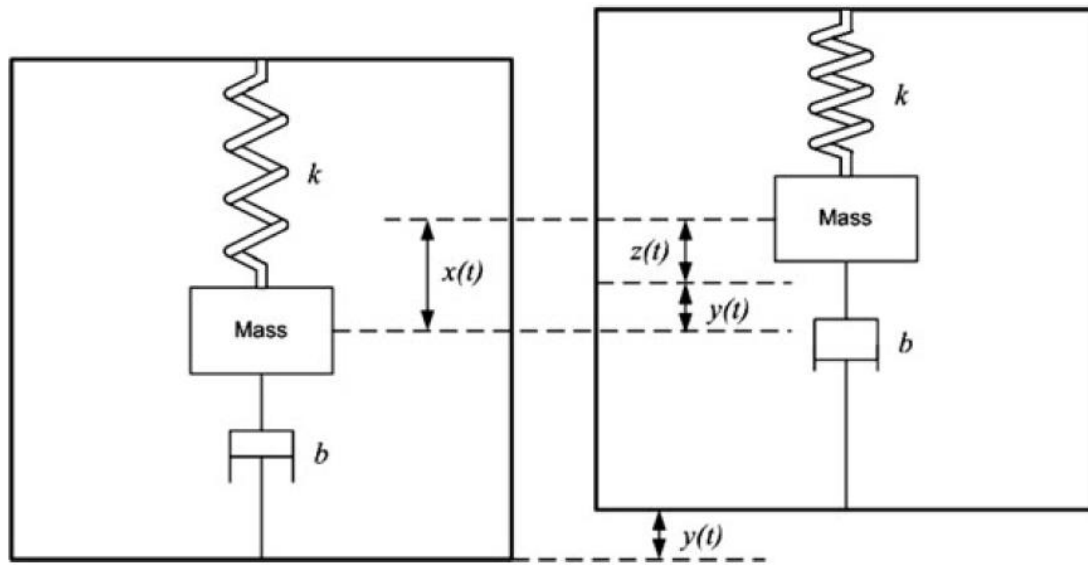


Figure 2 - Generic model of kinetic energy harvesters [1]

The system consists of an inertial mass, m , connected to a generator housing with a spring, k , and a damper, b . The damper has two parts, one is the mechanical damping (parasitic damping) b_m and the other is the electrical damping, b_e , which represents the transduction mechanism. Therefore, $b = b_m + b_e$.

When the generator vibrates, the inertial mass moves out of phase with the housing. There is either relative displacement between the mass and the housing or mechanical strain. This displacement is sinusoidal in amplitude and can drive a suitable transducer to generate electrical energy.

In figure 2, $x(t)$ represents the absolute displacement of the inertial mass, $y(t)$ is the displacement of the housing and $z(t)$ is the relative motion of the mass with respect to the housing. For a sinusoidal excitation, $y(t)$ can be written as $y(t) = Y \sin \omega t$, where Y is the amplitude of vibration and ω is the angular frequency of vibration. Electrical energy can then be extracted by transduction mechanisms exploiting either displacement or strain.

For the analysis, it is assumed that the mass of the vibration source is much greater than the mass of the inertial mass in the generator and the vibration source is unaffected by the movement of the generator. Then the differential equation of the movement of the mass with respect to the generator housing from the dynamic forces on the mass can be derived as follows:

$$m \cdot \frac{d^2 z(t)}{dt^2} + b \cdot \frac{dz(t)}{dt} + k \cdot z(t) = -m \cdot \frac{d^2 y(t)}{dt^2}$$

this can be written in the form after Laplace transform as

$$m \cdot s^2 \cdot z(s) + b \cdot s \cdot z(s) + k \cdot z(s) = -m \cdot a(s)$$

where $a(s)$ is the Laplace expression of the acceleration of the vibration $a(t)$ which is given by

$$a(t) = \frac{d^2 y(t)}{dt^2}$$

Therefore, the transfer function of the vibration-based micro-generator is

$$\frac{z(s)}{a(s)} = \frac{1}{s^2 + \frac{b}{m} \cdot s + \frac{k}{m}} = \frac{1}{s^2 + \frac{\omega_r}{Q} \cdot s + \omega_r^2}$$

where $Q = \frac{\sqrt{k \cdot m}}{b}$ is the quality factor and $\omega_r = \sqrt{\frac{k}{m}}$ is the resonant frequency.

As this is a resonant system, it generates maximum power when the resonant frequency of the generator matches ambient vibration frequency. Any difference between these two frequencies can result in a significant decrease in generated power. So, the main limitation to this technology is that the generator is, by definition, designed to work at a single frequency.

Recent development in adaptive kinetic energy harvesting increases the operating frequency range of such generators. One possible solution in consists in tuning resonant frequency of the generator by mechanical or electrical methods. In the first methods, the resonant frequency is altered by changing mechanical properties whereas electrical methods tune the resonant frequency by adjusting the electrical load.

For a cantilever with mass at the free end, the resonant frequency is given by:

$$f_r = \frac{1}{2\pi} \sqrt{\frac{Ywh^3}{4l^3(m + 0.24m_c)}}$$

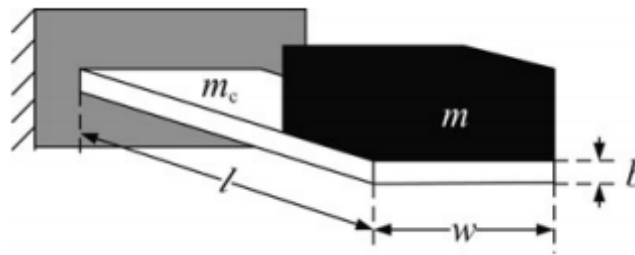


Figure 3 - Cantilever with a tip mass [1]

where Y is Young's modulus of the cantilever material, w , h and l are the width, thickness and length of the cantilever, respectively, and m_c is the mass of the cantilever. The resonant frequency can be tuned by adjusting any of these parameters. There are four different tuning methods:

- Changing dimensions
- Moving the centre of gravity of proof mass
- Variable spring stiffness
- Straining the structure

2.2.2. TRANSDUCTION MECHANISMS

As it was explained before, in kinetic energy harvesting, a particular transduction mechanism is used to extract electrical energy from motion. Currently, there are three main kinds of kinetic energy harvesters: electromagnetic, electrostatic and piezoelectric.

ELECTROMAGNETIC GENERATORS

They are based on the electromagnetic induction phenomenon discovered by Michael Faraday in 1831. His law of electromagnetic induction states the following: "An electrical current will be induced in any closed circuit when the magnetic flux through a surface bounded by the conductor changes".

In an electromagnetic generator, permanent magnets are used to produce strong magnetic field and a coil is used as the conductor. Either the permanent magnet or the coil is fixed to the frame while the other is attached to the inertial mass. The relative displacement caused by the vibration makes the transduction mechanism work and generate electrical energy. The induced voltage, also known as electromotive force (e.m.f.), across the coil is proportional to the strength of the magnetic field, the velocity of the relative motion and the number of turns of the coil.

Through Faraday's law, it is possible to distinguish between two different types of electromagnetic generators. In the first one (Figure 4a), the magnetic field is uniform

and the magnetic field cut by the coil varies with the relative displacement between magnets and the coil. In the second one (Figure 4b), the magnetic field varies with the distance apart from the magnet.

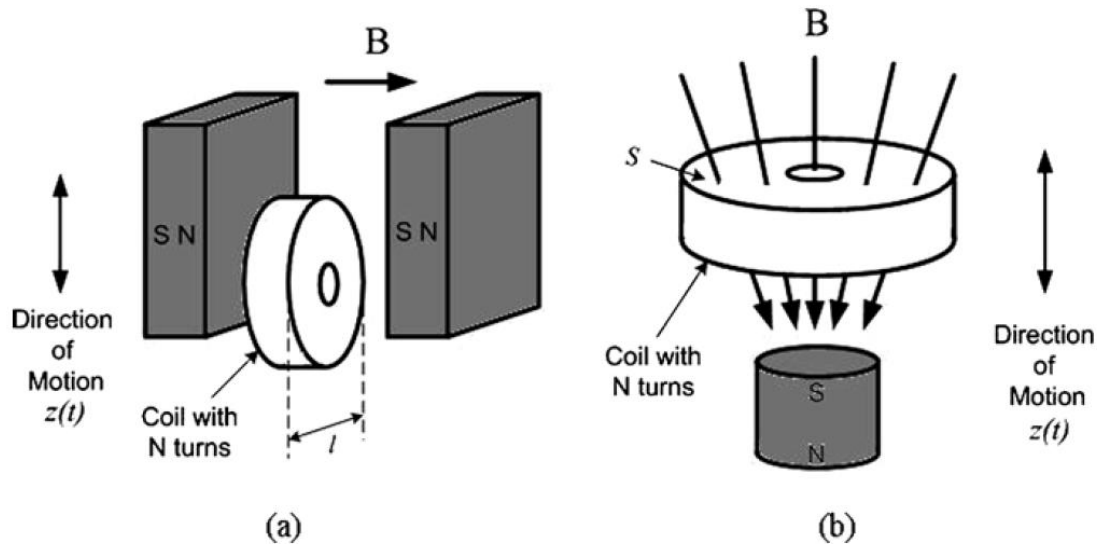


Figure 4 - Electromagnetic generators [1]

An electromagnetic generator is characterized by high output current level at the expense of low voltages.

ELECTROSTATIC GENERATORS

The basis of electrostatic generator is the variable capacitance structure which is driven by mechanical vibrations. The capacitance varies between maximum and minimum values. If the charge on the capacitor is constrained, charge will move from the capacitor to a storage device or to the load as the capacitance decreases. With this action, mechanical energy is converted to electrical energy.

There are three kinds of electrostatic generators:

- In-plane overlap (Figure 5a): it varies the overlap area between electrode fingers
- In-plane gap closing (Figure 5b): it varies the gap between electrode fingers
- Out-of-plane gap closing (Figure 5c): it varies the gap between two large electrode plates

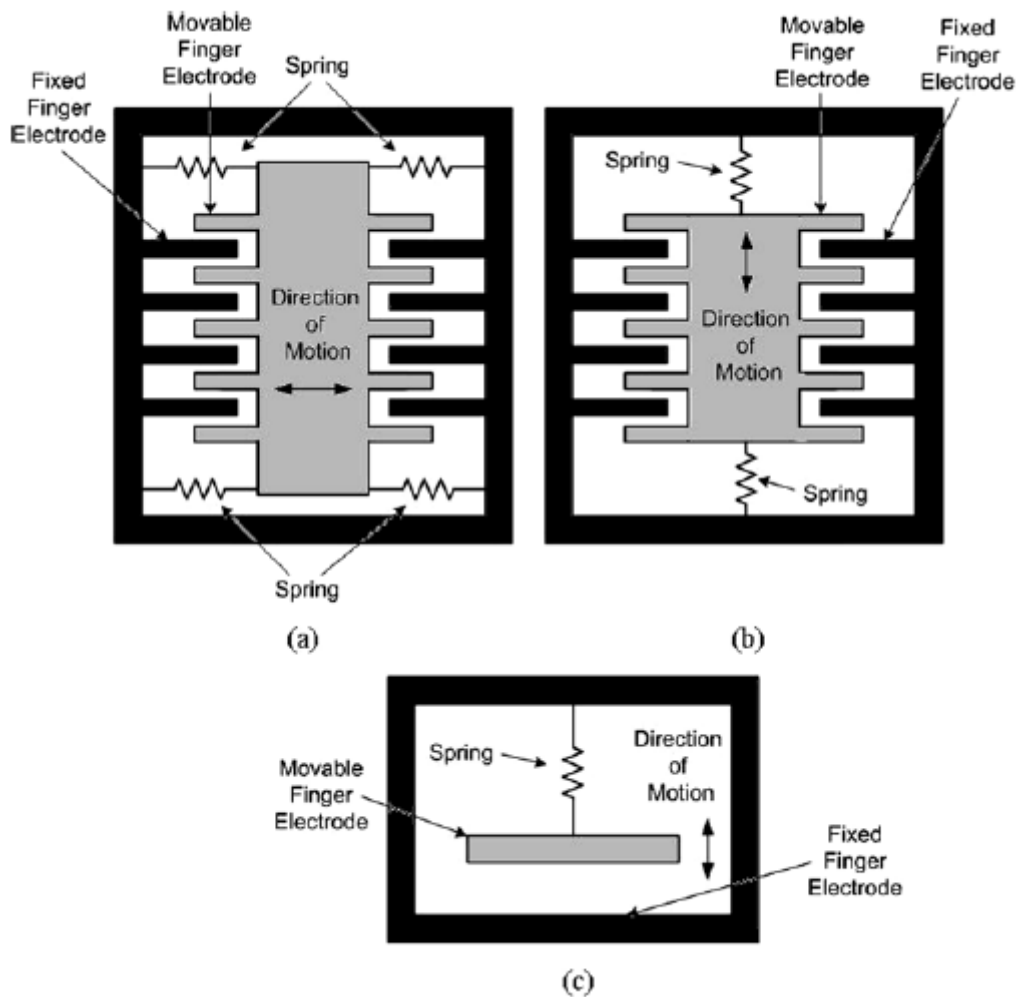


Figure 5 - Electrostatic generators [1]

PIEZOELECTRIC GENERATORS

The piezoelectric effect was discovered by Pierre and Jacques Curie in 1880. It is the ability of some materials (notably crystals and certain ceramics) to generate an electric potential in response to applied mechanical stress. The electrical polarization is proportional to the applied strain. Piezoelectric generators take advantage of this effect to transform mechanical into electrical energy.

Piezoelectric generators typically work in two different modes:

- 33 mode (Figure 6a): a force is applied in the same direction as the poling direction
- 31 mode (Figure 6b): a lateral force is applied in the direction perpendicular to the poling direction, an example of which is a bending beam that has electrodes on its top and bottom surfaces.

Although the 31 mode has a lower coupling coefficient than the 33 mode, it is the most commonly used because harvesting structures such as cantilevers or double-clamped beam use the lateral stress on the beam surface which is easily coupled to piezoelectric materials deposited onto the beam.

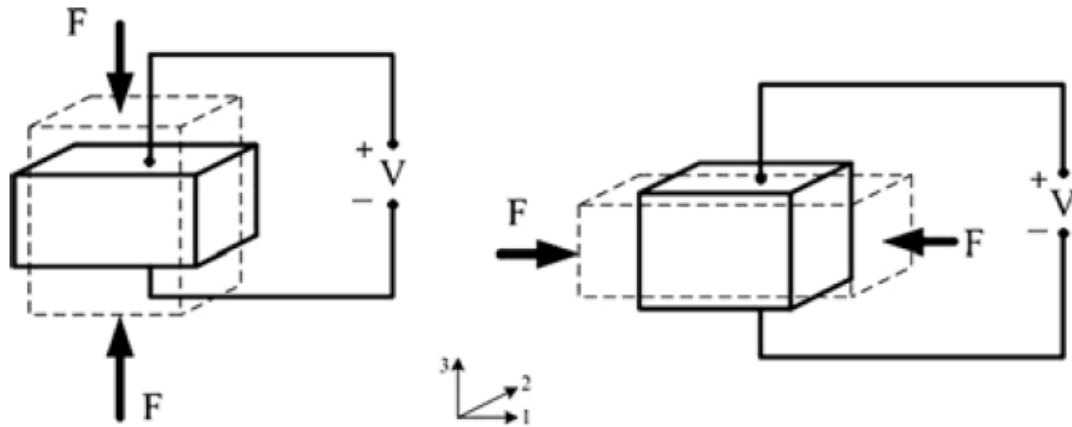


Figure 6 - Piezoelectric working modes [1]

OTHER TRANSDUCTION MECHANISMS. MAGNETOSTRICTIVE

Magnetostrictive materials are also used to extract electrical energy from ambient vibration. These materials deform when placed in a magnetic field and it can induce changes in magnetic field when it is strained. They are generally used in piezoelectric-magnetostrictive composites.

COMPARISON OF TRANSDUCTION MECHANISMS

On the following table the main advantages and disadvantages of each transduction mechanism can be seen:

Type	Advantages	Disadvantages
Electromagnetic	<ul style="list-style-type: none"> • No external voltage source • No mechanical constraints needed • High output current 	<ul style="list-style-type: none"> • Difficult to integrate with MEMS fabrication process • Poor performance in micro-scale • Low output voltage
Piezoelectric	<ul style="list-style-type: none"> • Simple structure • No external voltage source • Compatible with MEMS • High output voltage • No mechanical constraints needed 	<ul style="list-style-type: none"> • Thin films have poor coupling • Poor mechanical properties • High output impedance • Charge leakage • Low output current
Electrostatic	<ul style="list-style-type: none"> • Easy to integrate with MEMS fabrication process • High output voltage 	<ul style="list-style-type: none"> • Mechanical constraints needed • External voltage source or electrical precharged needed • High output impedance • Low output current
Magnetostrictive	<ul style="list-style-type: none"> • Ultra-high coupling coefficient • High flexibility 	<ul style="list-style-type: none"> • Non-linear effect • May need bias magnets • Difficult to integrate with MEMS fabrication process

Table 2 - Advantages and disadvantages of the transduction mechanisms [1]

From the table above, it can be seen that piezoelectric mechanisms have many advantages compared to the other energy harvesting methods. The main ones are their high output voltages and their easy application.

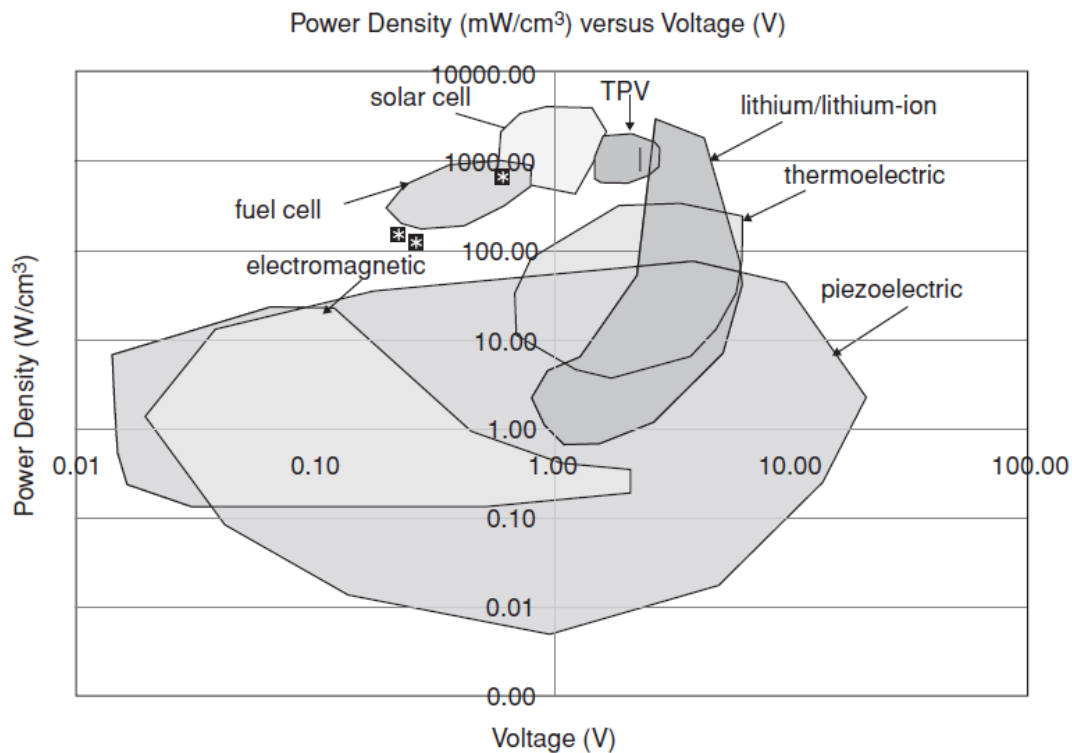


Figure 7 - Power Density vs. Voltage of energy harvesting systems [3]

As can be seen in figure 7, voltage outputs in electromagnetic energy harvesting are low and it is often required multistage post-processing in order to reach the voltage level. On the other hand, piezoelectric mechanisms have usable voltage outputs obtained from the piezoelectric material itself.

Another advantage is that piezoelectric energy harvesting emerges from the constitutive behaviour of the material, which eliminates the requirement of an external voltage input. Using electrostatic energy harvesting, an input voltage or charge is required so that the relative vibratory motion of the capacitor elements creates an alternating electrical output.

Moreover, piezoelectrics can be used in macro-scale or micro-scale applications. The reason of this fact is the well-established thick-film and thin-film techniques. On the other hand electromagnetic energy harvesting have limitations in enabling micro-scale because of poor properties of planar magnets and the limited number of turns that can be achieved using planar coils.

As can be seen, piezoelectric mechanisms have many advantages that can be useful for the following studies so that they will be the harvesting mechanisms that will be used.

2.3. PIEZOELECTRICITY

2.3.1. BASIS

As it was explained before, piezoelectricity is the ability of certain materials to generate a voltage when a corresponding mechanical stress is applied. The piezoelectric effect is reversible, as the shape of the piezoelectric materials will deform proportional to the applied voltage.

Piezoelectricity was first discovered by the brothers Pierre Curie and Jacques Curie in 1880. They predicted and demonstrated that crystalline materials like tourmaline, quartz, topaz, cane sugar, and Rochelle salt (sodium potassium tartrate tetrahydrate) can generate electrical polarization from mechanical stress. This is called the direct piezoelectric effect.

Inverse piezoelectricity was mathematically deduced from fundamental thermodynamic principles by Lippmann in 1881. Later the Curies confirmed the existence of the inverse piezoelectric effect.

These two effects coexist in a piezoelectric material, therefore, although only direct piezoelectric effect is interesting for kinetic energy harvesting, converse piezoelectric effect has to be taken into account.

2.3.2. CLASSIFICATION OF PIEZOELECTRIC MATERIALS

There are many materials, both natural and synthetic, that have piezoelectric properties. The main of them are now summarized.

NATURALLY OCCURRING CRYSTALS

- Quartz
- Berlinite (AlPO_4): a rare phosphate mineral that is structurally identical to quartz
- Sucrose (table sugar)
- Rochelle salt
- Topaz
- Tourmaline-group minerals
- Lead titanate (PbTiO_3): it occurs in nature as mineral macedonite but it is also synthesized for research and applications

OTHER NATURAL MATERIALS

- Bone
- Tendon
- Silk
- Wood
- Enamel
- Dentin
- DNA
- Viral proteins

SYNTHETIC CRISTALS

- Langasite ($\text{La}_3\text{Ga}_5\text{SiO}_{14}$): it is a quartz analogic crystal
- Gallium orthophosphate (GaPO_4), a quartz analogic crystal
- Lithium niobate (LiNbO_3)
- Lithium tantalate (LiTaO_3)

SYNTHETIC CERAMICS

- Barium titanate (BaTiO_3): it was the first piezoelectric ceramic discovered
- Lead zirconate titanate ($\text{Pb}[\text{Zr}_x\text{Ti}_{1-x}]\text{O}_3$ where $0 \leq x \leq 1$): it is more commonly known as PZT and it is the most common piezoelectric ceramic in use today
- Potassium niobate (KNbO_3)
- Sodium tungstate (Na_2WO_3)

POLYMERS

Unlike ceramics, where the crystal structure of the material creates the piezoelectric effect, in polymers the intertwined long-chain molecules attract and repel each other when an electric field is applied.

- Polyvinylidene fluoride (PVDF): it exhibits piezoelectricity several times greater than quartz

2.3.3. PIEZOELECTRIC MATHEMATICAL PARAMETERS

The constitutive equations of piezoelectric material combine strain, deformation and electrical behaviour and are as follows:

$$D = d^T \cdot \sigma + \varepsilon^T \cdot E \quad \text{Direct piezoelectric effect}$$

$$\varepsilon = S \cdot \sigma + d \cdot E \quad \text{Inverse piezoelectric effect}$$

where, D is the electrical displacement, ε is the strain, S is the compliance, σ is the stress, E is the electrical field, d is the piezoelectric strain coefficient and ε^T is permittivity (dielectric constant).

Most of the materials used in piezoelectric harvesting are orthotropic, that means that the material has two orthogonal planes of elastic symmetry.

Those equations can be written in the matrix form as follows:

$$\begin{bmatrix} D_1 \\ D_2 \\ D_3 \end{bmatrix} = \begin{bmatrix} 0 & 0 & 0 & 0 & 0 & d_{15} & 0 \\ 0 & 0 & 0 & 0 & d_{15} & 0 & 0 \\ d_{31} & d_{31} & d_{33} & 0 & 0 & 0 & 0 \end{bmatrix} + \begin{bmatrix} \varepsilon_{11}^T & 0 & 0 \\ 0 & \varepsilon_{11}^T & 0 \\ 0 & 0 & \varepsilon_{33}^T \end{bmatrix} \begin{bmatrix} E_1 \\ E_2 \\ E_3 \end{bmatrix}$$

$$\begin{bmatrix} \varepsilon_1 \\ \varepsilon_2 \\ \varepsilon_3 \\ \gamma_{23} \\ \gamma_{31} \\ \gamma_{12} \end{bmatrix} = \begin{bmatrix} S_{11} & S_{12} & S_{13} & 0 & 0 & 0 \\ S_{12} & S_{11} & S_{13} & 0 & 0 & 0 \\ S_{13} & S_{13} & S_{33} & 0 & 0 & 0 \\ 0 & 0 & 0 & S_{44} & 0 & 0 \\ 0 & 0 & 0 & 0 & S_{44} & 0 \\ 0 & 0 & 0 & 0 & 0 & S_{66} \end{bmatrix} \begin{bmatrix} \sigma_1 \\ \sigma_2 \\ \sigma_3 \\ \tau_{23} \\ \tau_{31} \\ \tau_{12} \end{bmatrix} + \begin{bmatrix} 0 & 0 & d_{31} \\ 0 & 0 & d_{31} \\ 0 & 0 & d_{33} \\ 0 & d_{15} & 0 \\ d_{15} & 0 & 0 \\ 0 & 0 & 0 \end{bmatrix} \begin{bmatrix} E_1 \\ E_2 \\ E_3 \end{bmatrix}$$

where $\varepsilon_1, \varepsilon_2$ and ε_3 are the normal strain and γ_{12}, γ_{31} and γ_{23} are the shear stress.

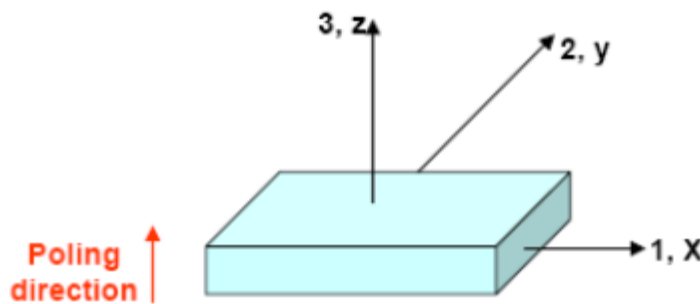


Figure 8 - Axis in piezoelectric materials [5]

Relative permittivity ϵ

The permittivity is defined as the dielectric displacement per unit electric field. The first subscript gives the direction of the dielectric displacement; the second gives the direction of the electric field.

ϵ_{11}^T is the permittivity for the dielectric displacement and electric field in direction 1 under conditions of constant stress.

ϵ_{33}^T is the permittivity for the dielectric displacement and electric field in direction 3 under conditions of constant stress.

Compliance S

The compliance of a material is defined as the strain produced per unit stress. It is the reciprocal of the modulus of elasticity. The first subscript refers to the direction of strain, the second to direction of stress. For example:

S_{11} is the compliance for a stress and accompanying strain in direction 1 under conditions of constant electric field.

Piezoelectric charge constants d

The piezoelectric charge constant is defined as the electric polarization generated in a material per unit mechanical stress applied to it. The first subscript refers to the direction of polarization generated in the material (at $E=0$) or to the applied field strength, the second refers respectively to the direction of the applied stress or to the direction of the induced strain. For example:

d_{31} is the induced polarization in direction 3 per unit stress applied in direction 1. Alternatively it is the mechanical strain induced in the material in direction 1 per unit electric field applied in direction 3. The induced polarization is in the direction parallel to the direction in which the ceramic element is polarized. The voltage output of this type is one order magnitude lower than for the d_{33} type, while the electrical current is larger. This makes this type better suited for energy harvesting, although the overall energy conversion is lower than the d_{33} type.

d_{33} is the induced polarization per unit applied stress in direction 3. Alternatively it is the induced strain per unit electric field in direction 3. The induced polarization is in the direction parallel to the direction in which the ceramic element is polarized. The advantage is its high energy conversion rate. However, the electrical output voltage is very high and the electrical current low. This makes this type less suitable for use with low energy consuming electronics, as the losses for converting the voltage and current to usable values are high.

Piezoelectric voltage constant g

The piezoelectric voltage constant is defined as the electric field generated in a material per unit mechanical stress applied to it. The first subscript refers to the direction of the electric field generated in the material or to the applied electric displacement; the second refers respectively to the direction of the applied stress or to the direction of the induced strain. For example:

g_{31} is the induced electric field in direction 3 per unit stress applied in direction 1. Alternatively it is the mechanical strain induced in the material in direction 1 per unit electric displacement applied in direction 3.

g_{31} is the induced electric field in direction 1 per unit shear stress applied about axis direction 2. Alternatively it is the shear strain induced in the material about axis 2 per unit electric displacement applied in direction 1.

Coupling factor k

The coupling factor is defined as a measure of the effectiveness with which electrical energy is converted into mechanical energy and vice versa.

$$k = \sqrt{\frac{\text{stored electrical energy}}{\text{applied mechanical energy}}}$$

k_{33} is the coupling factor for longitudinal vibrations of a very long, very slender rod under the influence of a longitudinal electric field.

k_{31} is the coupling factor for longitudinal vibrations of long rod under the influence of a transverse electrical field.

k_t is the coupling factor for longitudinal vibrations of a slender rod.

k_{15} describes shear mode vibrations of a piezoelectric body.

k_p is the planar coupling factor of a thin disc which represents the coupling between the electric field in direction 3 (parallel to the disc axis) and simultaneous mechanical effects in directions 1 and 2 that result in radial vibrations. It is known as radial coupling.

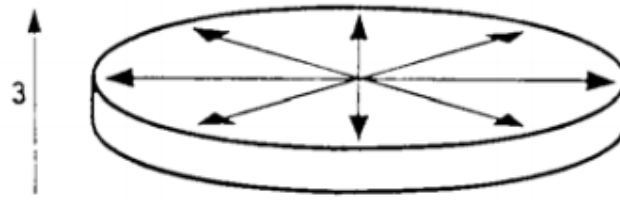


Figure 9 - Planar coupling model [6]

k_{eff} is given for PZT piezoceramic materials and it is obtained using the formula below, where f_n is the resonant frequency at minimal impedance and f_m the antiresonant frequency at maximal impedance.

$$k_{\text{eff}} = \sqrt{\frac{f_n^2 - f_m^2}{f_n^2}}$$

Most piezoelectric material parameters are determined by means of impedance measurements on special test bodies according to the European Standard EN 50324-2 at resonance, as can be seen as follow:

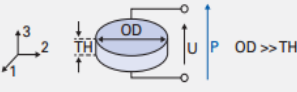


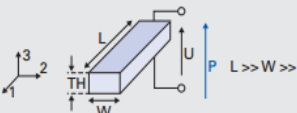
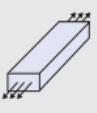
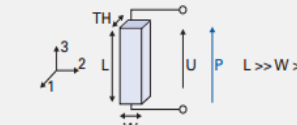

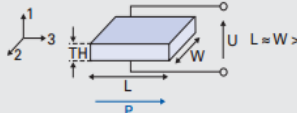

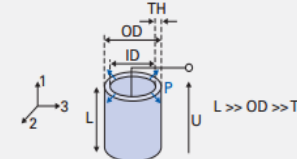


Shape	Oscillations		
	Type	Mechanical deformation	Series resonance frequency
Thin disk 	radial		$f_s = \frac{N_p}{OD}$
	thickness		$f_s = \frac{N_t}{TH}$
Plate 	transverse		$f_s = \frac{N_t}{L}$
Rod 	longitudinal		$f_s = \frac{N_s}{L}$
Shear plate 	thickness shear		$f_s = \frac{N_s}{TH}$
Tube 	transversal		$f_s = \frac{N_t}{L}$
	thickness		$f_s = \frac{N_t}{TH}$

Table 3 - Series resonance frequency depending on the shape [6]

Where f_s is the serial resonance that are related to the speed N of a wave traveling down the string by the equation:

$$f = \frac{nv}{2L}$$

L is the length of the string (for a string fixed at both ends) and $n=1, 2, 3 \dots$ (Harmonic in a closed and pipe). The speed of a wave through a string or wire is related to its tension T and the mass per unit length ρ :

$$v = \sqrt{\frac{T}{\rho}}$$

2.3.4. METHODS TO CHANGE THE RESPONSE CHARACTERISTICS

As it was explained before, piezoelectric energy harvesting devices give the maximum energy when they are working at the resonant frequency, like all kinetic energy harvesters. However, there are methods to achieve their proper functioning at different frequencies. The following images show these methods.

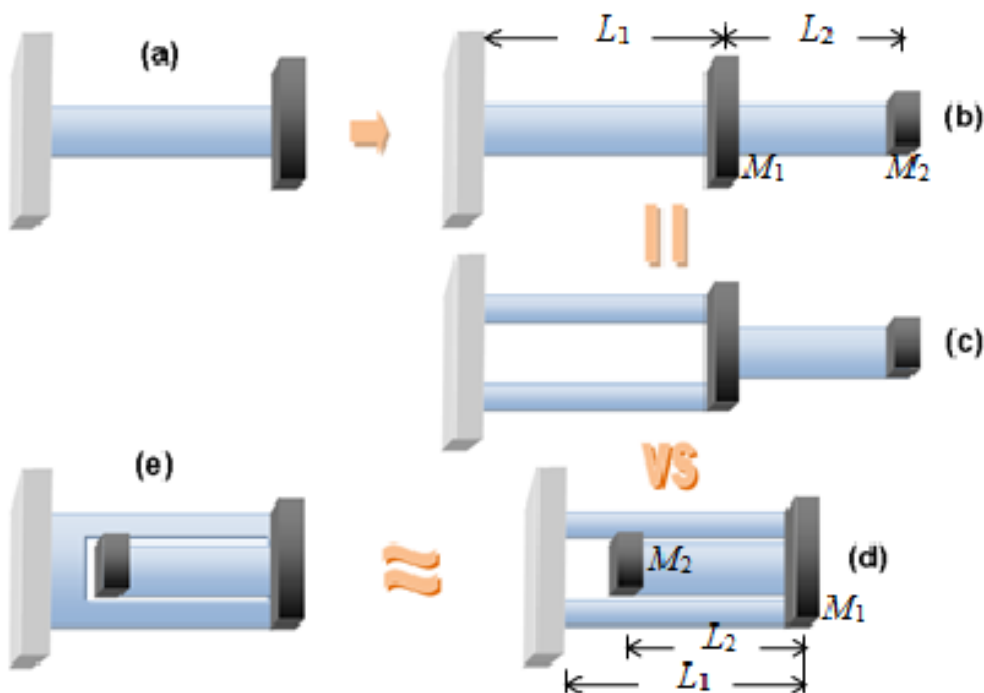


Figure 10

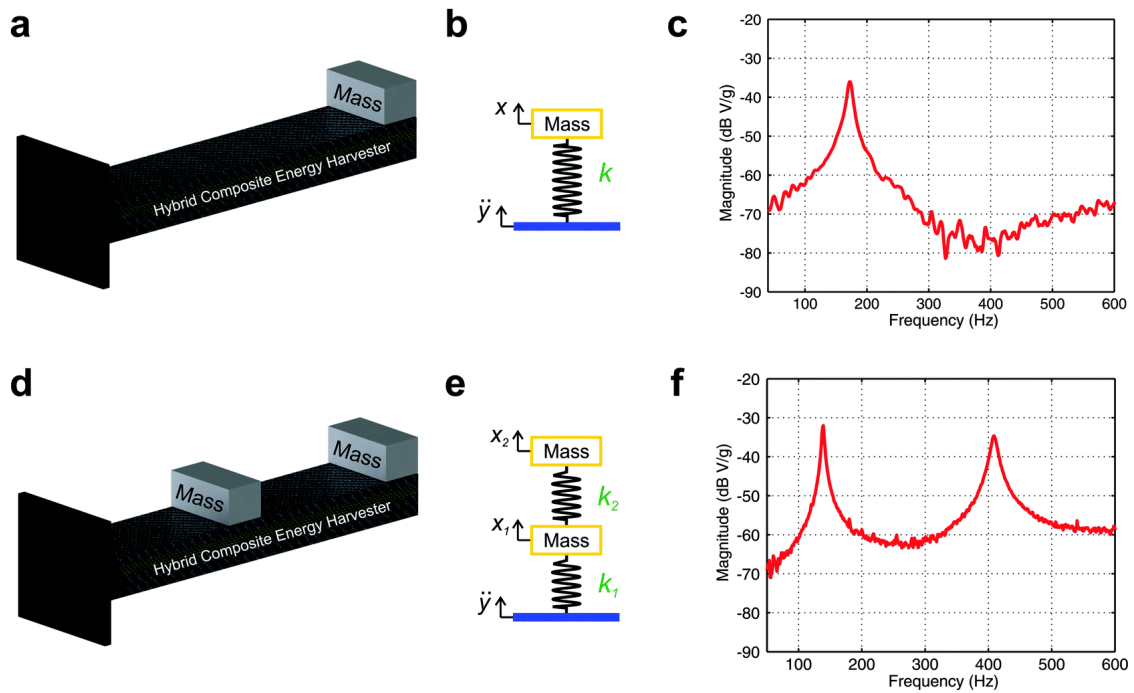


Figure 11

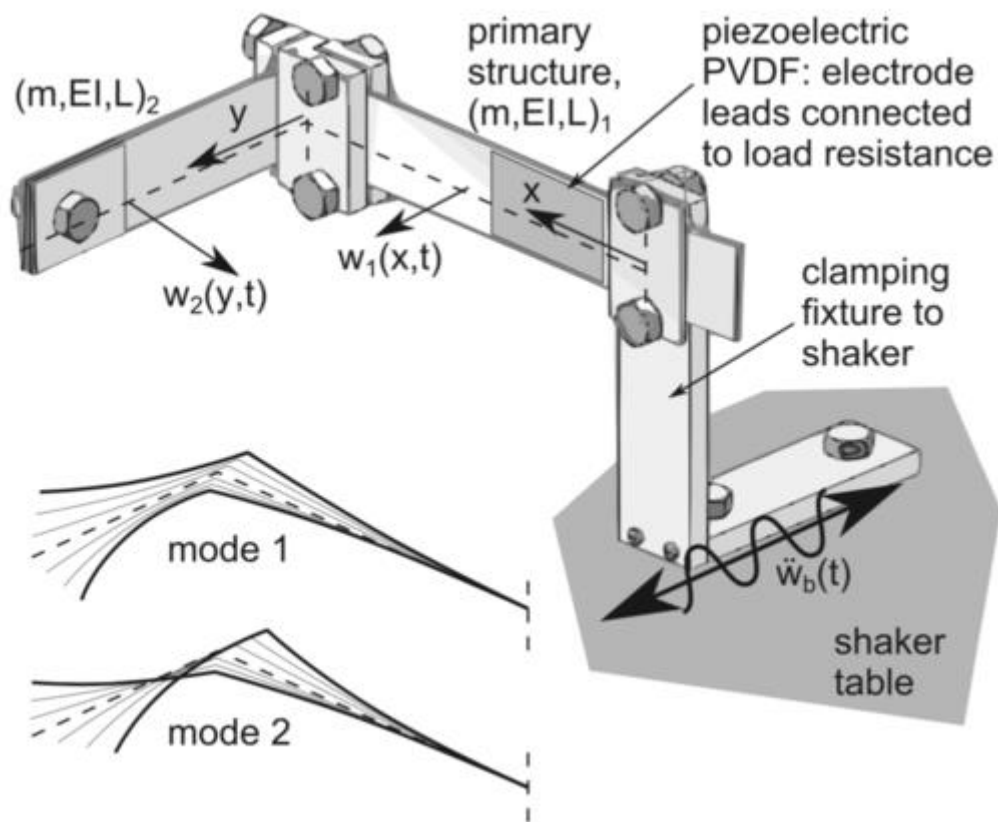


Figure 12

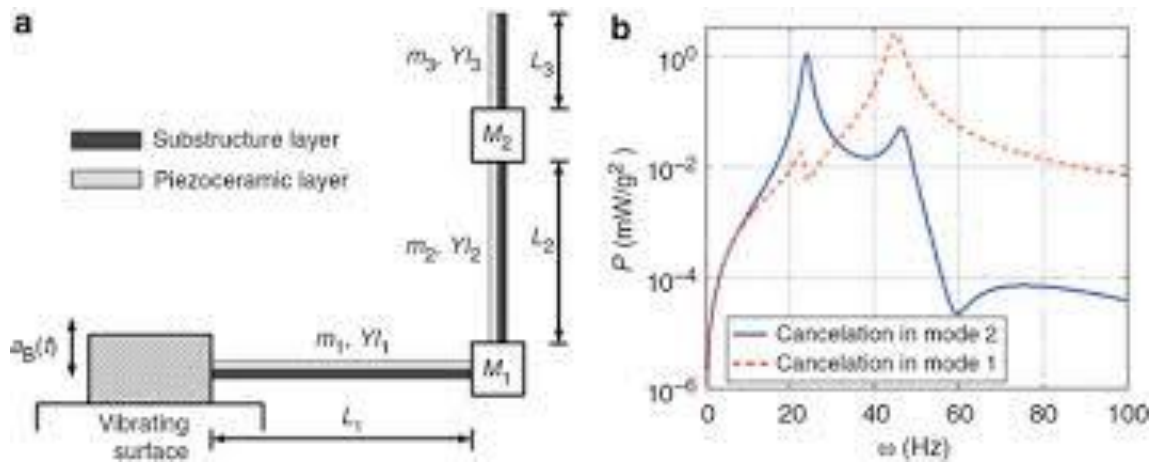


Figure 13

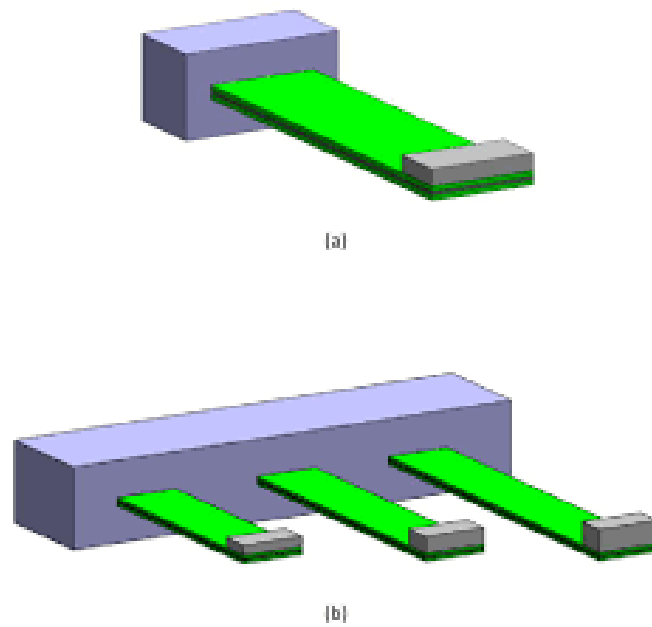


Figure 14

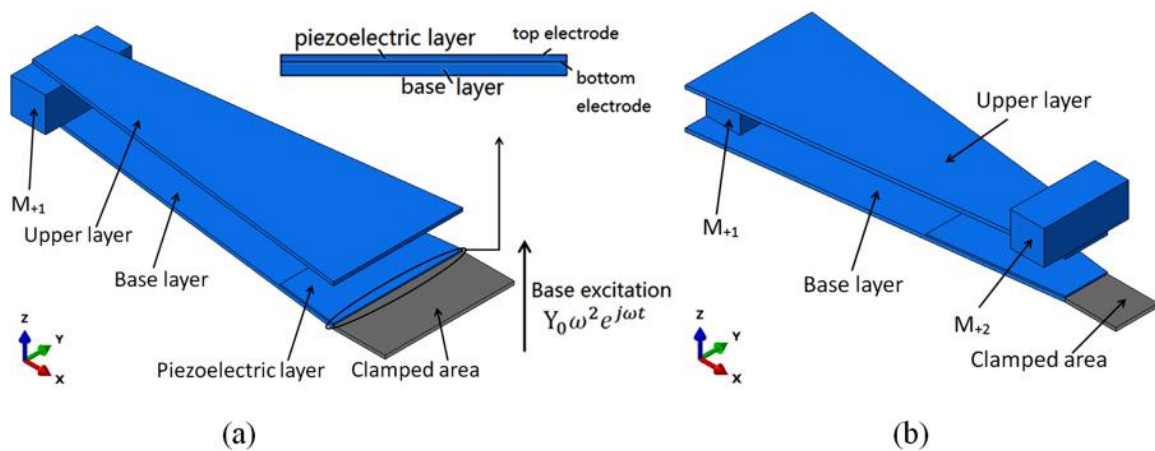


Figure 15

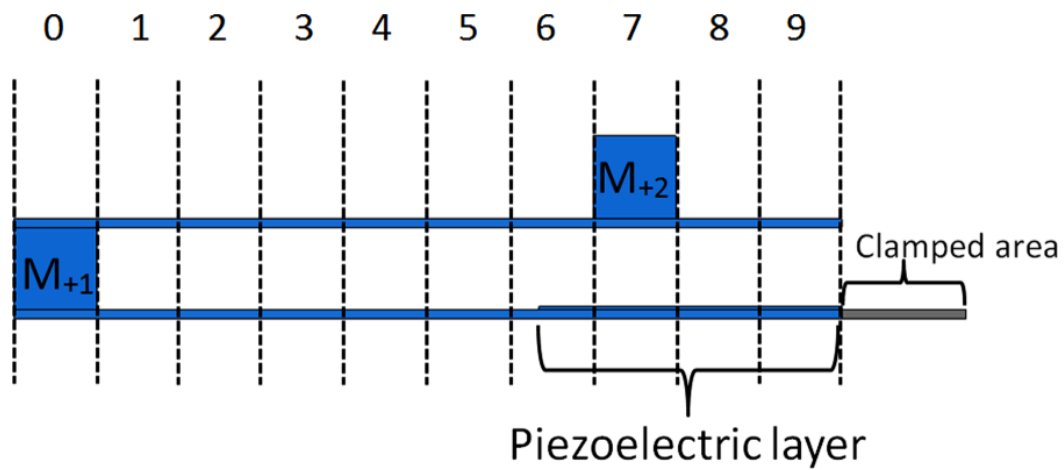


Figure 16

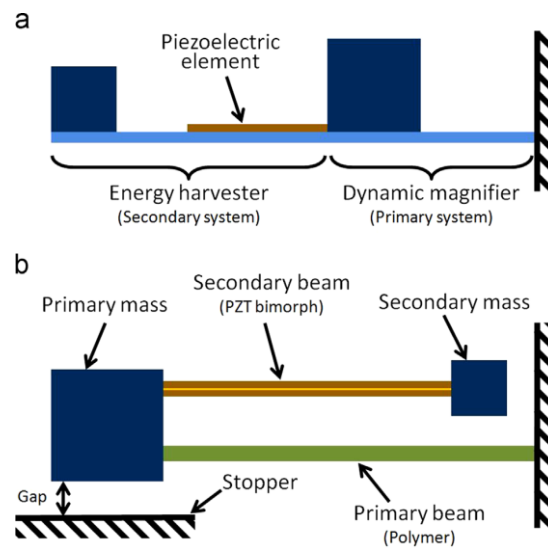


Figure 17

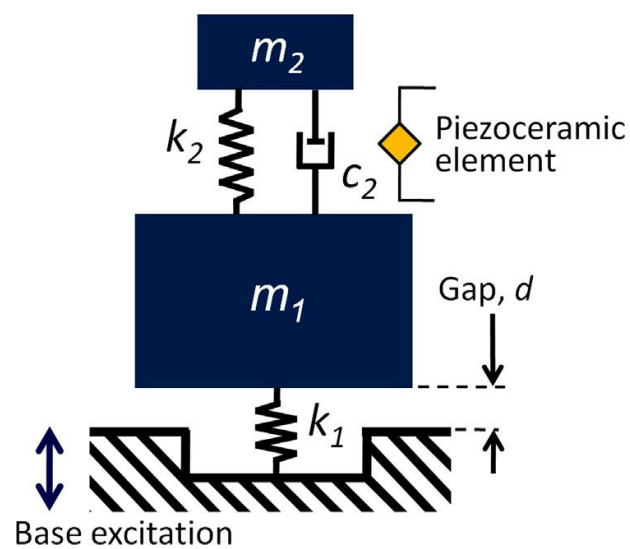


Figure 18

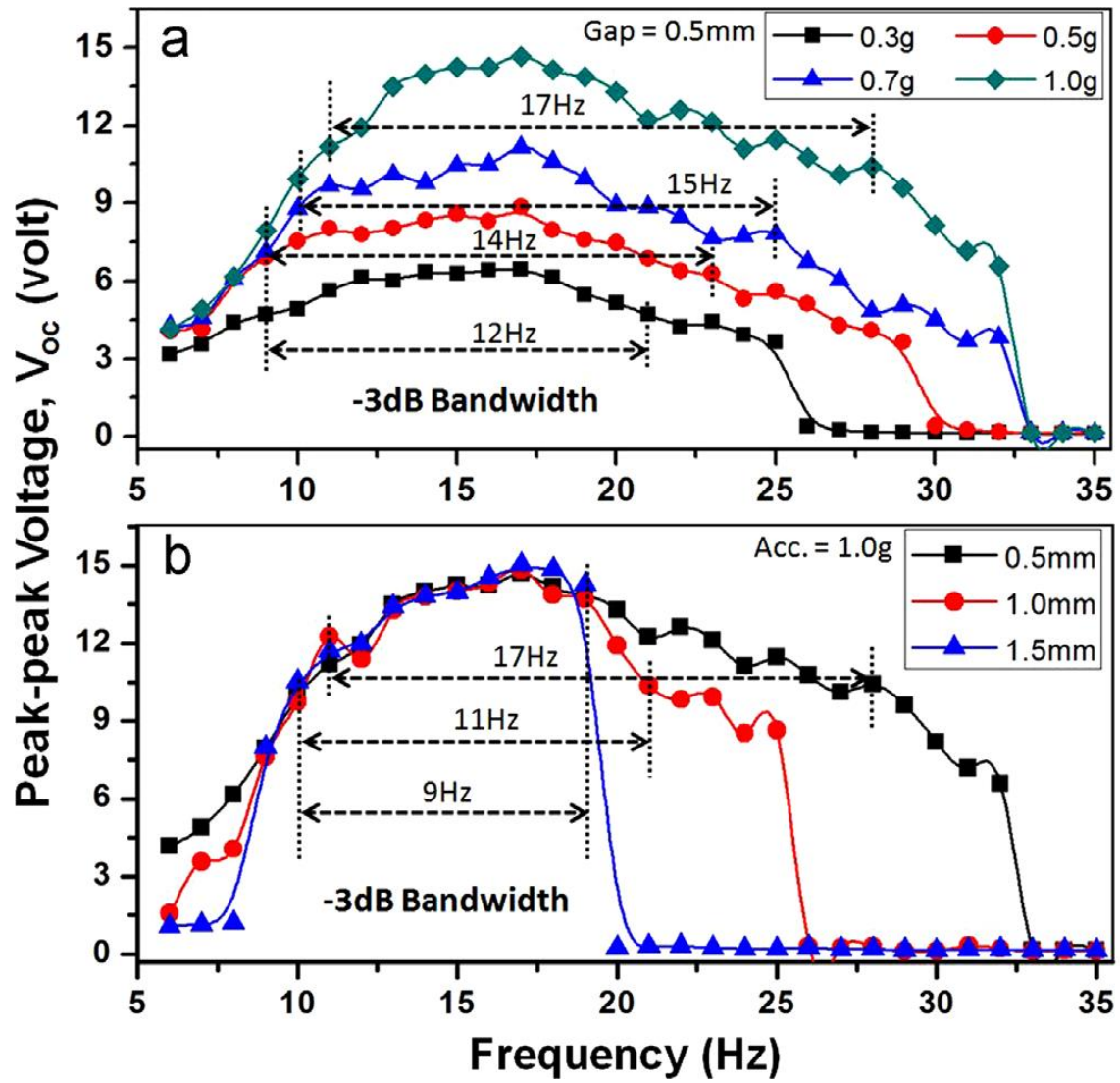


Figure 19

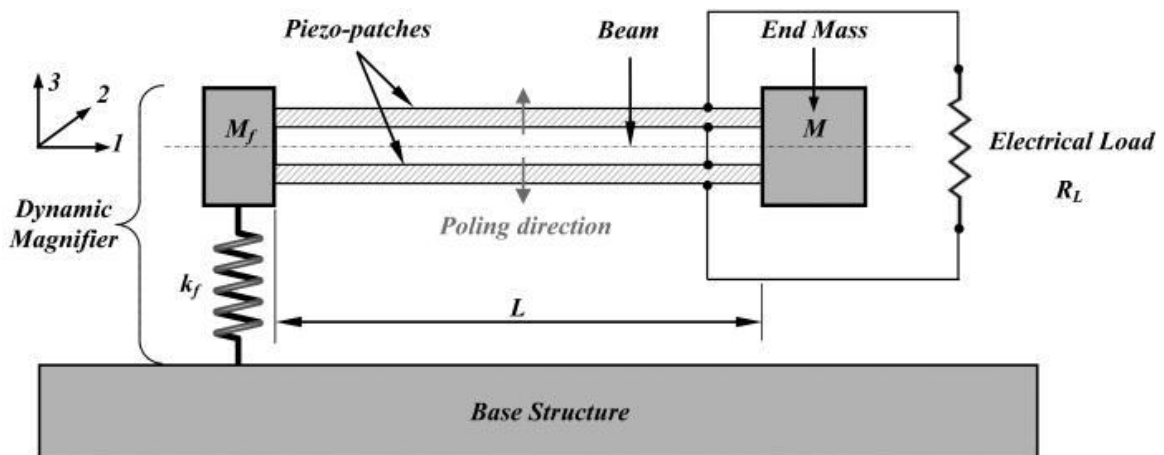


Figure 20

2.3.5. PIEZOELECTRIC MATERIALS APPLICATIONS FOR ENERGY HARVESTING

There are many different applications in which piezoelectric materials are used to harvest energy. Some of them are described now.

NIGHTCLUBS

This idea was implemented for the first time at Watt club in Rotterdam by the Sustainable Dance Club, and then imitated by the Club4Climate at London's Surya club. As people dance, the quartz crystals of the dance floor are pressed together. This creates a current which powers up the light, and the air conditioning. The clubber's movement can generate 60% of the energy needed to run the club.

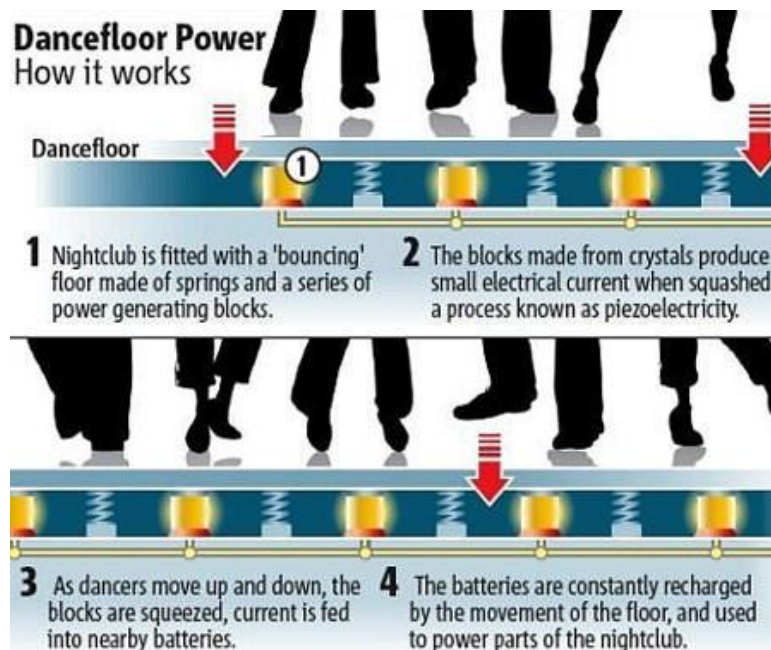


Figure 21 - Piezoelectric dance floor explanation [7]



Figure 22 - Piezoelectric dance floor [8]

BIOMECHANICAL ENERGY HARVESTING

Max Donelan at Simon Fraser University invented a device that exploits the energy of walking. The device wraps around the wearer's knee and generates power using the same principle that allows hybrid cars to recycle energy created by braking. A walker wearing harvesters on both knees could generate about 5 W of power, enough to charge 10 cell phones.



Figure 23 - Max Donelan's device [9]

The energy created by walking or running can also be harvested through piezoelectric devices installed on the footwear.



Figure 24 - Trainers with piezoelectric devices [10]

ROADWAYS, RAILROADS AND RUNWAYS

Israeli company Innowattech specialises in the development of custom piezoelectric generators for specific purposes such as harvesting mechanical energy imparted to roadways, railroads, pedestrian areas and runways. The company has previously used piezoelectric pads on Israeli highways and now they are planning to install piezoelectric pads throughout the country's railways to generate electricity.

A prototype of the energy-generating system was installed by the Technion University and Israel Railways in order to show the benefits of the technology. The project discovered that a railway track with trafficked by 10 to 20 ten-car trains could produce as much as 120 kWh, which could be used to power infrastructural systems such as signs and lights. Any surplus energy would then be uploaded to the country's power grid.

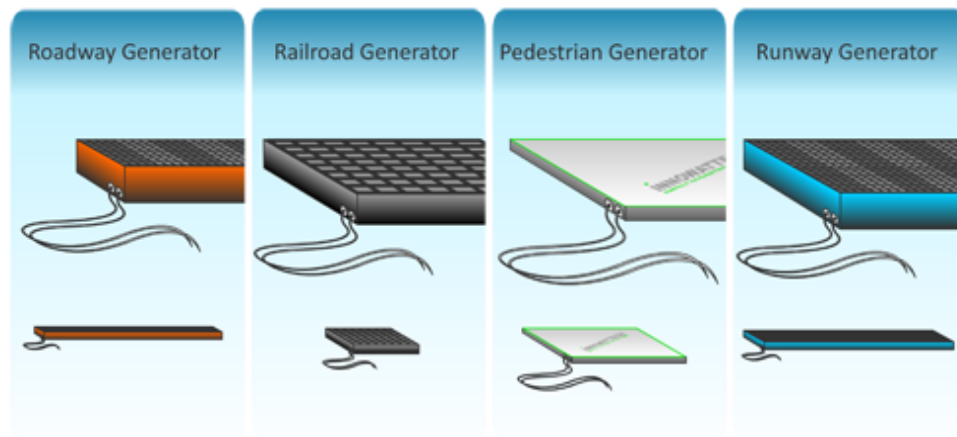


Figure 25 - Piezoelectric surfaces [11]



Figure 26 - Piezoelectric surface used in railways [12]

TRAIN STATIONS

The East Japan Railway Company (JR-East) is doing research on how to make its train stations more eco-friendly. One of the technologies they are working on is a ticket gate that has piezoelectric elements that would generate electricity as commuters walk through.

The system has been tested at the JR-East head office in Shibuya, where it is installed at the entrance to the reception area on the 4th floor. As visitors pass through the gate, a lamp lights up, signifying that electricity has been produced.



Figure 27 - Commuters at the Tokyo station [13]

TENNIS RACKETS

Tennis manufacturers, Head, were requested by players to design rackets with comfort as well as power. Previously, rackets had been designed to be stiff so that they return maximum energy to the ball when it is hit but this means that the racket transmits shock vibration to the player's arm.

To reduce vibration, piezoelectric fibres have been embedded around the racket throat and a computer chip has been installed inside the handle. The frame deflects slightly when the ball is hit so that the piezoelectric fibres bend and generate a charge (by the direct effect) which is collected. The associated current is carried to a silicon chip which boosts the current and sends it back to the fibres out of to reduce the vibration. The fibres then bend (by the converse effect) to counter the motion of the racket and reduce vibration.

The manufacturers claim 50% reduction in vibration compared with conventional rackets and the International Tennis Federation have approved them for tournament play.

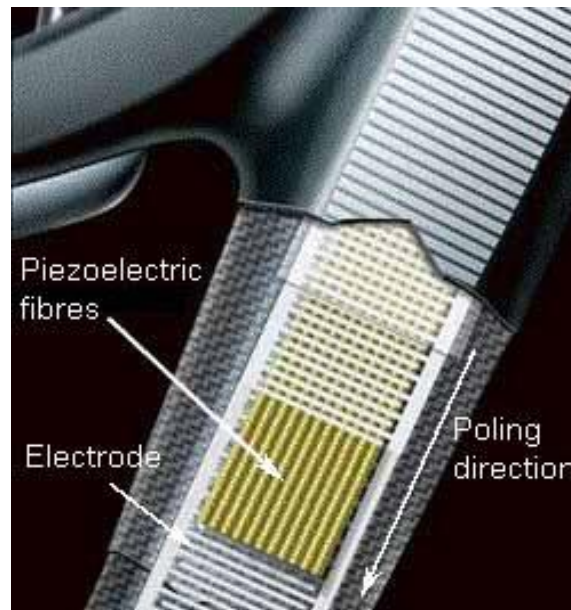


Figure 28 - Piezoelectric fibres installed in a tennis racket [14]

MUSIC INSTRUMENTS

The energy obtained by playing a music instrument can be harvested for later use. For example, the jingles of the tambourine shown in next figure are lined with piezoelectric elements, which generate voltage when impacted. This voltage is then harvested to turn on LED lights on the tambourine. The harder the tambourine is rattled, the greater the voltage generated by the piezoelectric elements and the brighter the light.



Figure 29 - Piezoelectric powered tambourine [15]

2.3.6. PIEZOELECTRIC ENERGY HARVESTERS PATENTS

There are many different patents for piezoelectric energy harvesters. Some examples are shown in this section.

US 4,467,236 – Piezoelectric acousto-electric generator

A piezoelectric generator for converting acoustic energy in a predetermined frequency range to electric energy including: a piezoelectric bending element; means for mounting the piezoelectric bending element in an acoustic energy path; tuning means mounted to the piezoelectric bending element to set the resonant frequency of oscillation of the piezoelectric bending element within the predetermined frequency range.

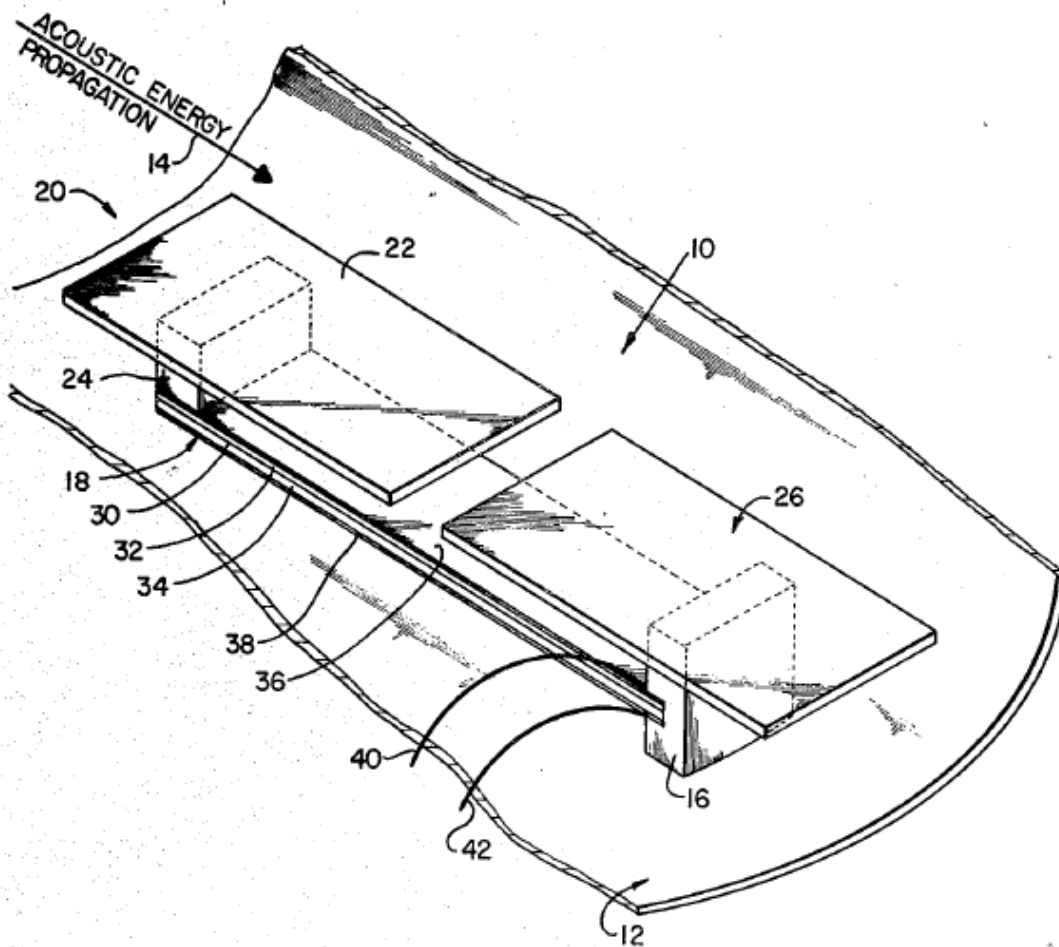


Figure 30 – US 4,467,236 patent [16]

US 6,407,484 – Piezoelectric energy harvester and method

A self-contained device for harvesting electrical energy from linear and rotary motion has a sensor with amplifiers for tensile stretching of a piezoelectric body with magnification of the applied force. The piezoelectric body is a monolithic plate with surface electrodes covering its top and bottom surfaces.

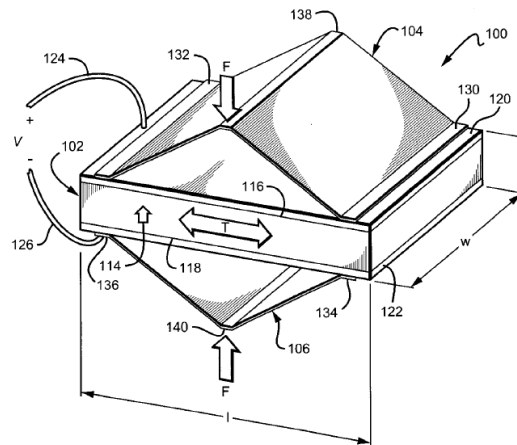


Figure 31 – US 6,407,484 patent [17]

US 6,858,970 – Multi-frequency piezoelectric energy harvester

A piezoelectric device connected to a vibration source converts vibration energy to electrical current. A plurality of pairs of oppositely polarized piezoelectric wafers deflect to produce an electrical current. Each pair of Wafers are arranged back-to-back and electrically joined together. The plurality of pairs of wafers are each connected to a set of micro-machined parts. Each pair of wafers form a birnorph, configured as a cantilevered beam attached to a set of parts to form an element. Each cantilevered beam has a mass weighted first end and is fixedly attached to one or more flexible sheaths on a second end. A plurality of elements form a cell unit. A plurality of cell units form an array. The electrical current produced varies by the number of elements per cell unit, and/or with the number of cell units per array.

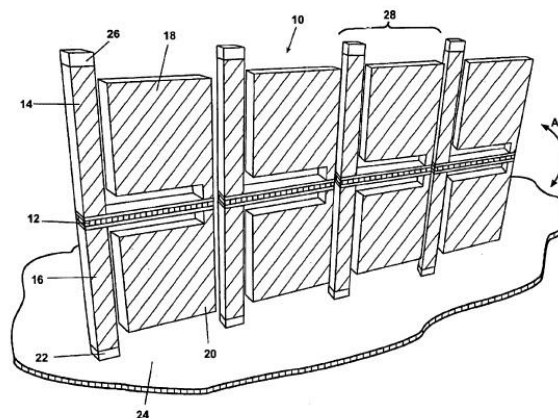


Figure 32 – US 6,858,970 patent [18]

US 7,439,657 – Broadband energy harvester apparatus and method

A broadband vibration energy harvesting apparatus and method. In one embodiment, a straight piezoelectric beam and a straight biasing beam are disposed parallel to one another and axially compressed by a support structure such that both of the beams are slightly bowed. This buckles and reduces the axial stiffness of both of the beams. The piezoelectric beam is secured to an external vibrating structure and supported by the structure. The flexing motion of the piezoelectric beam generates electrical signals that can be used to power a wide variety of devices. The apparatus is especially sensitive to small amplitude vibration signals and is able to harvest vibration energy over a wide range of frequencies, and is not limited to vibrations at discrete resonant frequencies. The apparatus is especially well suited for use in powering remotely located electrical sensors and actuators employed in automotive, aircraft and aerospace applications.

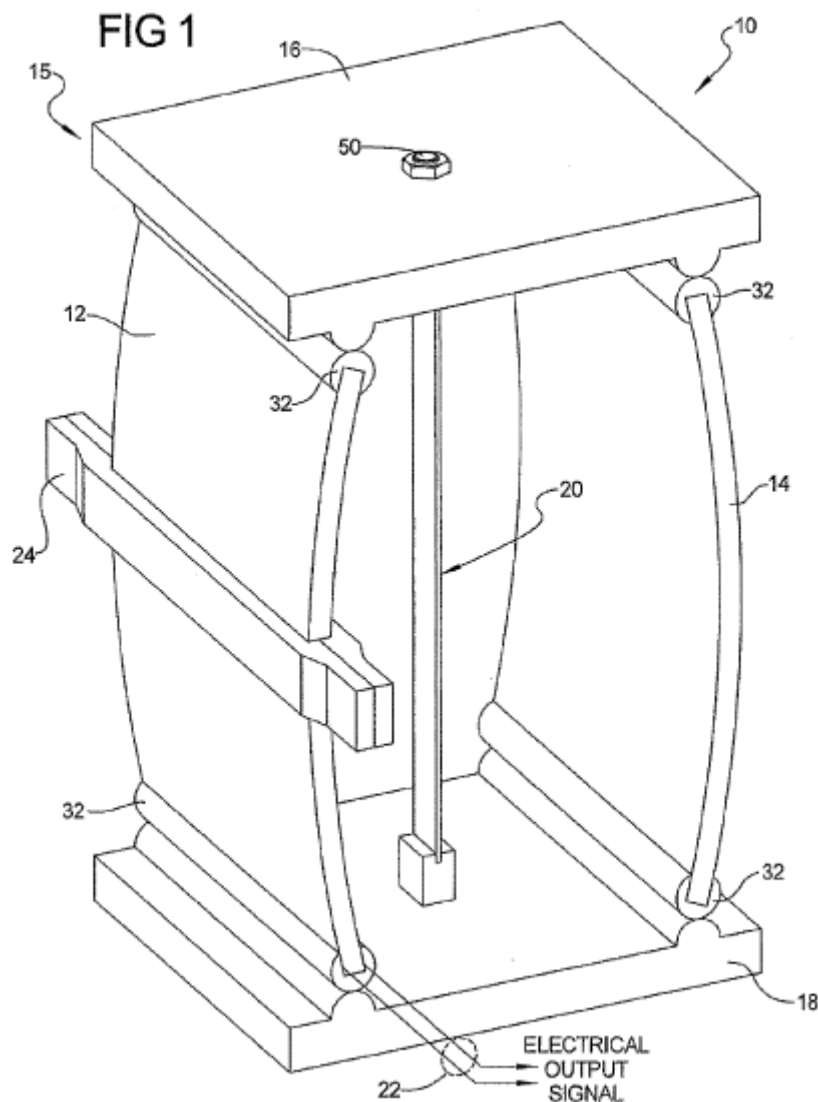


Figure 33 – US 7,439,657 patent [19]

US 7,446,459 – Hybrid piezoelectric energy harvesting transducer system

A hybrid piezoelectric energy harvesting transducer system includes: (a) first and second symmetric, pre-curved piezoelectric elements mounted separately on a frame so that their concave major surfaces are positioned opposite to each other; and (b) a linear piezoelectric element mounted separately on the frame and positioned between the pre-curved piezoelectric elements. The pre-curved piezoelectric elements and the linear piezoelectric element are spaced from one another and communicate with energy harvesting circuitry having contact points on the frame. The hybrid piezoelectric energy harvesting transducer system has a higher electromechanical energy than any known piezoelectric transducer.

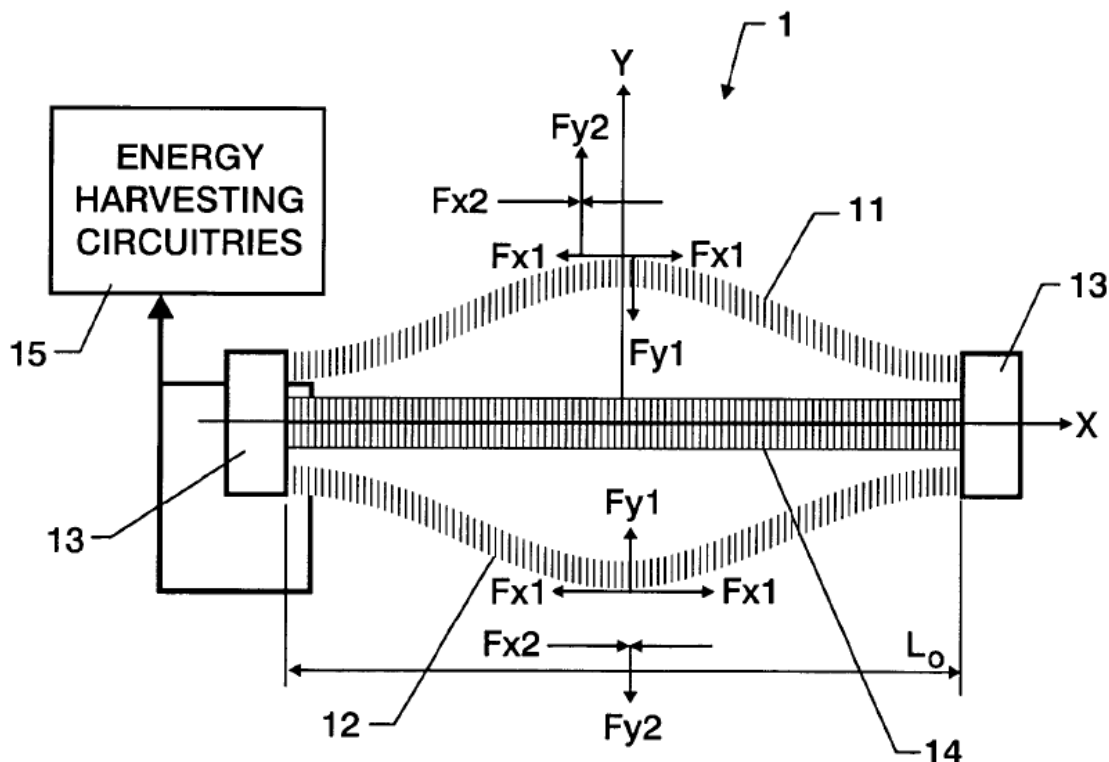


Figure 34 – US 7,446,459 patent [20]

US 7,649,305 – Piezoelectric energy harvester

A mechanism for capturing mechanical energy and converting it to electrical energy for use continually charging or providing emergency power to mobile, battery-powered devices comprises a plurality of elongated piezoelectric elements mounted at one or support points to one or more support structures. The plurality of piezoelectric elements are preferably structured and arranged so that at least each three dimensional coordinate axis has at least one element with a dominant mode of deflection in a plane normal to the axis, in order to permit harvesting energy from forces applied in any direction without regard to the orientation of the energy harvesting mechanism to the source of forces. This results in improved coupling of the transducer with the random movements

or vibrations that may not be confined to any particular plane or in a plane that is not necessarily aligned with the plane in which a piezoelectric element is designed to bend, thus improving the efficiency of energy capture.

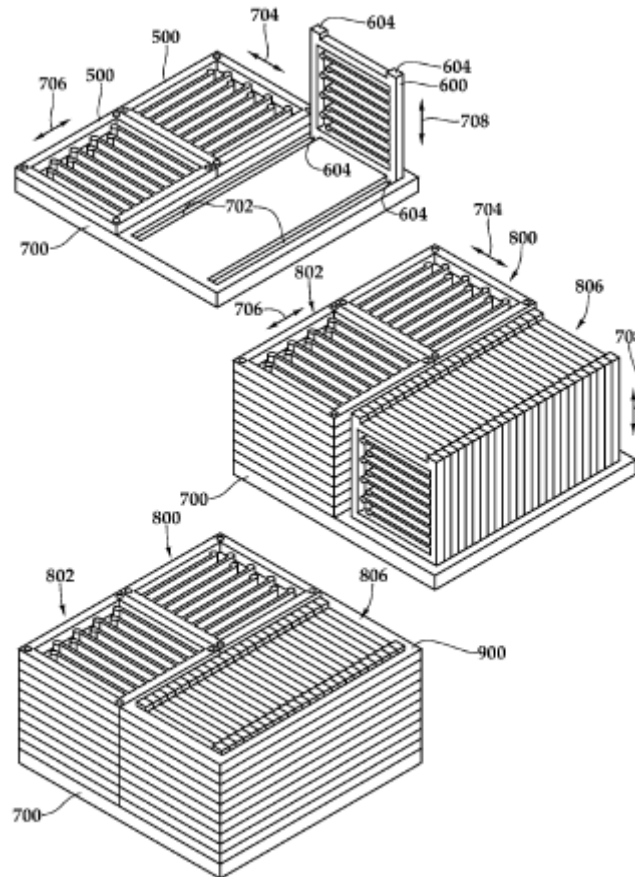


Figure 35 – US 7,649,305 patent [21]

US 7,812,508 – Power harvesting from railway: apparatus, system and method

The present invention relates to an apparatus system and method for power harvesting from a railroad using piezoelectric generator. The invention is to provide a system and method for power harvesting comprising a plurality of piezoelectric devices embedded in a railroad sleeper or attached to railroad rails and configured to produce electrical power when a train traverses their locations. The system includes a power conditioning unit and electrical conductors connecting said piezoelectric to said power conditioning unit. Harvested energy may be used locally in proximity to the energy generation location, stored for later use or transferred to be used in remote location.

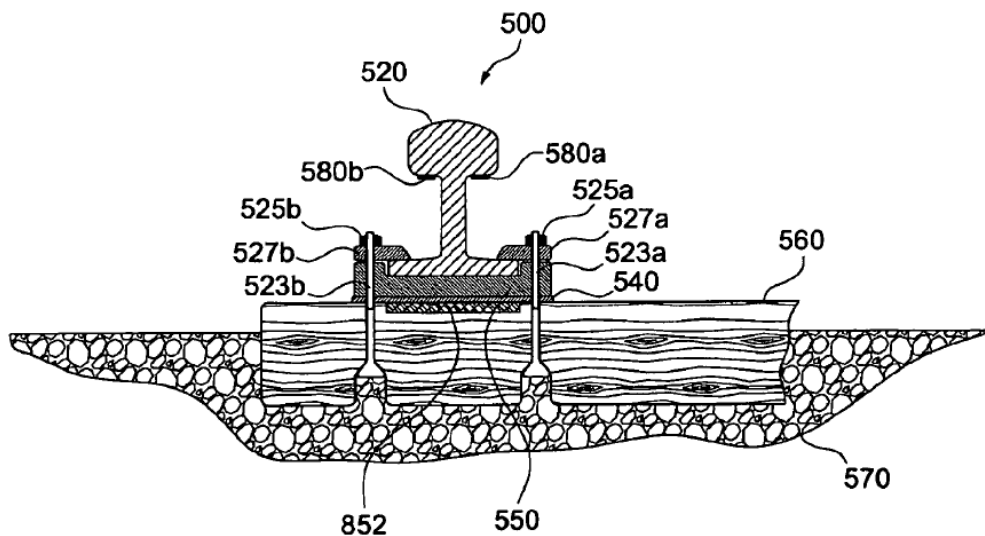


Figure 36 – US 7,812,508 patent [22]

US 7,839,058 – Wideband vibration energy harvester

In one embodiment a device comprises a composite structure that includes a piezoelectric flexure and a length-constraining element. The length-constraining element provides the piezoelectric flexure with a bowed shape. The piezoelectric flexure has a first stable bowed position and a second stable bowed position. The length-constraining element is one from the group consisting of a planar sheet and a columnar rod. In another embodiment a device comprises a piezoelectric flexure having a bowl shape. The piezoelectric flexure has a first stable bowl-shaped position and a second stable bowl-shaped position.

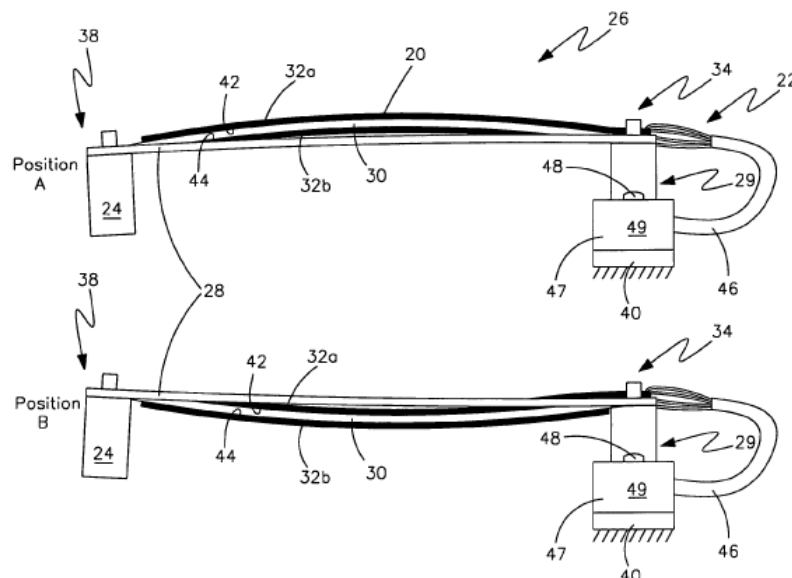


Figure 37 – US 7,839,058 patent [23]

US 2014/0285067 – Piezoelectric energy harvesting device or actuator

This invention concerns a piezoelectric energy harvesting device or actuator comprising a piezoelectric material (12) on a substrate (14). The piezoelectric material is divided into a plurality of discrete regions to provide a plurality of piezoelectric elements (16) on the substrate which are electrically insulated from each other. The elements are preferably disposed along the length of a cantilevered beam. The piezoelectric layer may be divided or further divided with an insulating gap extending in the longitudinal direction of the beam for energy harvesting in torsional mode(s) of beam vibration as well as bending modes.

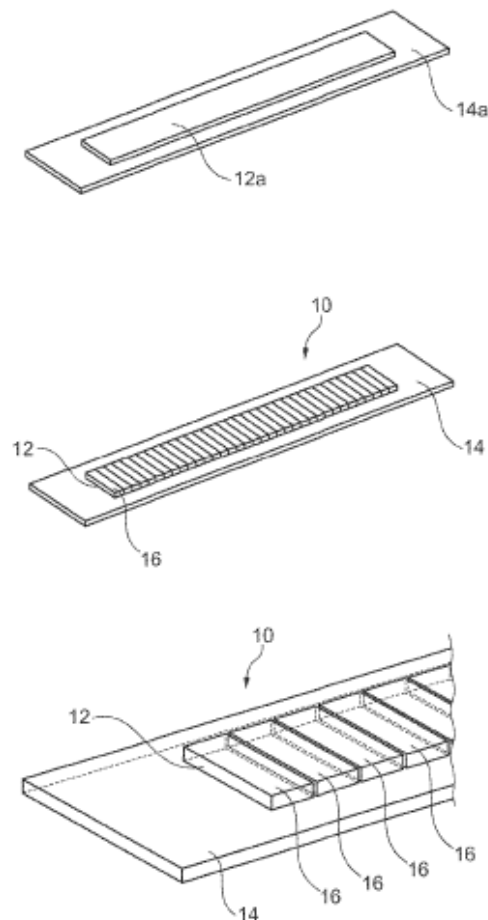


Figure 38 – US 2014/0285067 patent [24]

US 2014/0159542 – Piezoelectric energy harvesting device and method of fabricating the same

A flexible piezoelectric energy harvesting device includes a first flexible electrode substrate, a piezoelectric layer disposed on the first flexible electrode substrate, and a second flexible electrode substrate disposed on the piezoelectric layer. The piezoelectric layer may include a plurality of first piezoelectric lines spaced apart from each other in one direction and a plurality of second piezoelectric lines respectively filling spaces between the first piezoelectric lines.

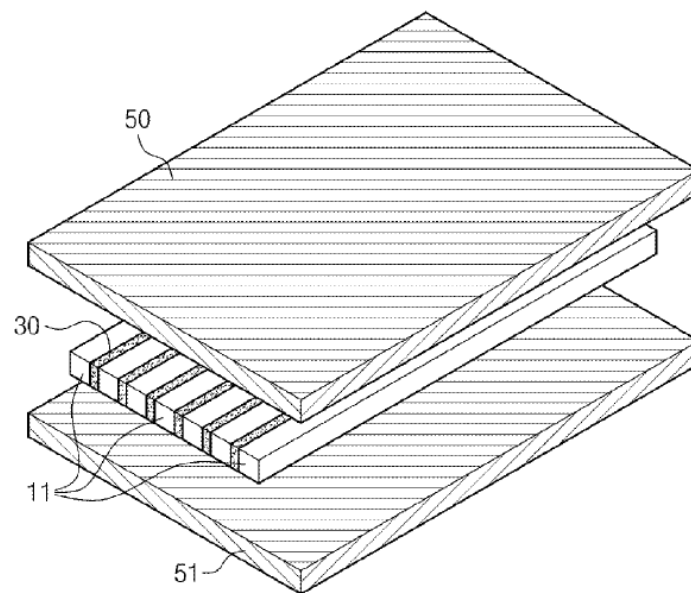


Figure 39 – US 2014/0159542 patent [25]

US 2013/0313946 – Piezoelectric energy harvesting array and method of manufacturing the same

The inventive concept discloses a piezoelectric energy harvesting array and a method of manufacturing the same. The manufacturing method may include forming a plurality of piezoelectric energy harvesting devices; connecting masses to one side of the piezoelectric energy harvesting devices and connecting the other side of the piezoelectric energy harvesting devices facing the masses to a base; and individually tuning a resonant frequency of each of the piezoelectric energy harvesting devices to prevent mismatch of resonant frequency when the masses vibrate.

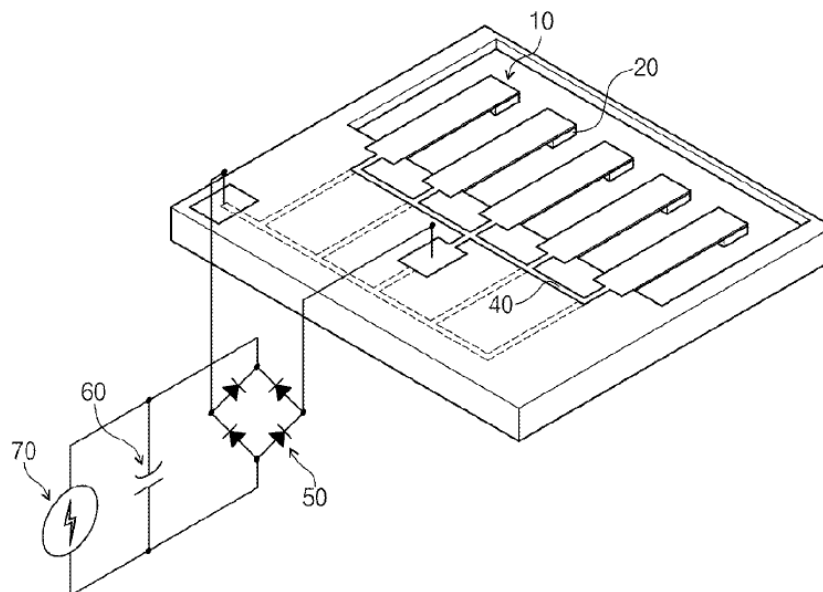


Figure 40 – US 2013/0313946 patent [26]

US 2012/0049694 – Micromachined piezoelectric energy harvester with polymer beam

A micromachined piezoelectric energy harvester and methods of fabricating a micromachined piezoelectric energy harvester are disclosed. In one embodiment, the micromachined piezoelectric energy harvester comprises a resonating beam formed of a polymer material, at least one piezoelectric transducer embedded in the resonating beam, and at least one mass formed on the resonating beam. The resonating beam is configured to generate mechanical stress in the at least one piezoelectric transducer, and the at least one piezoelectric transducer is configured to generate electrical energy in response to the mechanical stress.

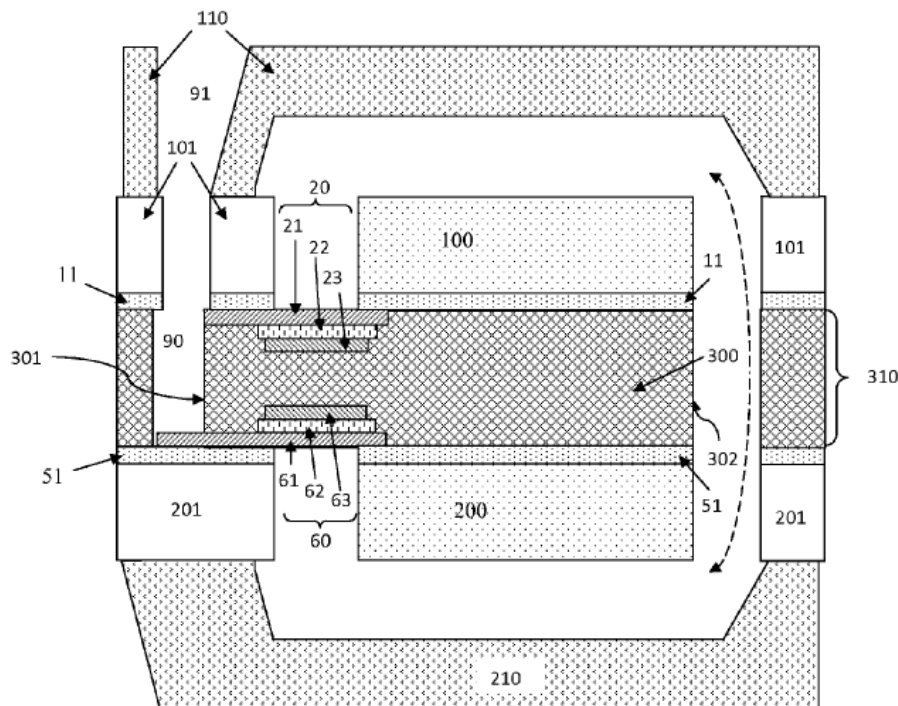


Figure 41 – US 2012/0049694 patent [27]

US 2010/0317978 – Implantable medical device housing modified for piezoelectric energy harvesting

Methods, systems, and apparatus for powering and/or recharging medical devices implanted within the body are described. An illustrative implantable sensor for sensing one or more physiologic parameters within a body lumen includes a housing having an exterior wall that has an inner surface and an outer surface and that defines an internal cavity. A portion of the housing includes an electrically conductive material that functions as a first electrical conductor. A flexible piezoelectric layer is disposed adjacent to a portion of the exterior wall and a second electrical conductor is disposed adjacent to the piezoelectric layer. The piezoelectric layer is configured to displace in

response to periodic pressure pulses within the body lumen and generate a voltage differential between the first and second electrical conductors.

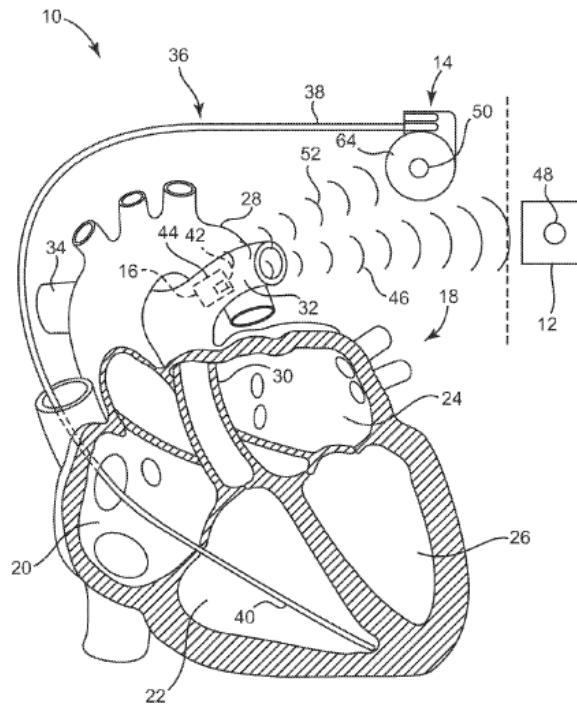


Figure 42 – US 2010/0317978 patent [28]

US 2007/0125176 – Energy harvesting device and methods

An energy harvesting device and related methods, with one embodiment comprising a micro-electromechanical structure fabricated as a plurality of members respectively resonant at different frequencies so that the structure can respond to a number of different vibration frequencies. Piezoelectric material converts the vibrations into an electric voltage difference across at least a portion of the structure.

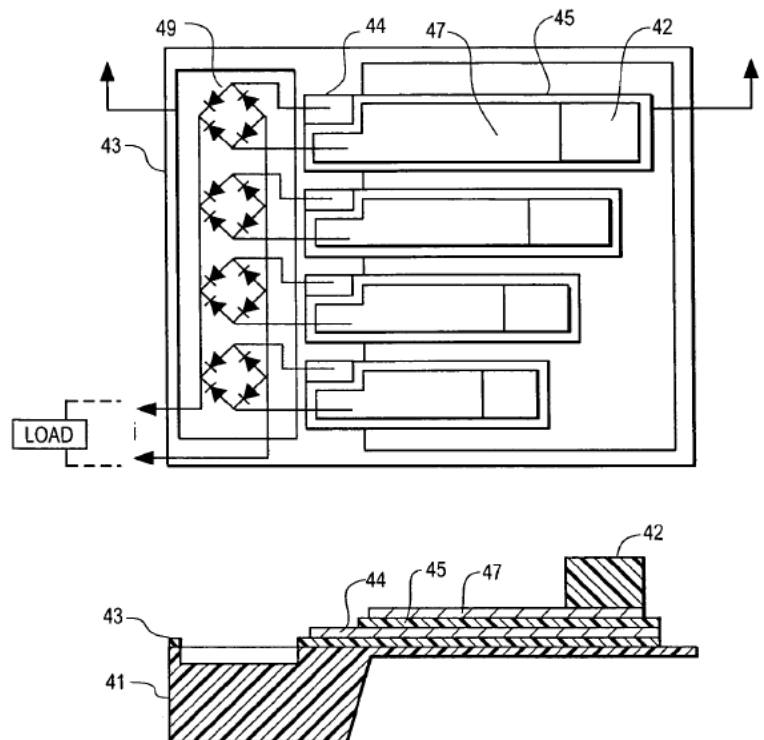


Figure 43 – US 2007/0125176 patent [29]

US 2006/0021261 – Footwear incorporating piezoelectric energy harvesting system

An article of footwear having a piezoelectric energy harvesting apparatus in the sole member. Walking or running applies a first force deforming a piezoelectric actuator, thereby generating electrical energy. An energy storage circuit stores electrical energy generated by the piezoelectric actuator for later application to electrical devices.

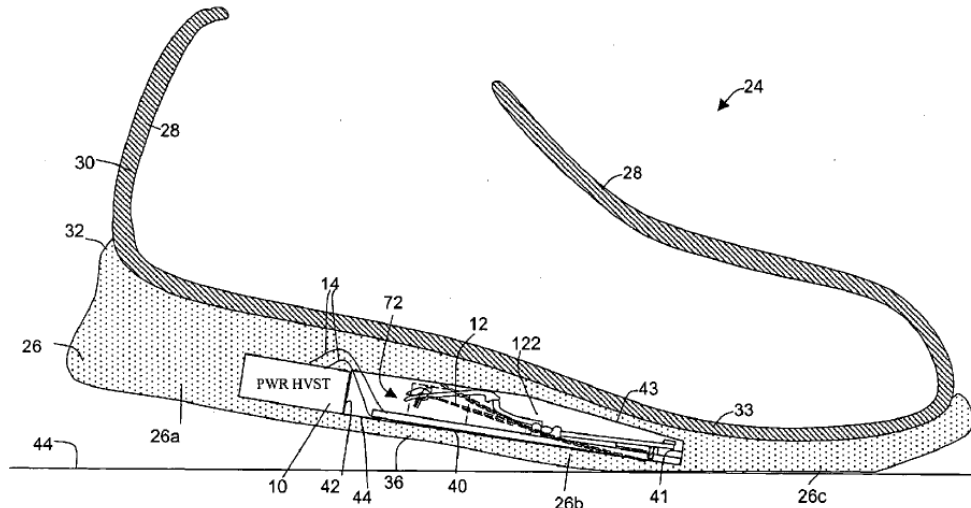
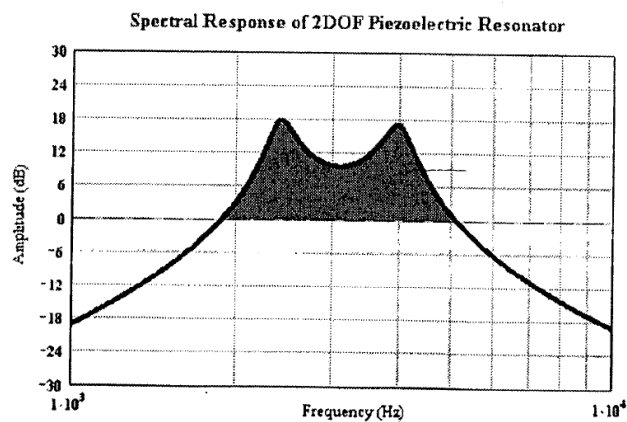
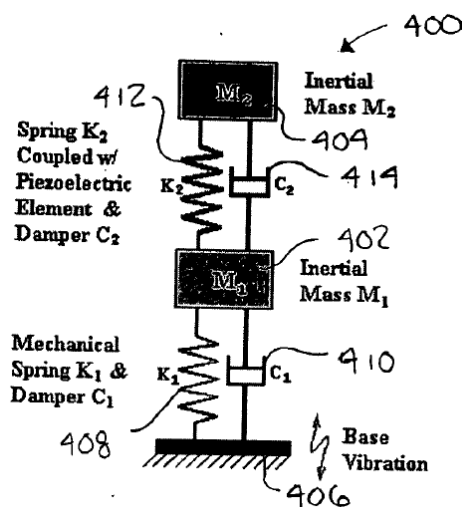


Figure 44 – US 2006/002161 patent [30]

US 2005/0134149 – Piezoelectric vibration energy harvesting device

A piezoelectric vibration energy harvesting device which is made up of a first mass, a second, a first spring coupled to the first mass, and a second spring coupled to the second mass. A piezoelectric element is bonded between the first mass and the second spring, so that a stress applied to the second spring is applied to the piezoelectric element.



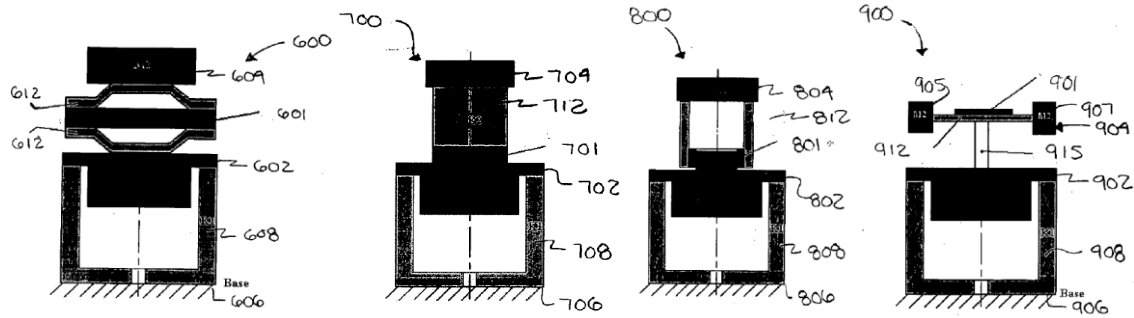


Figure 45 – US 2005/0134149 patent [31]

US 8,723,398 – Piezoelectric energy harvesting apparatus

Disclosed is a piezoelectric energy harvesting apparatus. The piezoelectric energy harvesting apparatus includes: a piezoelectric energy harvesting array that includes a plurality of piezoelectric energy harvesting devices converting an external vibration into electric energy; a plurality of switches that is connected in series to the piezoelectric energy harvesting devices, respectively, and fits the resonance frequency of the piezoelectric energy harvesting array to the frequency of the external vibration by adjusting the resonance frequencies of the piezoelectric energy harvesting devices through the operation of the switches; and at least one or more rectifiers that convert alternating voltage outputted from the piezoelectric energy harvesting array into direct voltage.

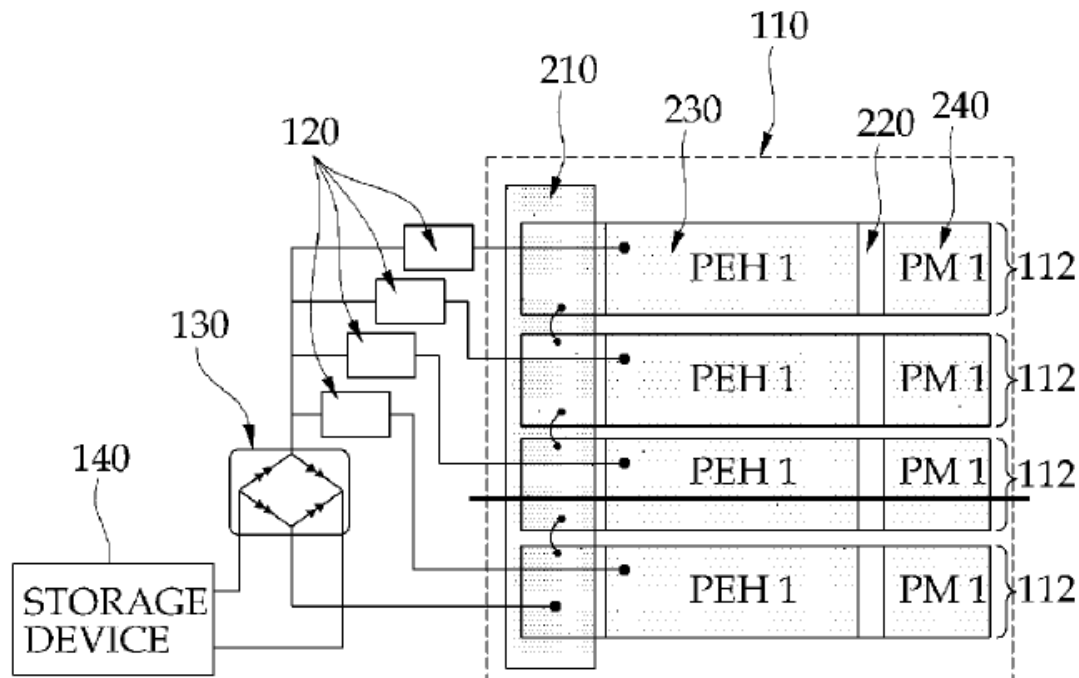


Figure 46 – US 8,723,398 patent [32]

US 8,581,475 – Generating device using piezoelectric energy harvester

Provided is a power generating apparatus using piezoelectric elements, which can increase an amount of electricity generated in the piezoelectric elements and can extend the life of the piezoelectric elements. The power generating apparatus includes: a plurality of piezoelectric elements; a main body in which the piezoelectric elements are received and fixed, with spaced apart from one another, so as to protect the piezoelectric elements; a piezoelectric element support reciprocatingly installed in the main body to support the piezoelectric elements such that the piezoelectric elements are deformed by a reciprocating motion of the piezoelectric element support; a driving unit provided in the main body to operate the piezoelectric element support; and a power transmission unit connecting the driving unit to the piezoelectric element support, such that the piezoelectric element support is reciprocated by a driving force of the driving unit.

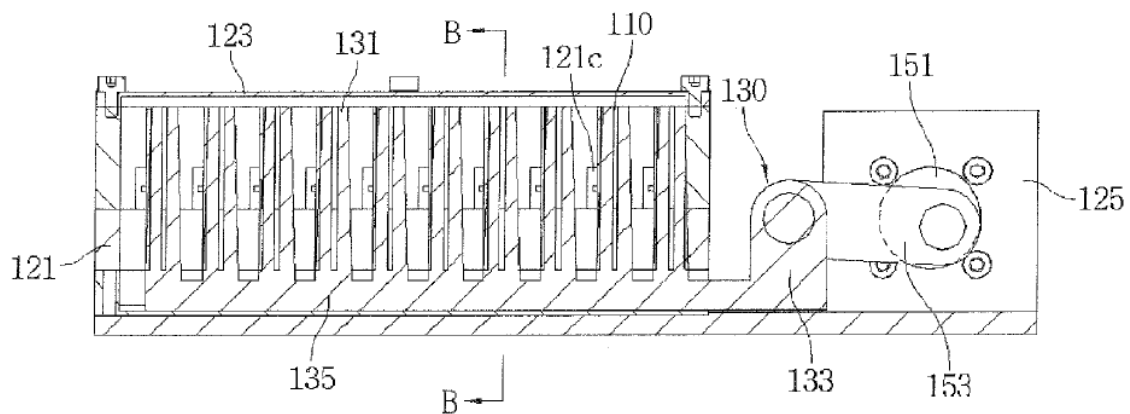


Figure 47 – US 8,581,475 patent [33]

3. DEVICE FOR THE VIBRATION ENERGY HARVESTING

3.1. CONSTRUCTION



Figure 48 - Piezoelectric device (V21BL)

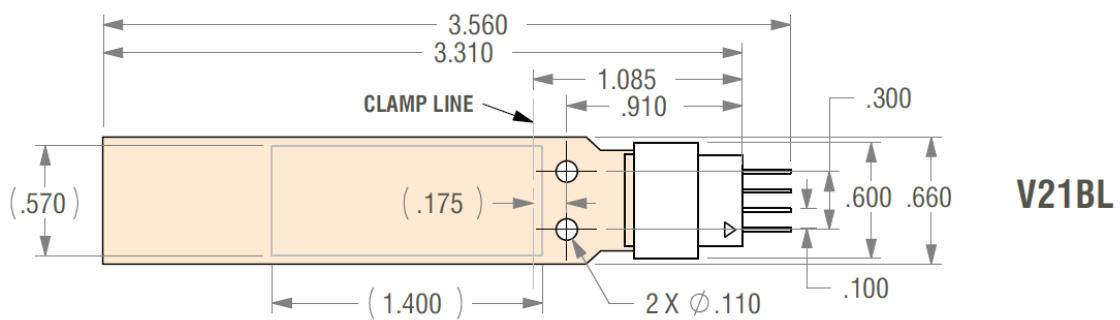


Figure 49 - Construction of the piezoelectric device (V21BL)

3.2. INPUT DATA

- 1) Vibration load

$$a_1 = 7.8 \frac{m}{s^2}$$

$$a_2 = 6 \frac{m}{s^2}$$

- 2) Working resonance frequency

$$f_n = 81.45 \text{ Hz}$$

4. EXPERIMENTAL STUDY

4.1. MEASURING SISTEM

4.1.1. EQUIPMENT USED

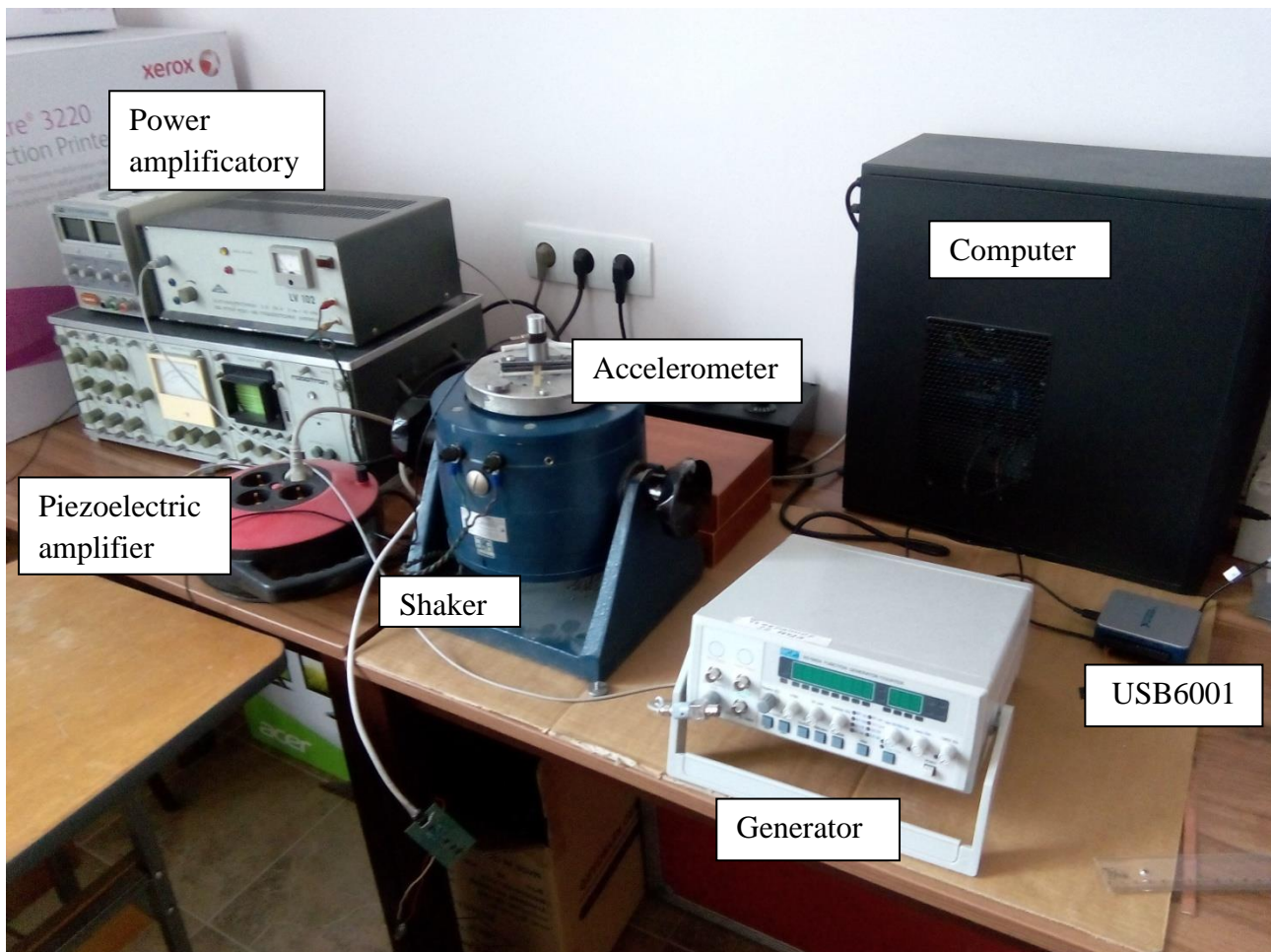
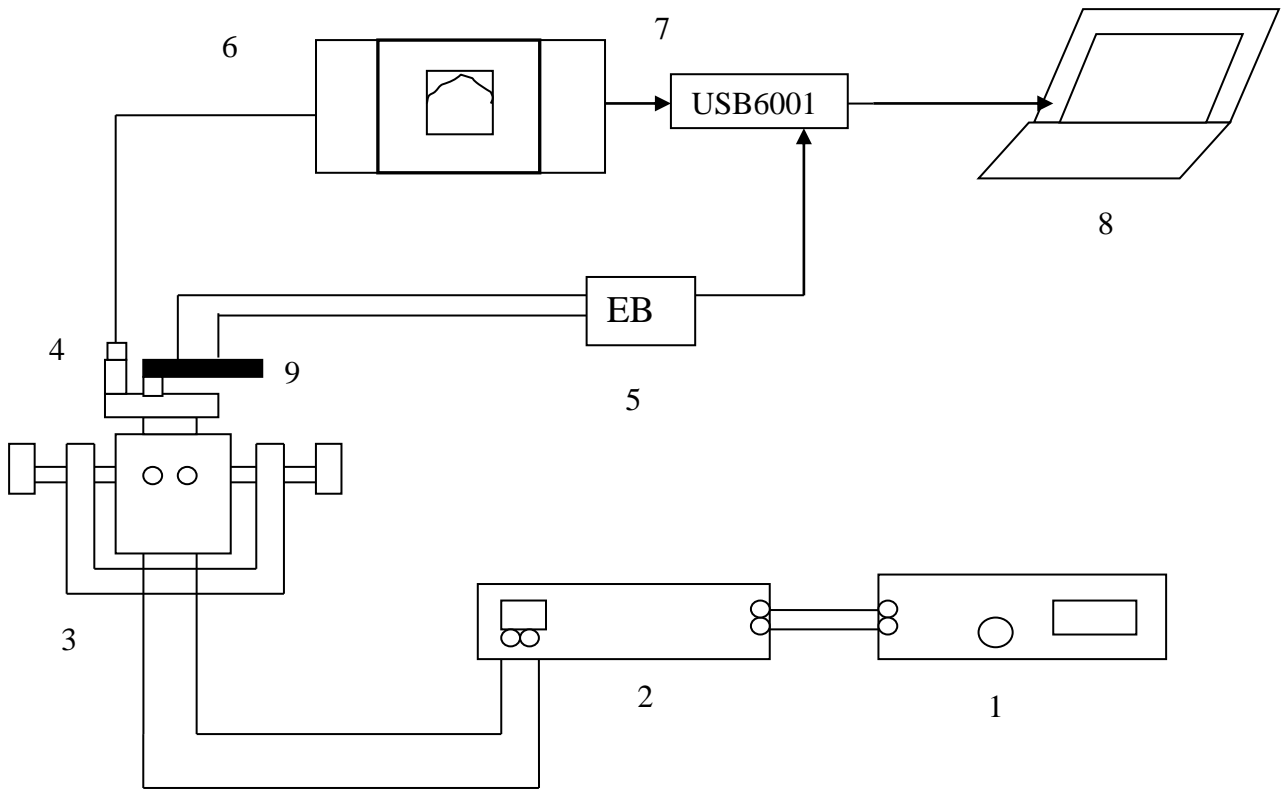


Figure 50 - Experimental setup used for the frequency response measurements of a uniform bimorph cantilever

4.1.2. SCHEME OF MEASUREMENT SYSTEM



The components are:

1. Signal Generator - SG 1642A MCP
2. Power amplification LV 102
3. Shaker ELN 138
4. IEPE accelerometer KD35
5. Rectifier (Model DB104) with additional components (EB)
6. Piezoelectric amplifier
7. Data acquisition system (Converter of the signal from analogical to digital) - USB 6001
8. Computer: System Design Software LabView – Cont Acq&Graph Voltage-Int Clk.vi
9. Piezoelectric cantilever device – V21BL.

4.1.3. PROGRAM MEASUREMENT AND VISUALIZATION

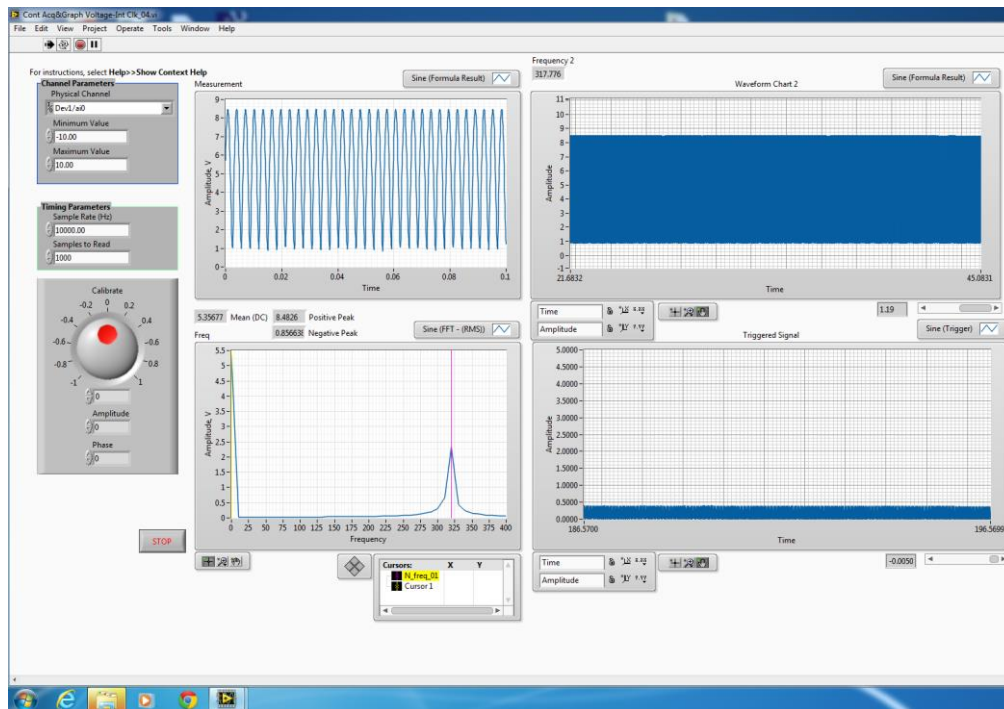


Figure 51 - Visualization of LabView using resistor

The scheme above shows the experimental setup that will excite the piezoelectric.

The vibration signal is generated from the signal generator, amplified via the power amplifier and finally utilized to control the vibration amplitude and frequency of the shaker. The piezoelectric cantilever device undergoes excitations and generates output voltage signal. Acceleration signals are measured by the accelerometer and amplified. This signal is converted from analogical into digital by the converter and finally it is shown in the computer.

A variable resistor or different discrete resistors are attached to the harvester output. This allows having different electrical loading conditions and makes possible to determine the output electrical energy with easy. Measuring the voltage over this resistor the power output can be obtained. The excitation signal frequency is matched to the resonant frequency of the beam in order to maximize the power output.

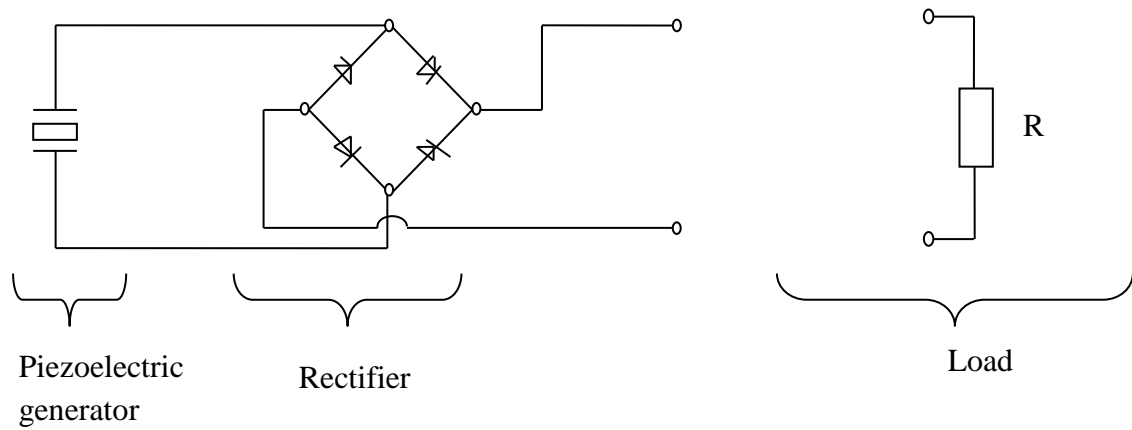


Figure 52 - Scheme of the construction

The resonant frequency of the system is obtained by exciting the system with a constant acceleration and looking for the frequency at which the maximum acceleration amplitude occurs. The resonant frequency of the harvester is determined by varying the excitation frequency and by measuring the power output while keeping the mechanical power input constant.

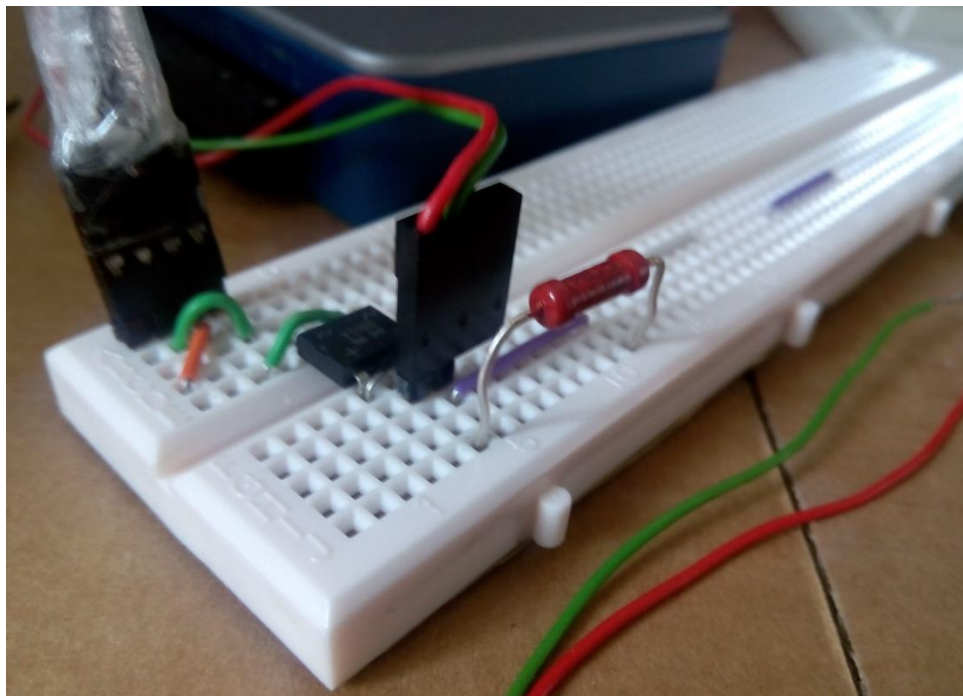


Figure 53 - Circuit with resistor

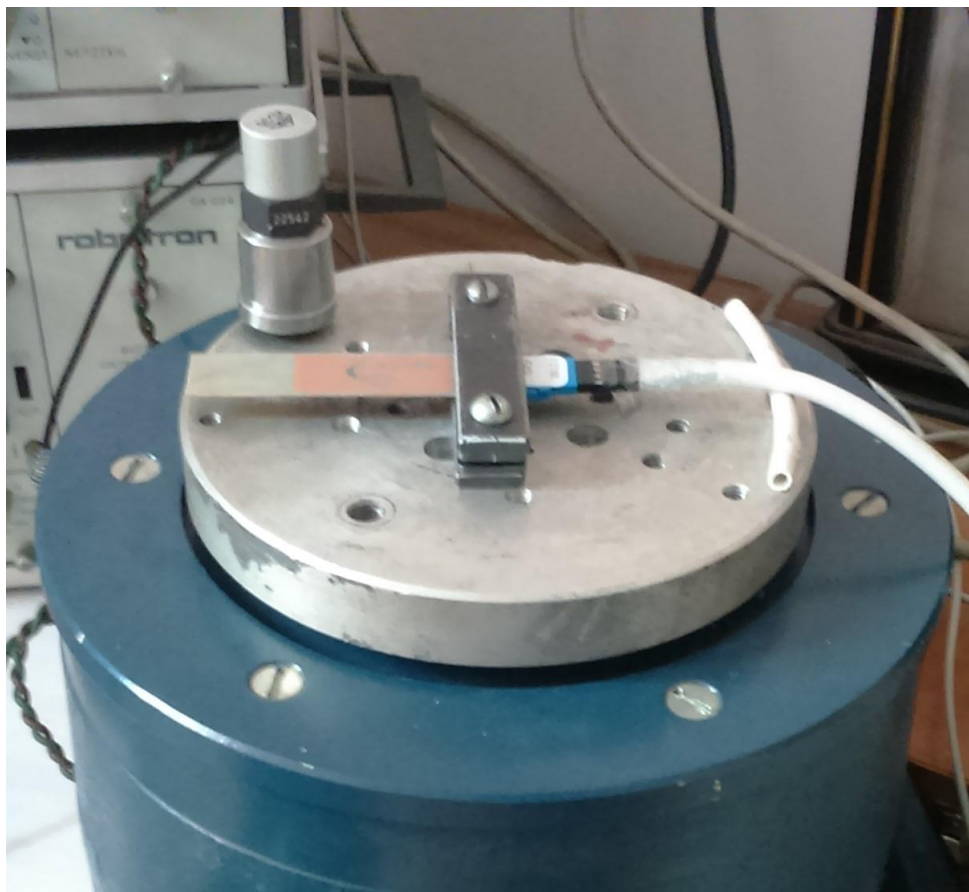


Figure 54 - Shaker, accelerometer and piezoelectric device

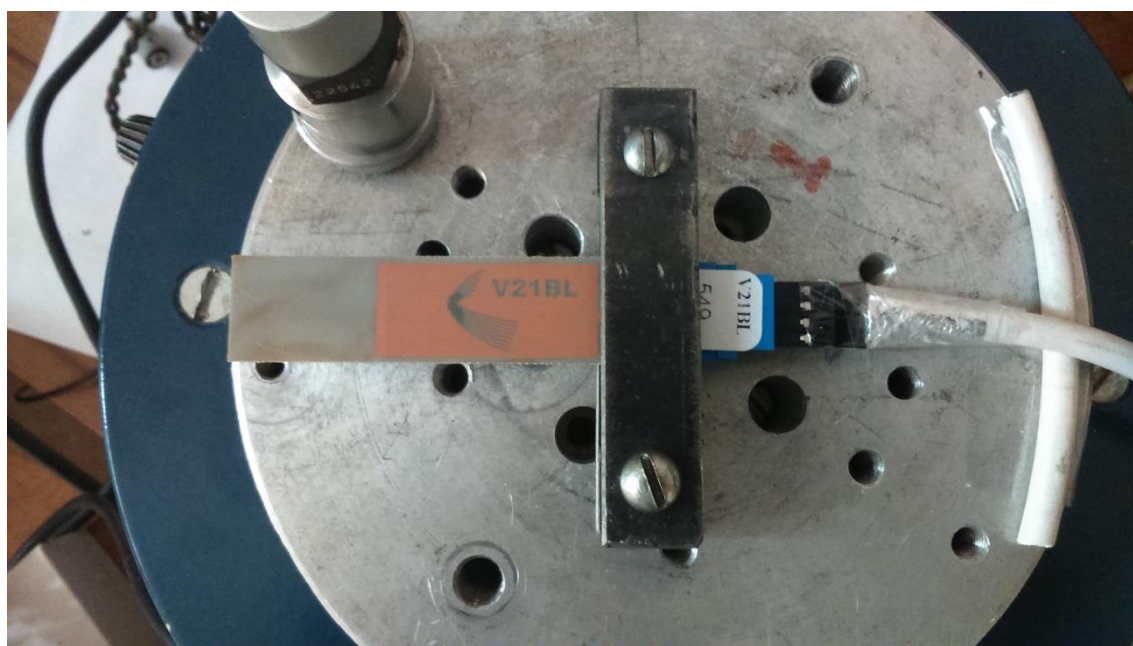


Figure 55 - Detail picture of the piezoelectric device

4.2. METHODS OF MEASUREMENT

The power generated by the piezoelectric device can be determined by the following expression:

$$P_{i,max} = \frac{U_i^2}{R_i} [mW]$$

$i = 1 \div 2$ – Measurements at various accelerations

U_i – Maximum value of the measured output voltage [V]

R_i – Resistance load [kΩ]

$P_{i,max}$ – Maximum value of the measured power output [mW]

The average power per cubic centimetre is calculated by the equation:

$$P_{i,avg,V} = \frac{P_{i,max}}{V} \left[\frac{mW}{cm^3} \right]$$

$V = 2.415 \cdot 10^{-4} \text{ cm}^3$ – Volume of the piezomaterial

The average power per square centimetre is determined using this expression:

$$P_{i,avg,S} = \frac{P_{i,max}}{S} \left[\frac{mW}{cm^2} \right]$$

$S = 0.105 \text{ cm}^2$ – Surface of the piezomaterial

Finally, the electric current is obtained by the equation:

$$I_i = \frac{U_i}{R_i} [mA]$$

I_i – Maximum value of the measured electric current output [mA]

4.3. EXPERIMENTAL RESULTS

$f_n=81.45 \text{ Hz}, a_1=7.8 \text{ m/s}^2$						
Nº	$R_1 \text{ [k}\Omega\text{]}$	$U_{1,\max} \text{ [V]}$	$P_1 \text{ [mW]}$	$P_1 \text{ [mW/cm}^3\text{]}$	$P_1 \text{ [mW/cm}^2\text{]}$	$I_1 \text{ [mA]}$
1	2	1,41	0,994	4116,149	9,467	0,705
2	10	3,86	1,490	6169,607	14,190	0,386
3	20	5,8	1,682	6964,803	16,019	0,290
4	43	7,89	1,448	5994,713	13,788	0,183
5	68	8,64	1,098	4545,707	10,455	0,127
6	150	9,58	0,612	2533,510	5,827	0,064
7	330	9,88	0,296	1224,850	2,817	0,030

Table 4 - Experimental results for $a=7.8 \text{ m/s}^2$

$f_n=81.45 \text{ Hz}, a_2=6 \text{ m/s}^2$						
Nº	$R_2 \text{ [k}\Omega\text{]}$	$U_{2,\max} \text{ [V]}$	$P_2 \text{ [mW]}$	$P_2 \text{ [mW/cm}^3\text{]}$	$P_2 \text{ [mW/cm}^2\text{]}$	$I_2 \text{ [mA]}$
1	2	1,14	0,650	2690,683	6,189	0,570
2	10	3,47	1,204	4985,880	11,468	0,347
3	20	5,2	1,352	5598,344	12,876	0,260
4	43	6,96	1,127	4664,798	10,729	0,162
5	68	7,67	0,865	3582,322	8,239	0,113
6	150	8,5	0,482	1994,479	4,587	0,057
7	800	9,2	0,106	438,095	1,008	0,012

Table 5 - Experimental results for $a=6 \text{ m/s}^2$

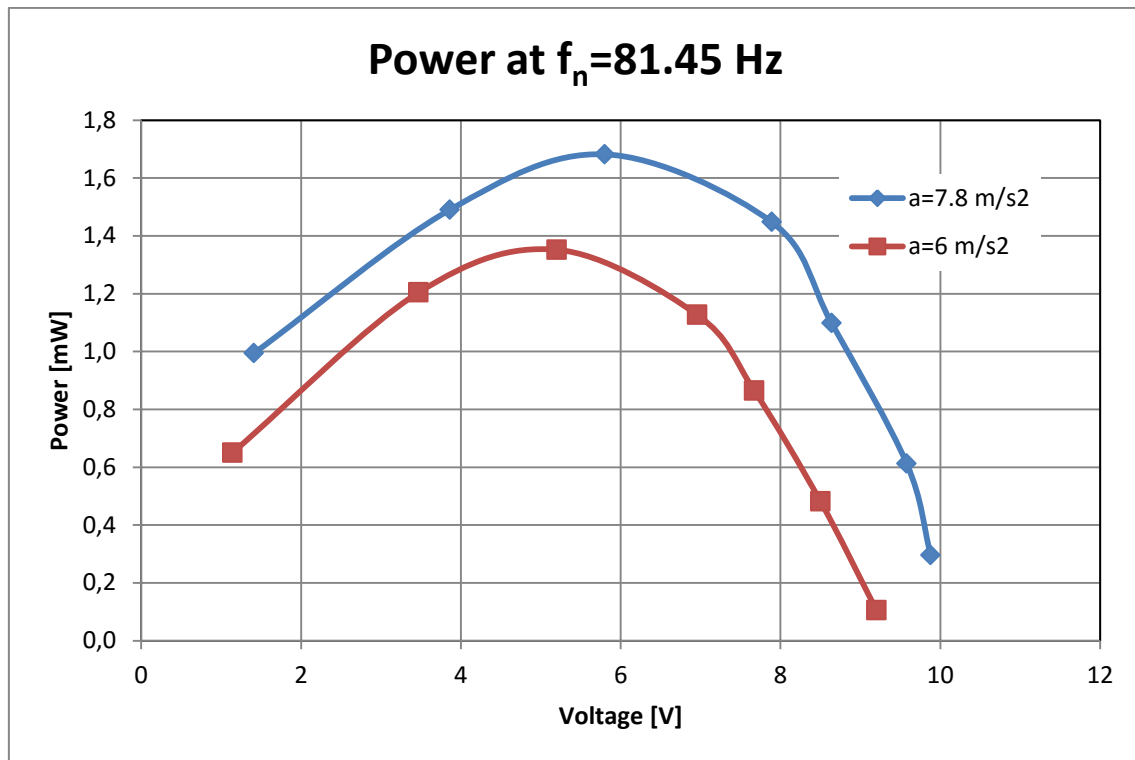


Figure 56 – Variation of the output power according to the output voltage for different accelerations of forced oscillation cantilever beam

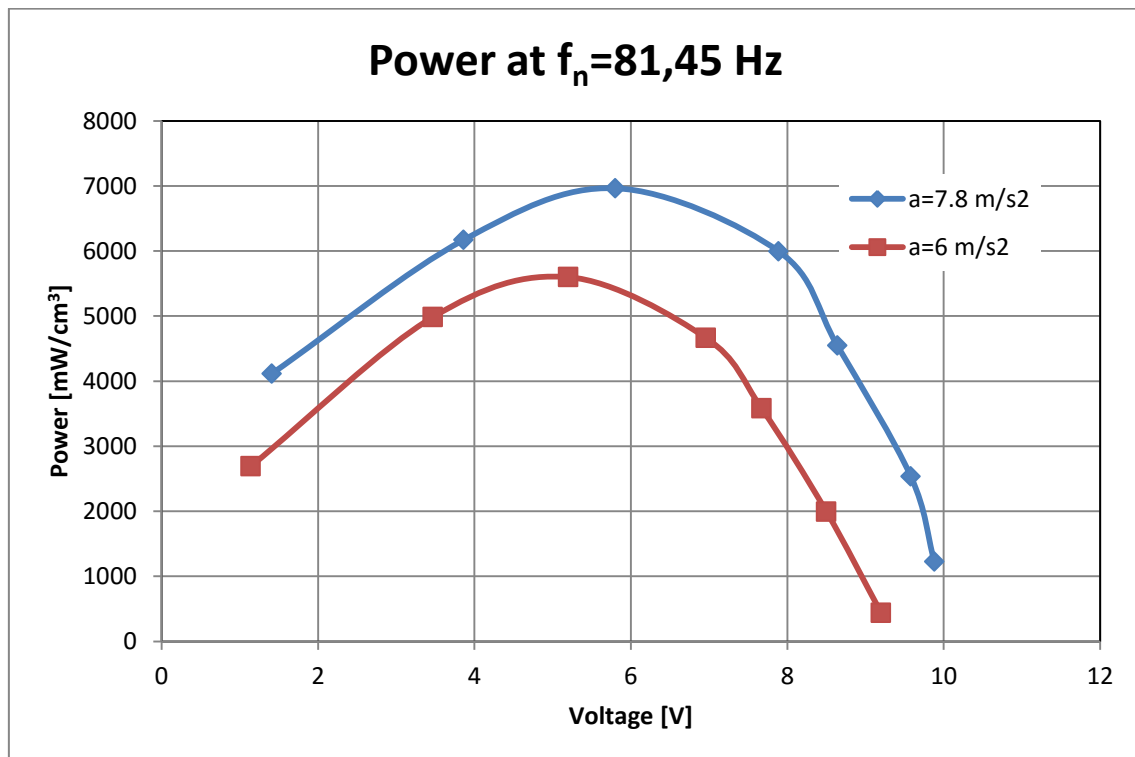


Figure 57 – Variation of the output power according to the output voltage for different accelerations of forced oscillation cantilever beam

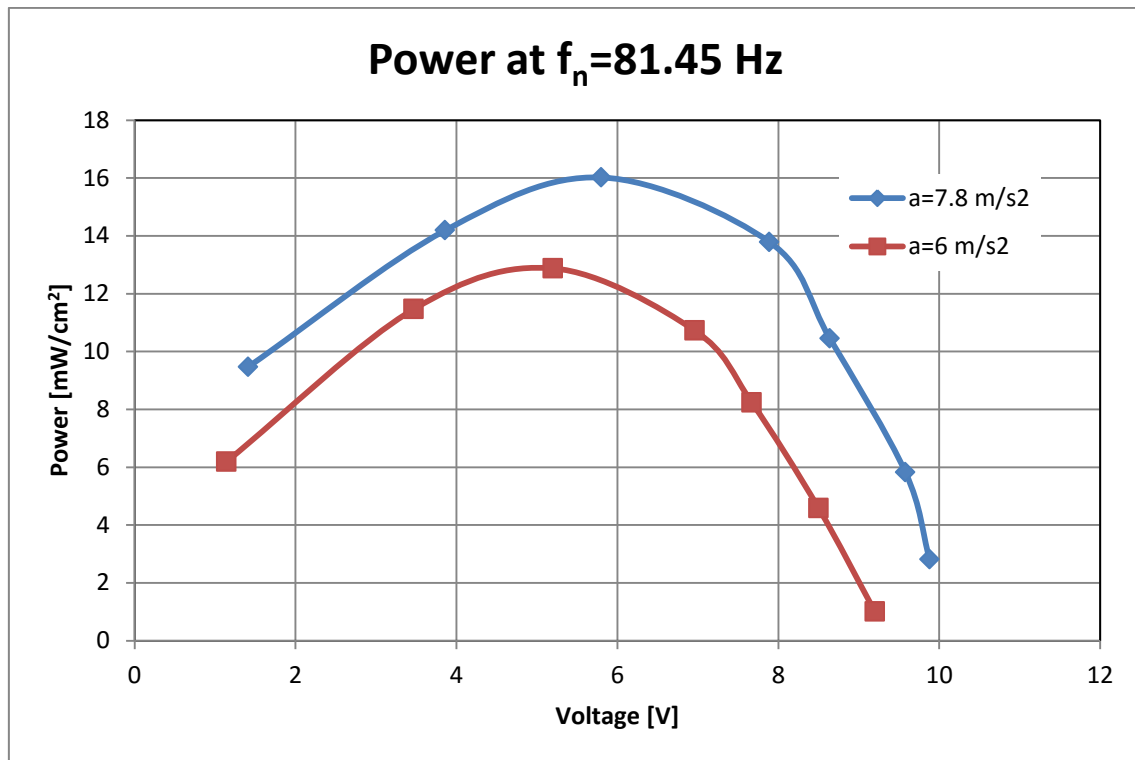


Figure 58 – Variation of the output power according to the output voltage for different accelerations of forced oscillation cantilever beam

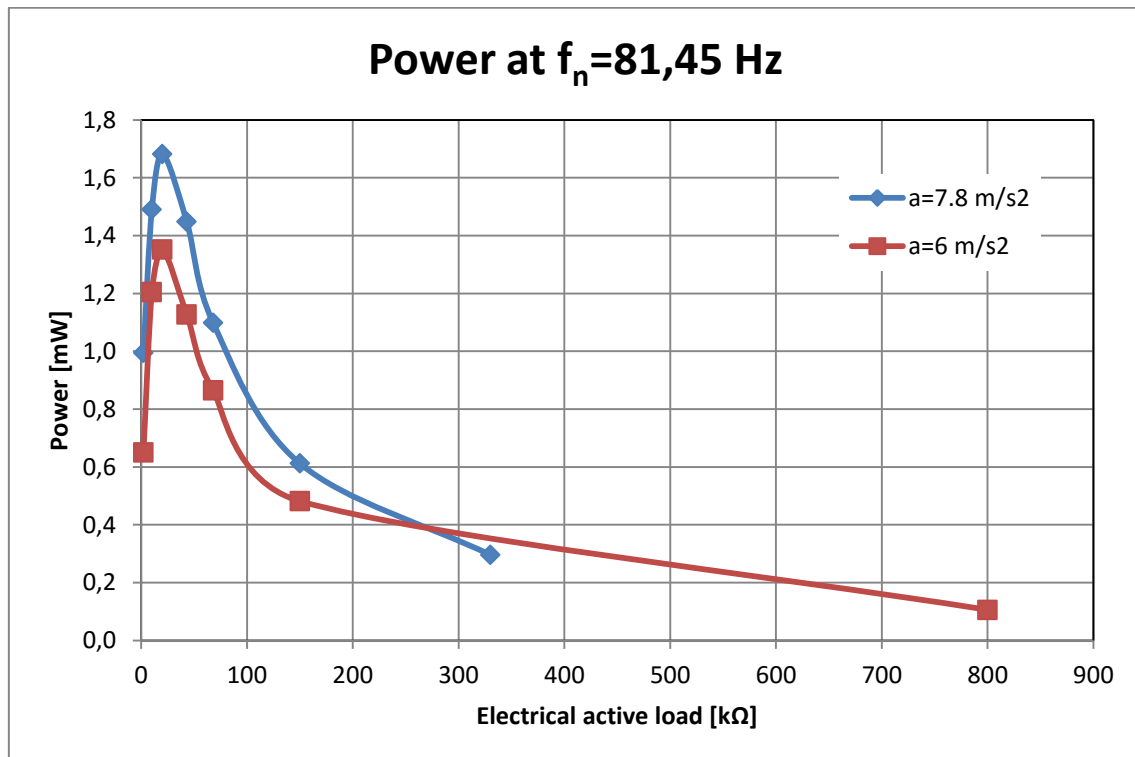


Figure 59– Variation of the output power according to the electrical active load for different accelerations of forced oscillation cantilever beam

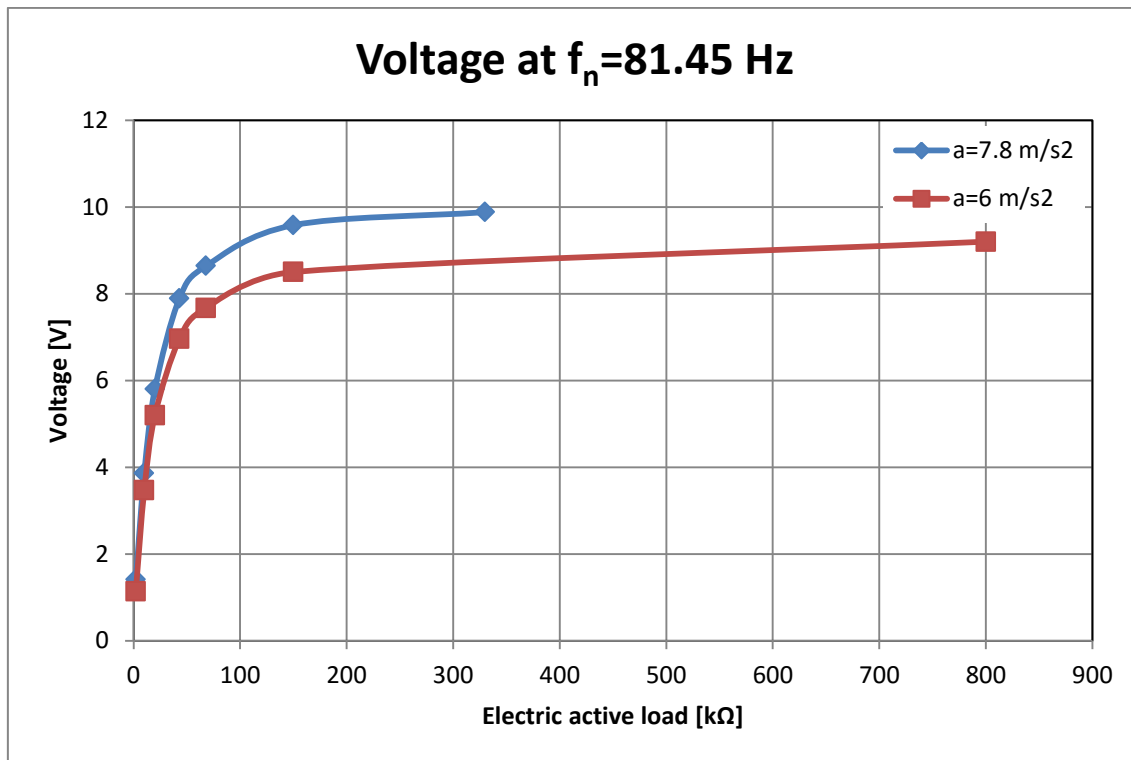


Figure 60– Variation of the output voltage according to the electrical active load for different accelerations of forced oscillation cantilever beam

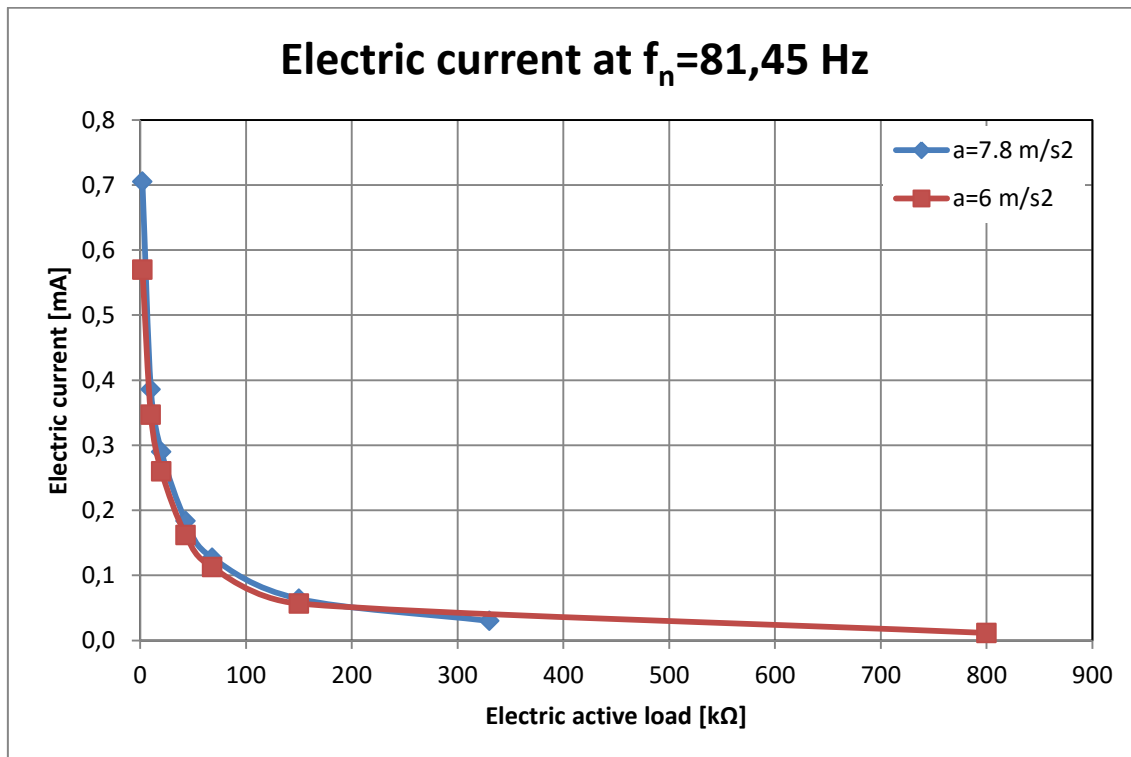


Figure 61– Variation of the output electric current according to the electrical active load for different accelerations of forced oscillation cantilever beam

5. MODELLING THE STRUCTURE IN ANSYS

5.1. DIAGRAM OF MODELING AND SIMULATION

This shows the basic block diagram of the steps that are followed to make the simulation in ANSYS. It is divided into these blocks:

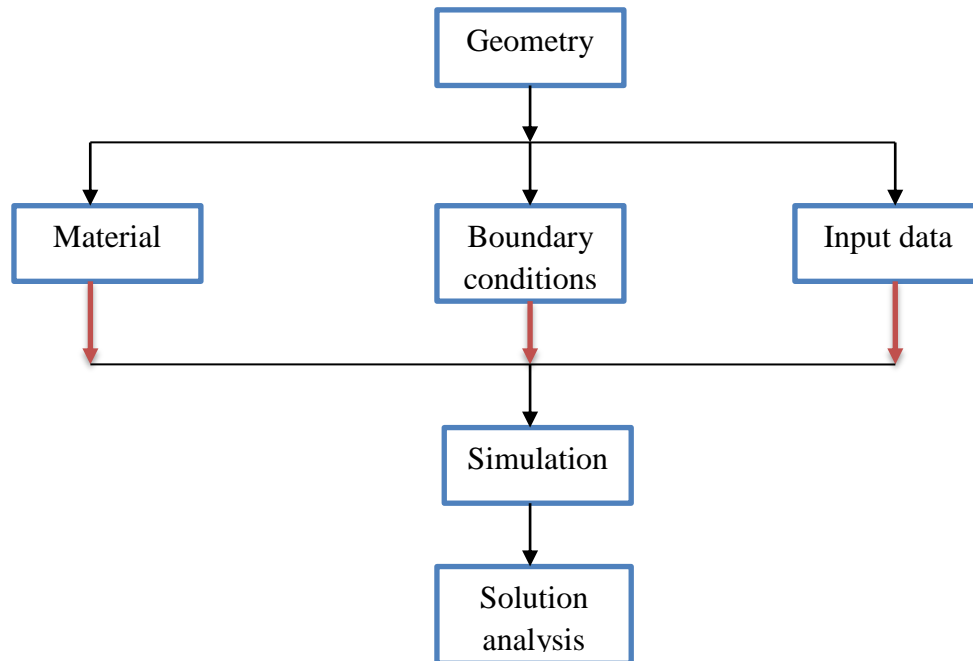


Figure 62 - Diagram of modelling and simulation

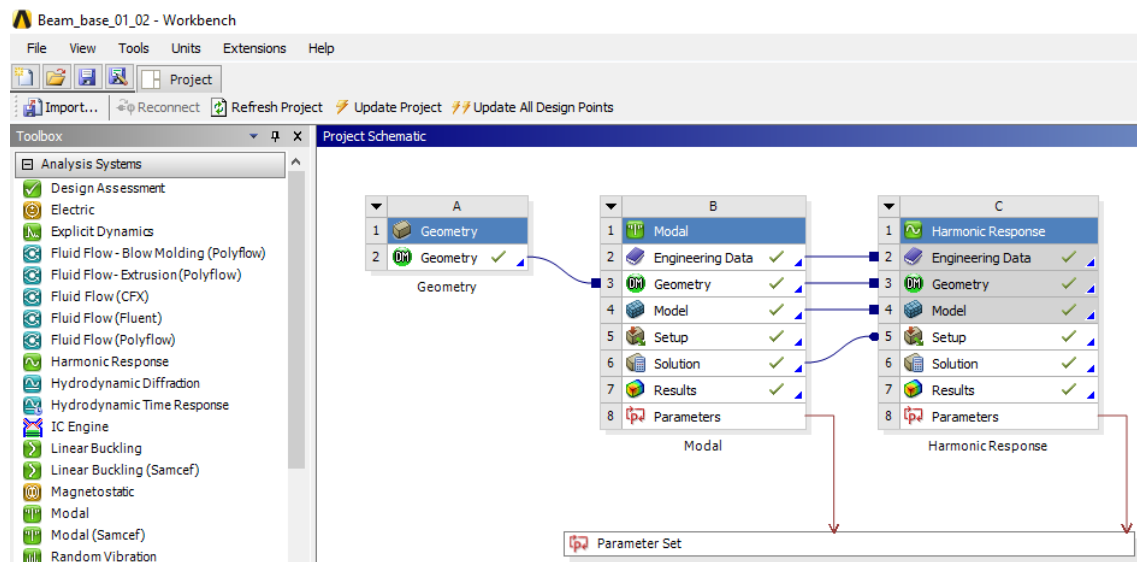


Figure 63 - Diagram of modelling and simulation

5.2. BASE MODEL

5.2.1. CONSTRUCTION



Figure 64 - Piezoelectric device (V21BL)

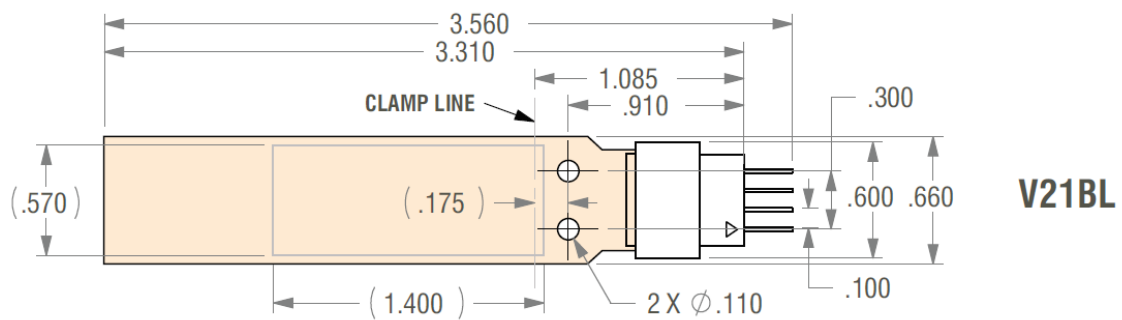


Figure 65 - Geometry of the piezoelectric device (V21BL)

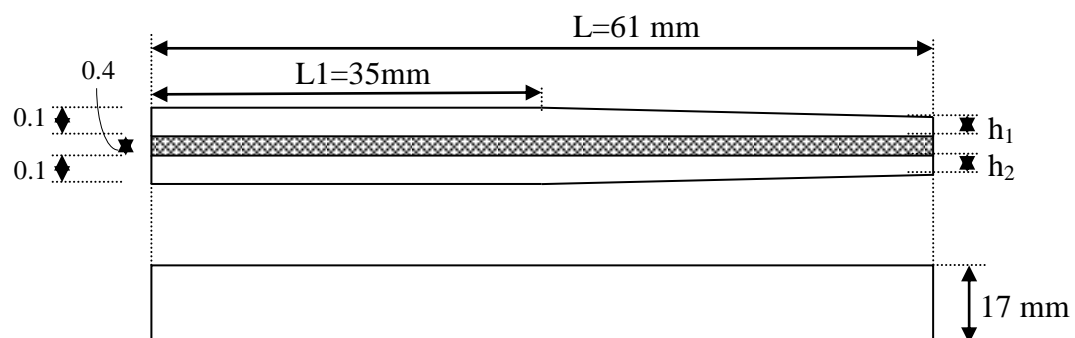


Figure 66 - Draw of the piezoelectric device (V21BL)

5.2.2. DRAWING OF THE MODEL

The geometry of the mechanism can be introduced using the tools of the Design Modeler. It is also possible the introduction of a geometry from another CAD software.



Figure 67 - Draw of the model (V21BL)

5.2.3. MODEL OF THE CONSTRUCTION

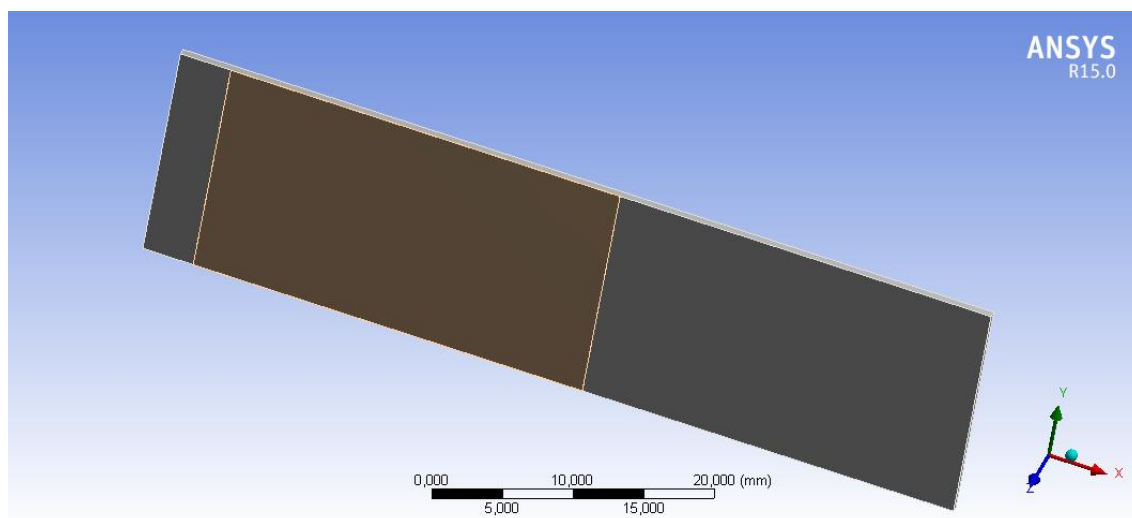


Figure 68 - Model of the construction

Object Name	Beam	Piezo_01
State	Meshed	
Graphics Properties		
Visible	Yes	
Transparency	1	
Definition		
Suppressed	No	
Stiffness Behavior	Flexible	
Coordinate System	Default Coordinate System	
Reference Temperature	By Environment	
Material		
Assignment	Tekstolit	Structural Steel
Nonlinear Effects	Yes	
Thermal Strain Effects	Yes	
Bounding Box		
Length X	6,1e-002 m	2,928e-002 m
Length Y	1,7e-002 m	
Length Z	6,e-004 m	1,8e-005 m
Properties		
Volume	6,222e-007 m³	8,9597e-009 m³
Mass	8,0886e-004 kg	7,0333e-005 kg
Centroid X	3,05e-002 m	1,844e-002 m
Centroid Y	8,5e-003 m	8,5e-003 m
Centroid Z	3,e-004 m	6,09e-004 m
Moment of Inertia Ip1	1,9504e-008 kg·m²	1,6939e-009 kg·m²
Moment of Inertia Ip2	2,5084e-007 kg·m²	5,0248e-009 kg·m²
Moment of Inertia Ip3	2,7029e-007 kg·m²	6,7187e-009 kg·m²
Statistics		
Nodes	1388	686
Elements	175	84
Mesh Metric	None	

5.2.4. BOUNDARY CONDITIONS

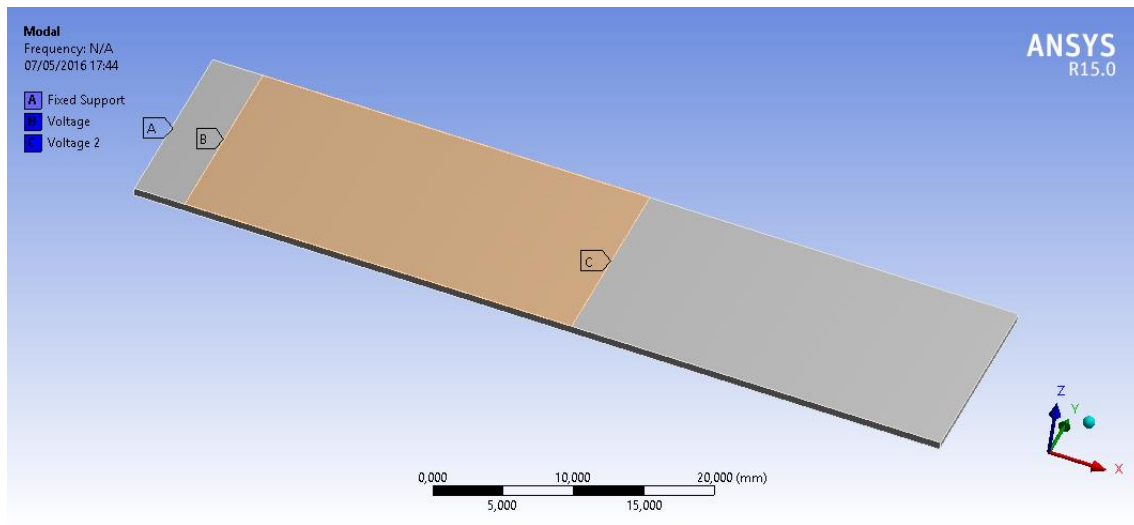


Figure 69 - Boundary conditions of the model

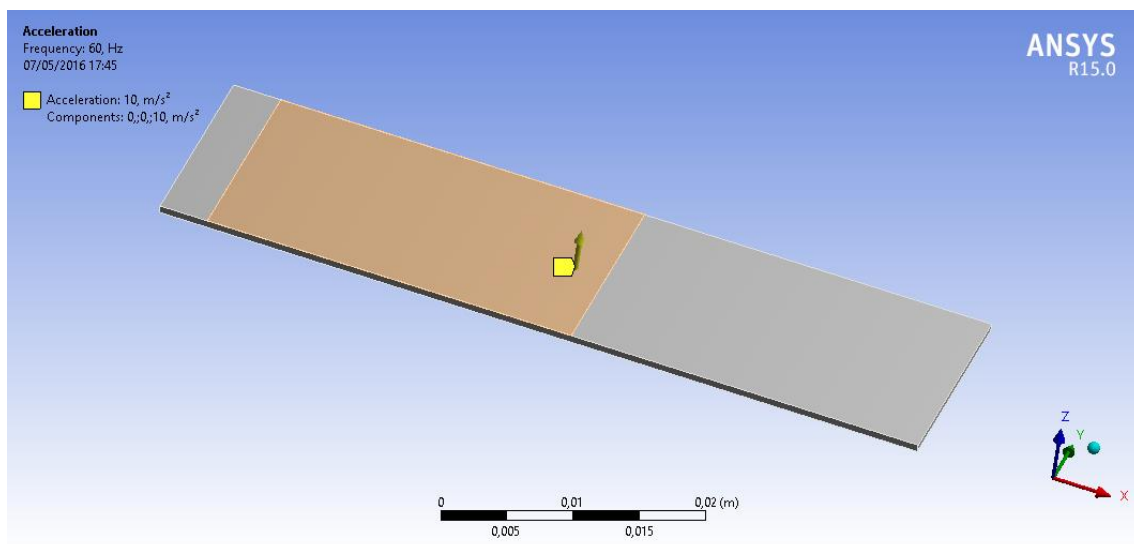


Figure 70 - Boundary conditions of the model

5.2.5. MESH

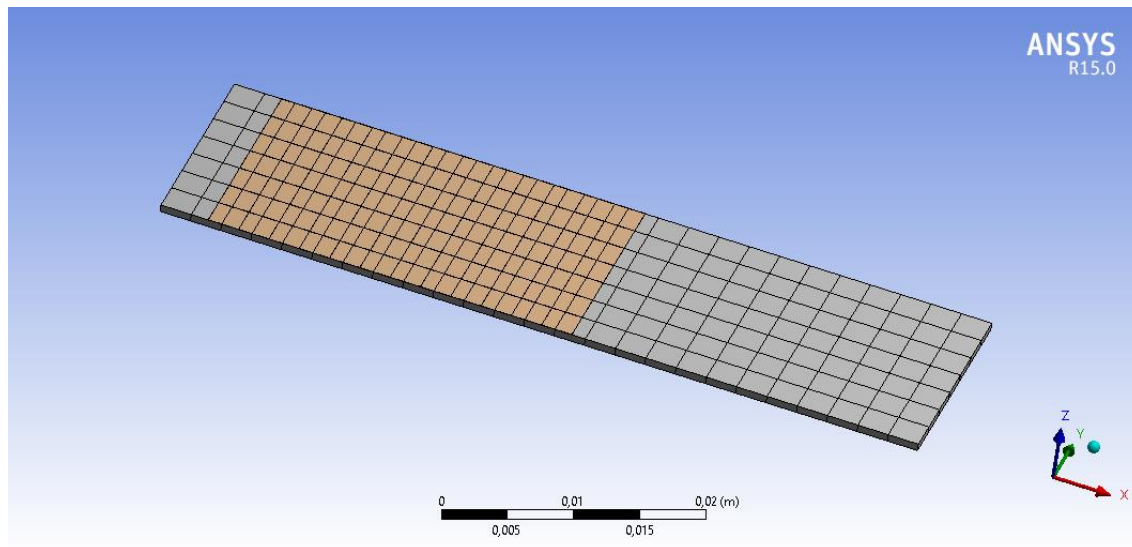


Figure 71 - Mesh of the model

Object Name	Mesh
State	Solved
Defaults	
Physics Preference	Mechanical
Relevance	0
Sizing	
Use Advanced Size Function	Off
Relevance Center	Coarse
Element Size	Default
Initial Size Seed	Active Assembly
Smoothing	Medium
Transition	Fast
Span Angle Center	Coarse
Minimum Edge Length	1,34e-005 m
Inflation	
Use Automatic Inflation	None
Inflation Option	Smooth Transition
Transition Ratio	0,272
Maximum Layers	5
Growth Rate	1,2
Inflation Algorithm	Pre
View Advanced Options	No
Patch Conforming Options	
Triangle Surface Mesher	Program Controlled
Patch Independent Options	
Topology Checking	Yes

Advanced	
Number of CPUs for Parallel Part Meshing	Program Controlled
Shape Checking	Standard Mechanical
Element Midside Nodes	Program Controlled
Straight Sided Elements	No
Number of Retries	Default (4)
Extra Retries For Assembly	Yes
Rigid Body Behavior	Dimensionally Reduced
Mesh Morphing	Disabled
Defeaturing	
Pinch Tolerance	Please Define
Generate Pinch on Refresh	No
Automatic Mesh Based Defeaturing	On
Defeaturing Tolerance	Default
Statistics	
Nodes	2074
Elements	259
Mesh Metric	None

5.2.6. MATERIAL

Inside the Engineering Data Sources different materials can be found or there is the possibility of importing data.

Tekstolit > Constants

Density 1300, kg m⁻³

Tekstolit > Isotropic Elasticity

Temperature C	Young's Modulus Pa	Poisson's Ratio	Bulk Modulus Pa	Shear Modulus Pa
	7,e+009	0,4	1,1667e+010	2,5e+009

Piezo_volture_01 > Constants

Density 7800, kg m⁻³

Piezo_volture_01 > Anisotropic Elasticity

D[* ,1] Pa	D[* ,2] Pa	D[* ,3] Pa	D[* ,4] Pa	D[* ,5] Pa	D[* ,6] Pa
7,49e+010					
-3,42e+009	7,49e+010				
-1,385e+010	-1,385e+010	4,319e+010			
0,	0,	0,	2,105e+010		
0,	0,	0,	0,	2,257e+010	
0,	0,	0,	0,	0,	2,257e+010

Piezo_volture_01 > Constant Damping Coefficient

Constant Damping Coefficient
0,

Object Name	Piezoelectric Body_01	Piezoelectric Body_02	Voltage	Voltage 2	Voltage 3	Voltage 4
State	Fully Defined					
Scope						
Scoping Method	Geometry Selection					
Geometry	1 Body			1 Face		
Definition						
Polarization Axis	X					
Permittivity Constant	8.854E-12 [A A sec sec sec sec kg^-1 m^-1 m^-1 m^-1]					
PIEZ e31	-6.7 [A sec m^-1 m^-1]					
PIEZ e33	15.4 [A sec m^-1 m^-1]					
PIEZ e15	18.1 [A sec m^-1 m^-1]					
DPER ep11	2000					
DPER ep33	1000					
RSVX	0 [kg m m m A^-1 A^-1 sec^-1 sec^-1 sec^-1]					
RSVY	0 [kg m m m A^-1 A^-1 sec^-1 sec^-1 sec^-1]					
RSVZ	0 [kg m m m A^-1 A^-1 sec^-1 sec^-1 sec^-1]					
Voltage (Real)				0 [kg m m A^-1 sec^-1 sec^-1 sec^-1]		

5.2.7. SIMULATION

Using the input data, the simulation of the model is made by ANSYS. Can be used harmonic response analysis in order to obtain the deformation and the output voltage in the model or the modal analysis for obtaining all of the natural frequencies of the model and their deformation and voltage.

5.2.8. SOLUTION ANALYSIS

Information about deformation, frequency or output voltage can be obtained after the simulation. This solution can be studied and the simulation can be repeated in order to look for another behaviour of the model using another input data.

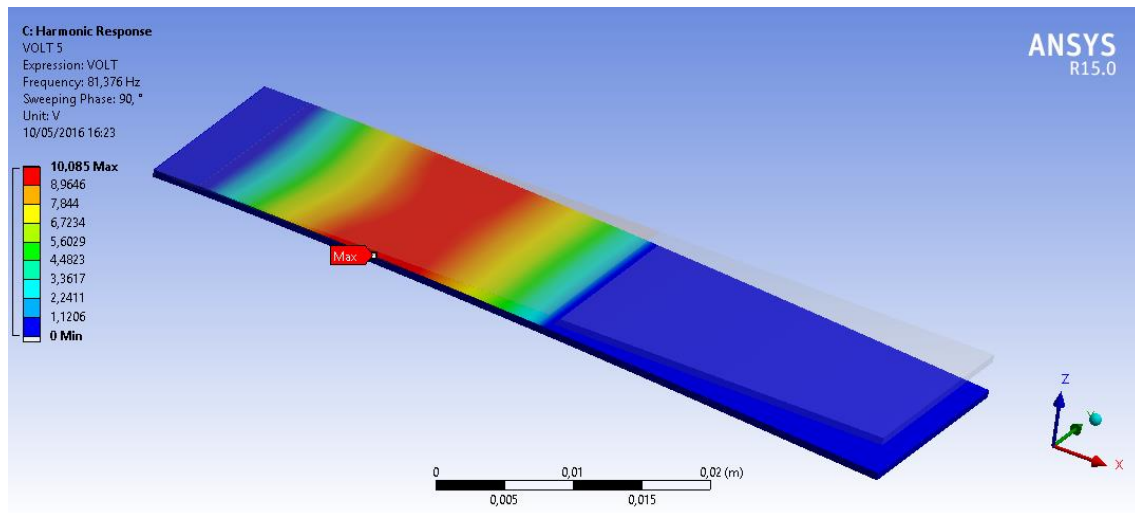


Figure 72 - Voltage at $a=7.8 \text{ m/s}^2$ and $f=81.376 \text{ Hz}$

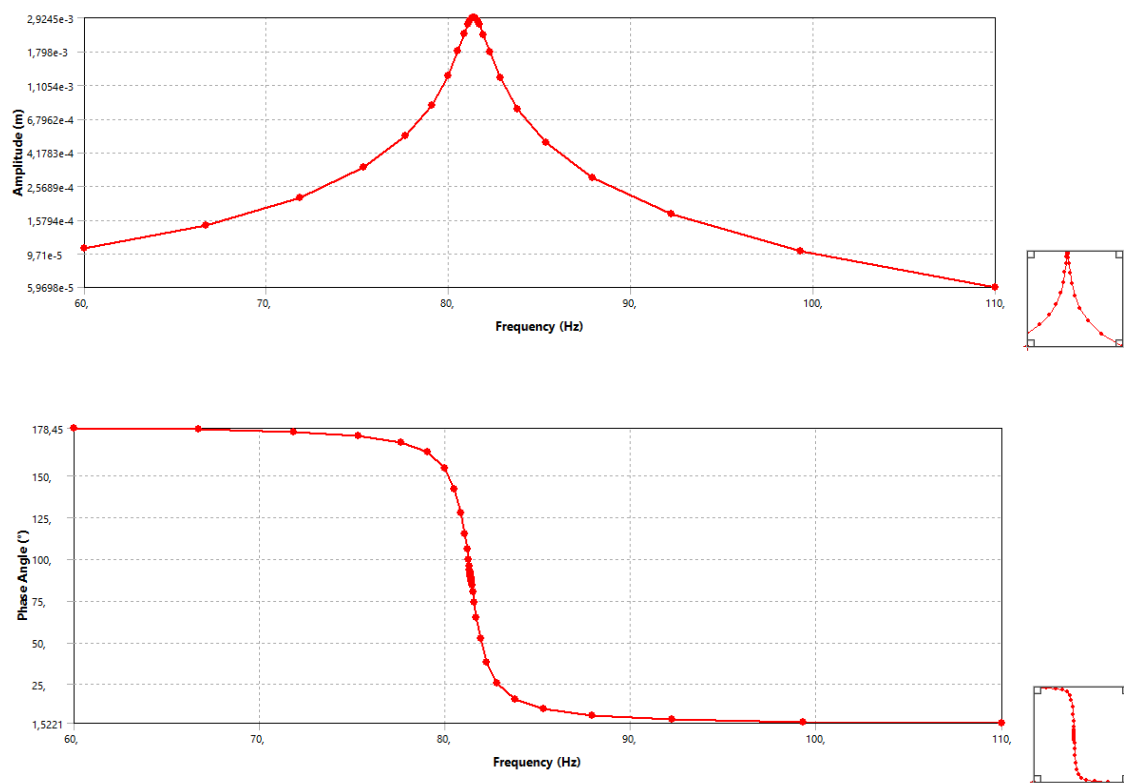


Figure 73 - Frequency response and phase of the deformation of free end of the cantilever at $a=7.8 \text{ m/s}^2$

5.3. MODEL WITH SPRING

5.3.1. MODEL OF THE CONSTRUCTION

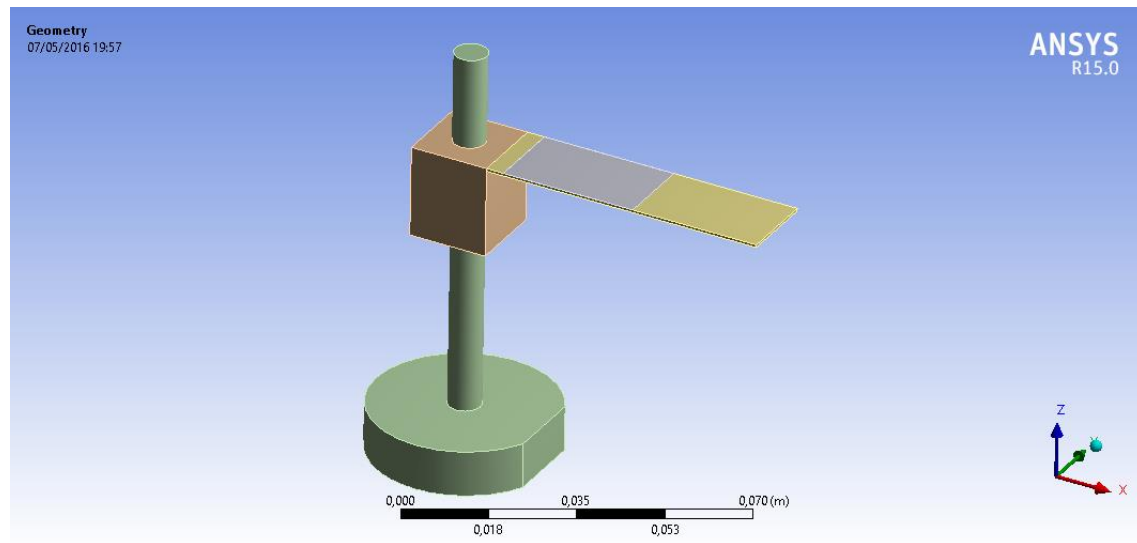


Figure 74 - Model of the construction

Object Name	<i>CBeam_01-1</i>	<i>Mass_02-1</i>	<i>Mass_01-1</i>	<i>Piezo_plast-1</i>	<i>Piezo_plast-2</i>
State	Meshed				Suppressed
Graphics Properties					
Visible	Yes				No
Transparency	1				
Definition					
Suppressed	No				Yes
Stiffness Behavior	Flexible				
Coordinate System	Default Coordinate System				
Reference Temperature	By Environment				
Material					
Assignment	Tekstolit	Structural Steel			
Nonlinear Effects	Yes				
Thermal Strain Effects	Yes				
Bounding Box					
Length X	6,1e-002 m	3,8e-002 m	1,7e-002 m	2,928e-002 m	
Length Y	1,7e-002 m	3,9997e-002 m	1,7e-002 m		
Length Z	6,e-004 m	9,e-002 m	2,e-002 m	1,34e-005 m	
Properties					
Volume	6,222e-007 m³	1,541e-005 m³	5,0103e-006 m³	6,67e-009 m³	
Mass	8,0886e-004 kg	0,12097 kg	3,9331e-002 kg	5,2359e-005 kg	

Centroid X	3,9e-002 m	-2,7865e-004 m	5,4216e-010 m	2,694e-002 m	
Centroid Y	4,6194e-010 m	5,0655e-020 m	5,1431e-010 m	4,6194e-010 m	
Centroid Z	6,97e-002 m	1,3934e-002 m	6,e-002 m	7,0007e-002 m	6,94e-002 m
Moment of Inertia Ip1	1,9504e-008 kg·m ²	6,2154e-005 kg·m ²	2,387e-006 kg·m ²	1,261e-009 kg·m ²	
Moment of Inertia Ip2	2,5084e-007 kg·m ²	6,1539e-005 kg·m ²	2,387e-006 kg·m ²	3,7407e-009 kg·m ²	
Moment of Inertia Ip3	2,7029e-007 kg·m ²	1,9041e-005 kg·m ²	2,149e-006 kg·m ²	5,0017e-009 kg·m ²	
Statistics					
Nodes	2156	1093	1368	1068	0
Elements	279	529	231	135	0
Mesh Metric	None				

5.3.2. BOUNDARY CONDITIONS

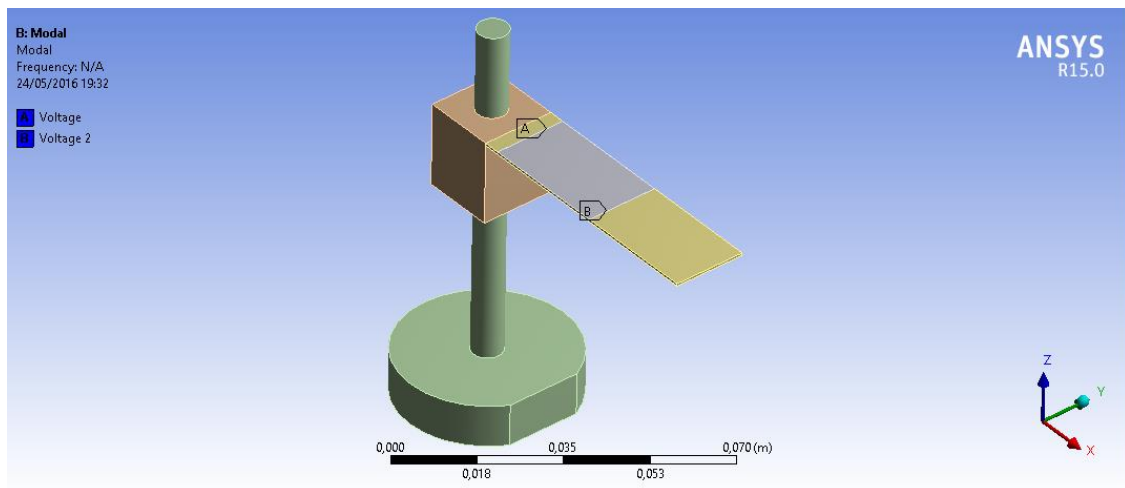


Figure 75 - Boundary conditions of the model

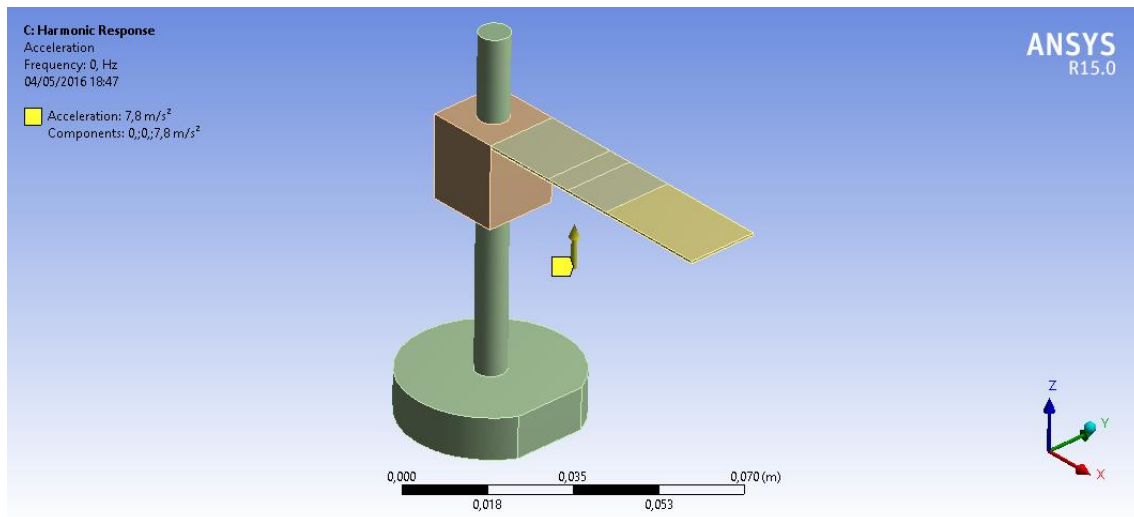


Figure 76 - Boundary conditions of the model

5.3.3. MESH

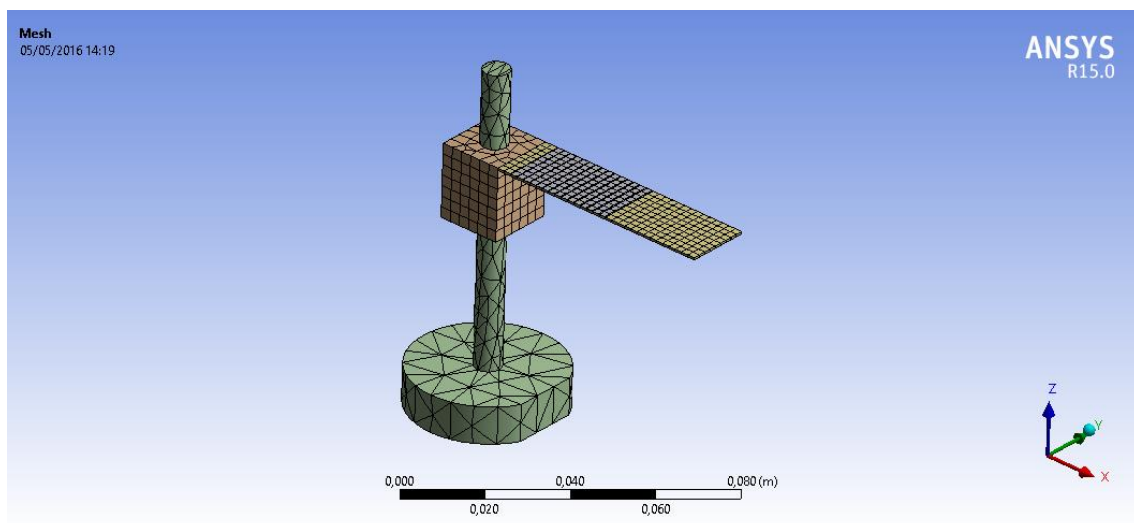


Figure 77 - Mesh of the model

Object Name	Mesh
State	Solved
Defaults	
Physics Preference	Mechanical
Relevance	0
Sizing	
Use Advanced Size Function	Off
Relevance Center	Coarse
Element Size	Default
Initial Size Seed	Active Assembly
Smoothing	Medium
Transition	Fast

Span Angle Center	Coarse
Minimum Edge Length	1,34e-005 m
Inflation	
Use Automatic Inflation	None
Inflation Option	Smooth Transition
Transition Ratio	0,272
Maximum Layers	5
Growth Rate	1,2
Inflation Algorithm	Pre
View Advanced Options	No
Patch Conforming Options	
Triangle Surface Mesher	Program Controlled
Patch Independent Options	
Topology Checking	Yes
Advanced	
Number of CPUs for Parallel Part Meshing	Program Controlled
Shape Checking	Standard Mechanical
Element Midside Nodes	Program Controlled
Straight Sided Elements	No
Number of Retries	Default (4)
Extra Retries For Assembly	Yes
Rigid Body Behavior	Dimensionally Reduced
Mesh Morphing	Disabled
Defeaturing	
Pinch Tolerance	Please Define
Generate Pinch on Refresh	No
Automatic Mesh Based Defeaturing	On
Defeaturing Tolerance	Default
Statistics	
Nodes	5685
Elements	1174
Mesh Metric	None

5.3.4. MATERIAL

Inside the Engineering Data Sources different materials can be found or there is the possibility of importing data.

Tekstolit > Constants

Density	1300, kg m ⁻³
---------	--------------------------

Tekstolit > Isotropic Elasticity

Temperature C	Young's Modulus Pa	Poisson's Ratio	Bulk Modulus Pa	Shear Modulus Pa
	7,e+009	0,4	1,1667e+010	2,5e+009

Structural Steel > Constants

Density	7850, kg m ⁻³
Coefficient of Thermal Expansion	1,2e-005 C ⁻¹
Specific Heat	434, J kg ⁻¹ C ⁻¹
Thermal Conductivity	60,5 W m ⁻¹ C ⁻¹
Resistivity	1,7e-007 ohm m

Structural Steel > Compressive Ultimate Strength

Compressive Ultimate Strength Pa
0,

Structural Steel > Compressive Yield Strength

Compressive Yield Strength Pa
2,5e+008

Structural Steel > Tensile Yield Strength

Tensile Yield Strength Pa
2,5e+008

Structural Steel > Tensile Ultimate Strength

Tensile Ultimate Strength Pa
4,6e+008

Structural Steel > Isotropic Secant Coefficient of Thermal Expansion

Reference Temperature C
22,

Structural Steel > Alternating Stress Mean Stress

Alternating Stress Pa	Cycles	Mean Stress Pa
3,999e+009	10,	0,
2,827e+009	20,	0,
1,896e+009	50,	0,
1,413e+009	100,	0,

1,069e+009	200,	0,
4,41e+008	2000,	0,
2,62e+008	10000	0,
2,14e+008	20000	0,
1,38e+008	1,e+005	0,
1,14e+008	2,e+005	0,
8,62e+007	1,e+006	0,

Structural Steel > Strain-Life Parameters

Strength Coefficient Pa	Strength Exponent	Ductility Coefficient	Ductility Exponent	Cyclic Strength Coefficient Pa	Cyclic Strain Hardening Exponent
9,2e+008	-0,106	0,213	-0,47	1,e+009	0,2

Structural Steel > Isotropic Elasticity

Temperature C	Young's Modulus Pa	Poisson's Ratio	Bulk Modulus Pa	Shear Modulus Pa
	2,e+011	0,3	1,6667e+011	7,6923e+010

Structural Steel > Isotropic Relative Permeability

Relative Permeability
10000

Piezo_vulture_01 > Constants

Density	7800, kg m ⁻³
---------	--------------------------

Piezo_vulture_01 > Anisotropic Elasticity

D[* ,1] Pa	D[* ,2] Pa	D[* ,3] Pa	D[* ,4] Pa	D[* ,5] Pa	D[* ,6] Pa
7,49e+010					
-3,42e+009	7,49e+010				
-1,385e+010	-1,385e+010	4,319e+010			
0,	0,	0,	2,105e+010		
0,	0,	0,	0,	2,257e+010	

0,	0,	0,	0,	0,	2,257e+010
----	----	----	----	----	------------

Piezo_vulture_01 > Constant Damping Coefficient

Constant Damping Coefficient
0,

Object Name	<i>Piezoelectric Body</i>	<i>Piezoelectric Body</i> 2	<i>Voltage</i>	<i>Voltage</i> 2	<i>Voltage</i> 3	<i>Voltage</i> 4
State	Fully Defined					
Scope						
Scoping Method	Geometry Selection					
Geometry	1 Body			1 Face		
Definition						
Polarization Axis	X					
Permittivity Constant	8.854E-12 [A A sec sec sec sec kg^-1 m^-1 m^-1 m^-1]					
PIEZ e31	-6.7 [A sec m^-1 m^-1]					
PIEZ e33	18.1 [A sec m^-1 m^-1]					
PIEZ e15	15.4 [A sec m^-1 m^-1]					
DPER ep11	2000					
DPER ep33	1000					
RSVX	0 [kg m m m A^-1 A^-1 sec^-1 sec^-1 sec^-1]					
RSVY	0 [kg m m m A^-1 A^-1 sec^-1 sec^-1 sec^-1]					
RSVZ	0 [kg m m m A^-1 A^-1 sec^-1 sec^-1 sec^-1]					
Voltage (Real)				0 [kg m m A^-1 sec^-1 sec^-1 sec^-1]		

5.3.5. SIMULATION

Using the input data, the simulation of the model is made by ANSYS. Can be used harmonic response analysis in order to obtain the deformation and the output voltage in the model or the modal analysis for obtaining all of the natural frequencies of the model and their deformation and voltage.

5.3.6. SOLUTION ANALYSIS

Information about deformation, frequency or output voltage can be obtained after the simulation. This solution can be studied and the simulation can be repeated in order to look for another behaviour of the model using another input data.

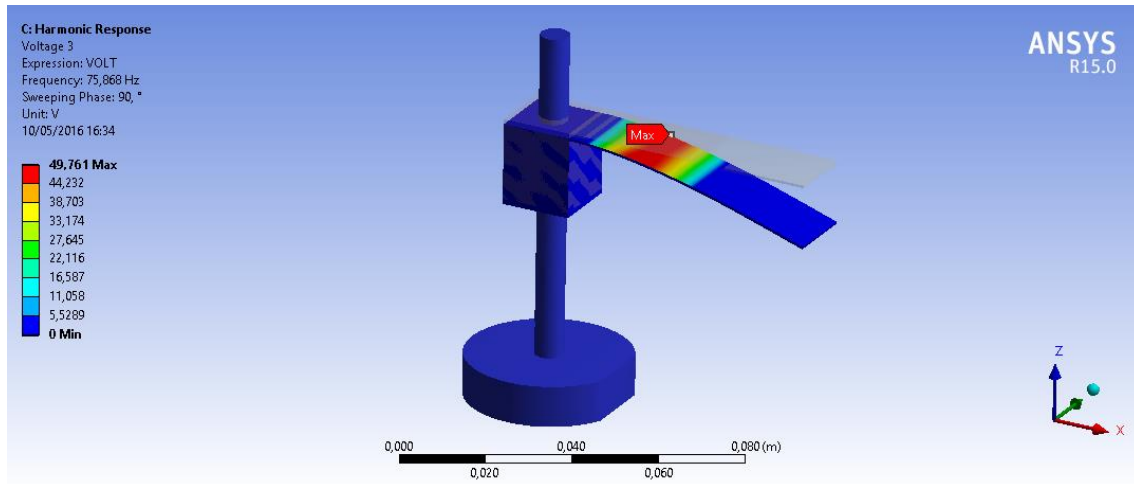


Figure 78 - Voltage at $a=7.8 \text{ m/s}^2$, $C=10000 \text{ N/m}$ and $f=75.868 \text{ Hz}$

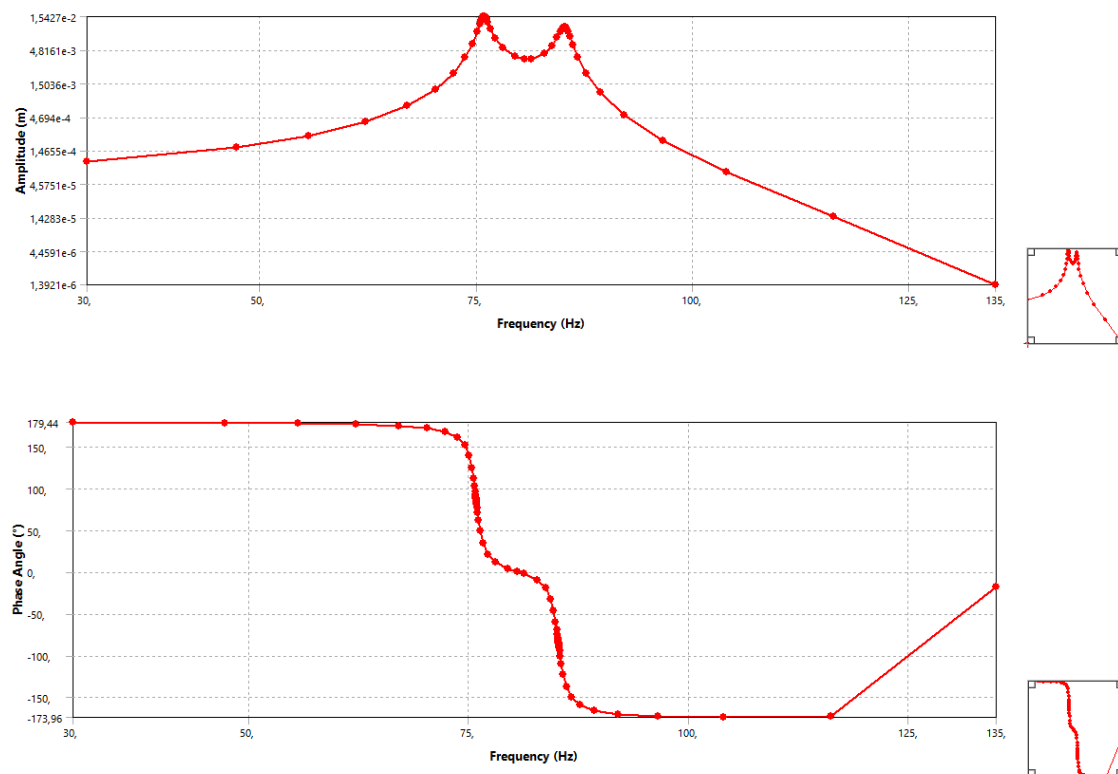


Figure 79 - Frequency response and phase of the deformation of free end of the cantilever at $a=7.8 \text{ m/s}^2$ and $C=10000 \text{ N/m}$

5.4. STUDY THE EFFECTS OF AMPLITUDE OF VIBRATIONS OR OF THE SPRING CONSTANT ON VOLTAGE GENERATED

5.4.1. BASE MODEL

For the base model, the study consists in varying the acceleration and see how the output voltage changes for different frequencies.

f (Hz) a (m/s^2)	60	65	70	75	81,376	85	90	95	100
2	0,104	0,13132	0,18113	0,29695	2,5859	0,46018	0,19341	0,11549	0,074937
3	0,156	0,19698	0,2717	0,44543	3,8789	0,69026	0,29011	0,17323	0,11241
4	0,208	0,26264	0,36226	0,5939	5,1719	0,92035	0,38681	0,23098	0,14987
5	0,26001	0,3283	0,45283	0,74238	6,4648	1,1504	0,48352	0,28872	0,18734
6	0,31201	0,39395	0,54339	0,89085	7,7578	1,3805	0,58022	0,34647	0,22481
7,8	0,40561	0,51214	0,70641	1,1581	10,085	1,7947	0,75429	0,45041	0,29226
9	0,41601	0,52527	0,72452	1,1878	10,344	1,8407	0,77363	0,46196	0,29975
10	0,52001	0,65659	0,90565	1,4848	12,93	2,3009	0,96704	0,57745	0,37469

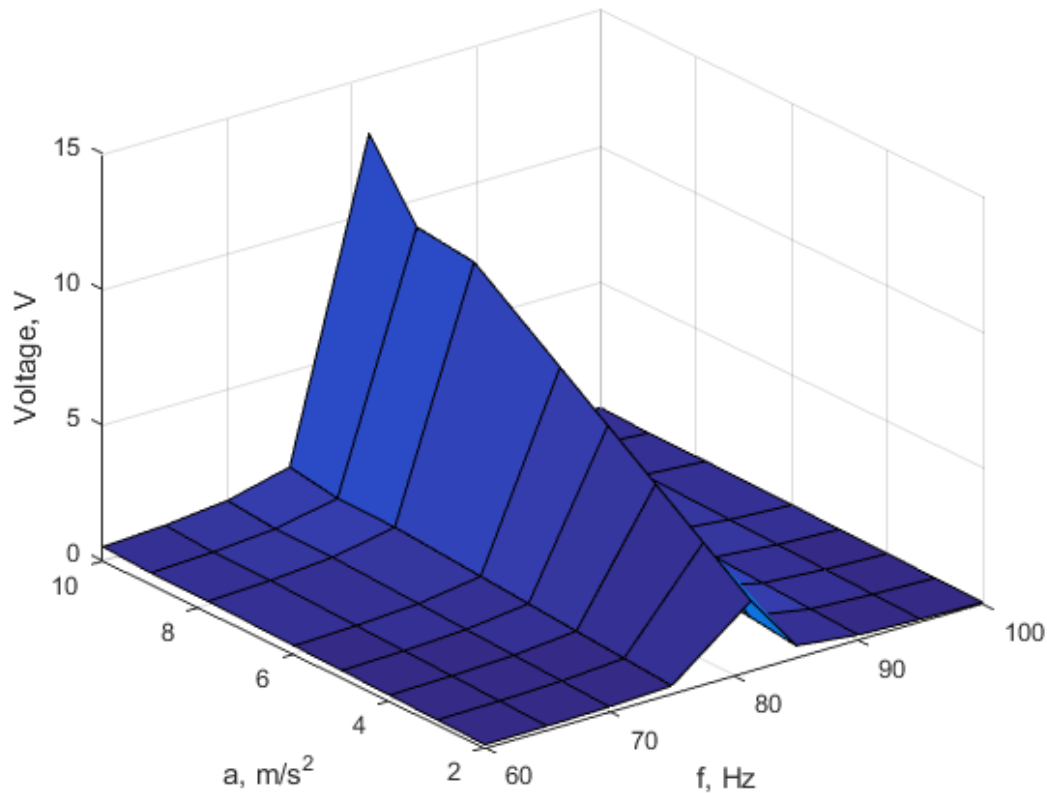


Figure 80 - Frequency response of the voltage output for different accelerations

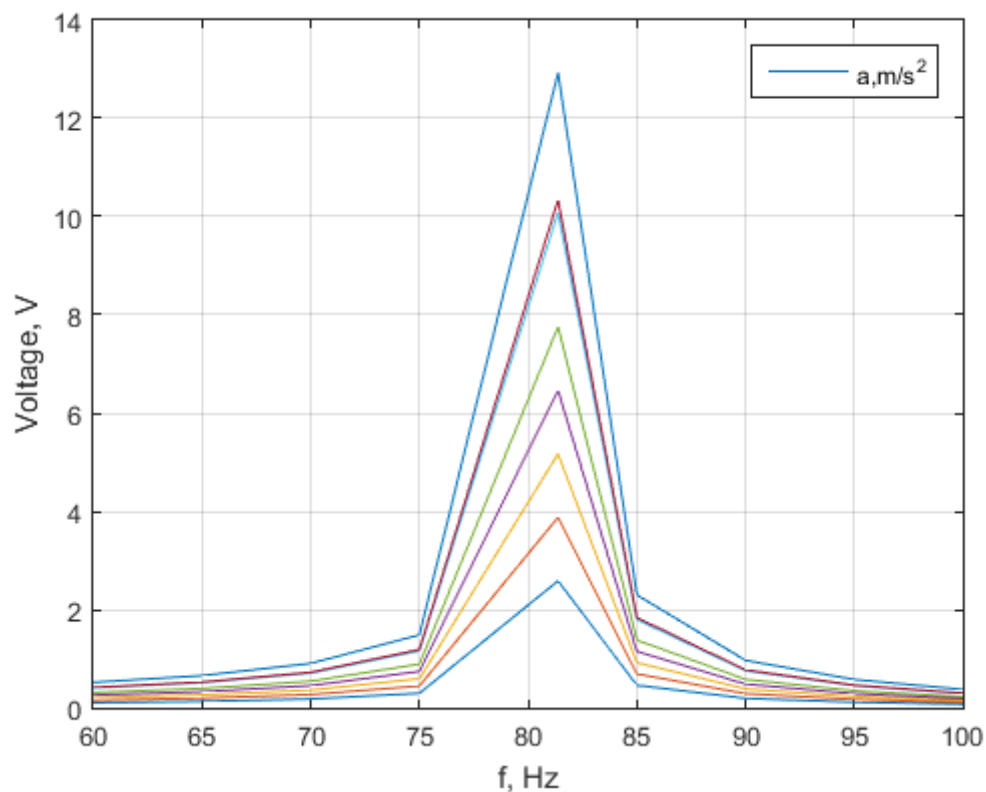


Figure 81 - Frequency response of the voltage output for different accelerations

5.4.2. MODEL WITH SPRING

In this model, the spring constant is varied in order to see how the voltage changes with the frequency.

C (N/m)=2000									
f (Hz)	30	33	35,445	339	59	79	81,606	85	88
Voltage(V)	0,80193	1,7894	14,678	1,2561	0,21681	0,65243	2,3441	0,40422	0,18884

C (N/m)=4000									
f (Hz)	44	47	50,003	53	66	79	81,808	85	88
Voltage(V)	1,2004	2,5197	18,351	2,6973	0,68758	1,6402	6,0041	1,0837	0,49197

C (N/m)=6000									
f (Hz)	55	58	60,966	64	71,5	79	82,176	85	88
Voltage(V)	1,8967	3,8195	24,651	4,4139	1,9058	3,2581	12,292	2,4047	1,0473

C (N/m)=8000									
f (Hz)	64	67	69,702	73	76,5	80	82,995	86	89
Voltage(V)	2,9001	6,709	36,246	7,7377	5,4786	7,3881	23,881	4,1519	1,7475

C (N/m)=10000									
f (Hz)	70	73	75,868	79	80,5	82	85,247	89	92
Voltage(V)	3,6385	8,7285	49,76	14,146	11,998	13,133	37,402	4,6595	1,9736

C (N/m)=12000									
f (Hz)	73	76	78,659	82	84,5	87	90,069	93	96
Voltage(V)	3,6372	8,71	43,035	11,135	8,7251	10,584	30,671	5,587	2,4103

C (N/m)=14000									
f (Hz)	74	77	79,624	83	88	93	96,105	99	102
Voltage(V)	3,1321	7,1041	32,456	7,4751	4,4185	6,4878	20,079	4,0791	1,8736

C (N/m)=16000									
f (Hz)	74	77	80,037	83	91	99	102,21	105	108
Voltage(V)	2,4778	5,2599	26,271	6,3756	2,5578	4,3513	13,878	3,2273	1,4765

C (N/m)=18000									
f (Hz)	74	77	80,257	83	94	105	108,11	111	114
Voltage(V)	2,1757	4,3191	22,617	5,6431	1,6828	3,2729	10,209	2,472	1,1539

C (N/m)=20000									
f (Hz)	74	77	80,393	83	97	111	113,76	117	120
Voltage(V)	1,9792	3,7606	20,268	5,1434	1,1994	2,864	7,8559	1,7743	0,89185

C (N/m)=26000									
f (Hz)	75	78	80,599	84	105	126	129,37	132	135
Voltage(V)	1,9501	4,0461	16,568	3,2844	0,58872	1,4136	4,1304	1,252	1,282

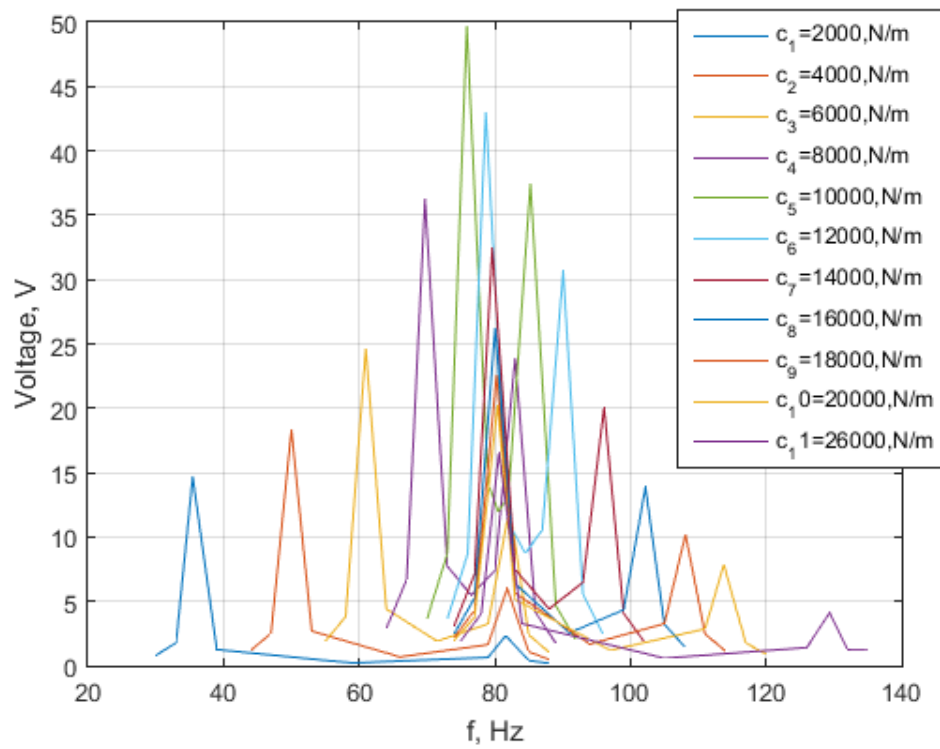


Figure 82 - Frequency response of the voltage output for different spring constants

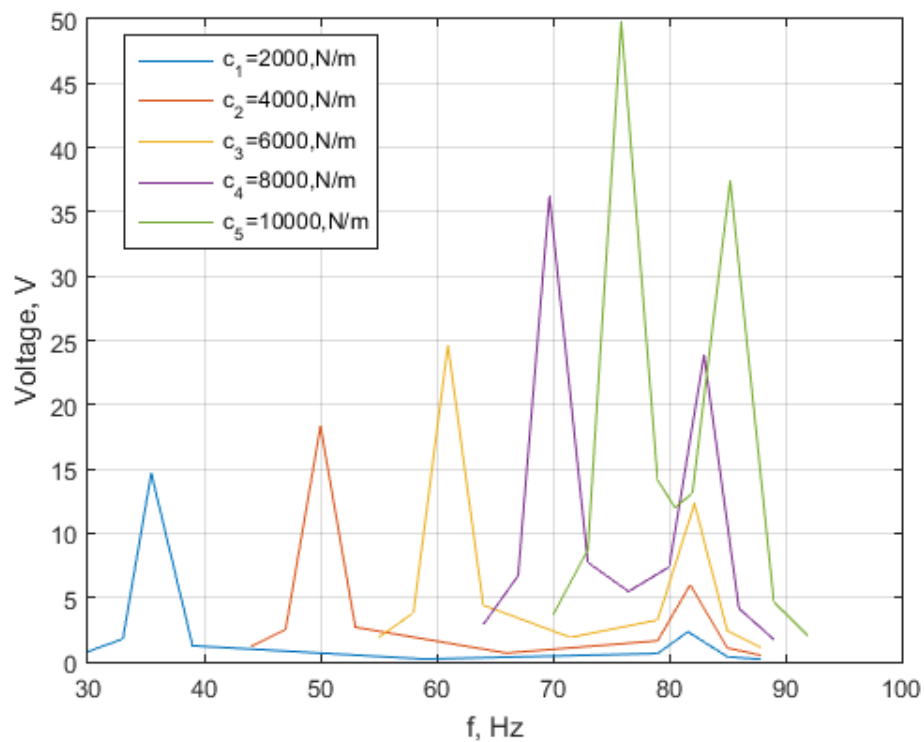


Figure 83 - Frequency response of the voltage output for different spring constants
(from 2000 N/m to 10000 N/m)

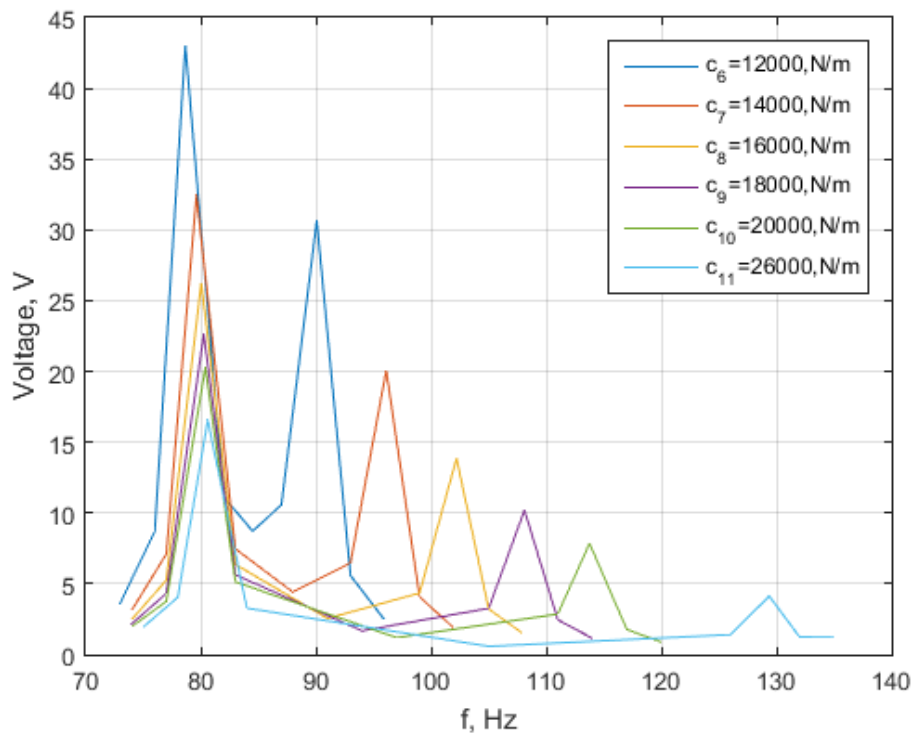


Figure 84 - Frequency response of the voltage output for different spring constants (from 12000 N/m to 26000 N/m)

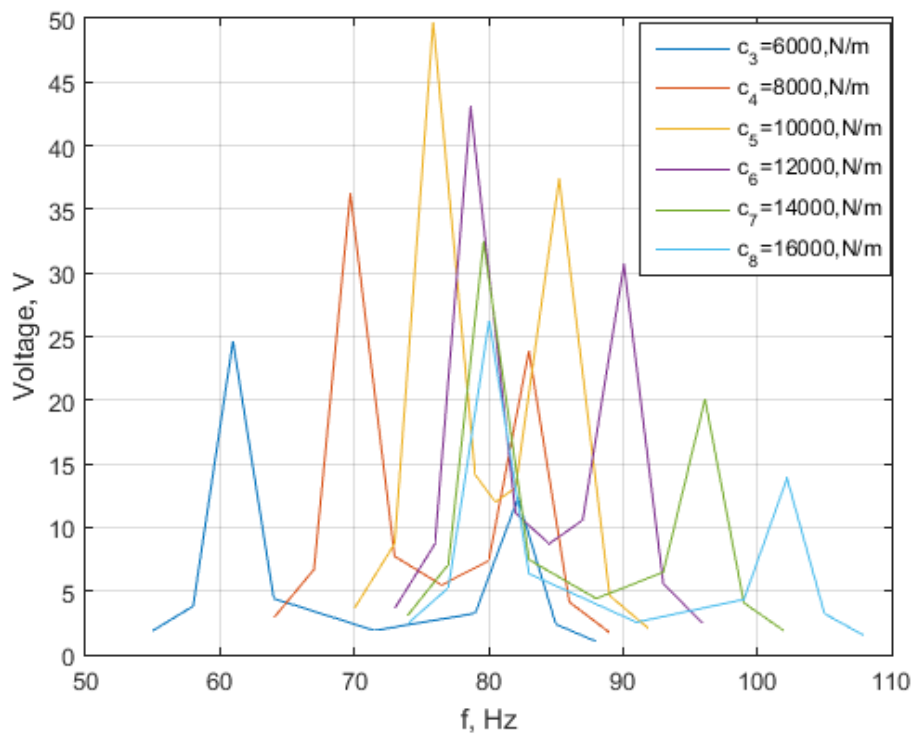


Figure 85 - Frequency response of the voltage output for different spring constants (from 6000 N/m to 16000 N/m)

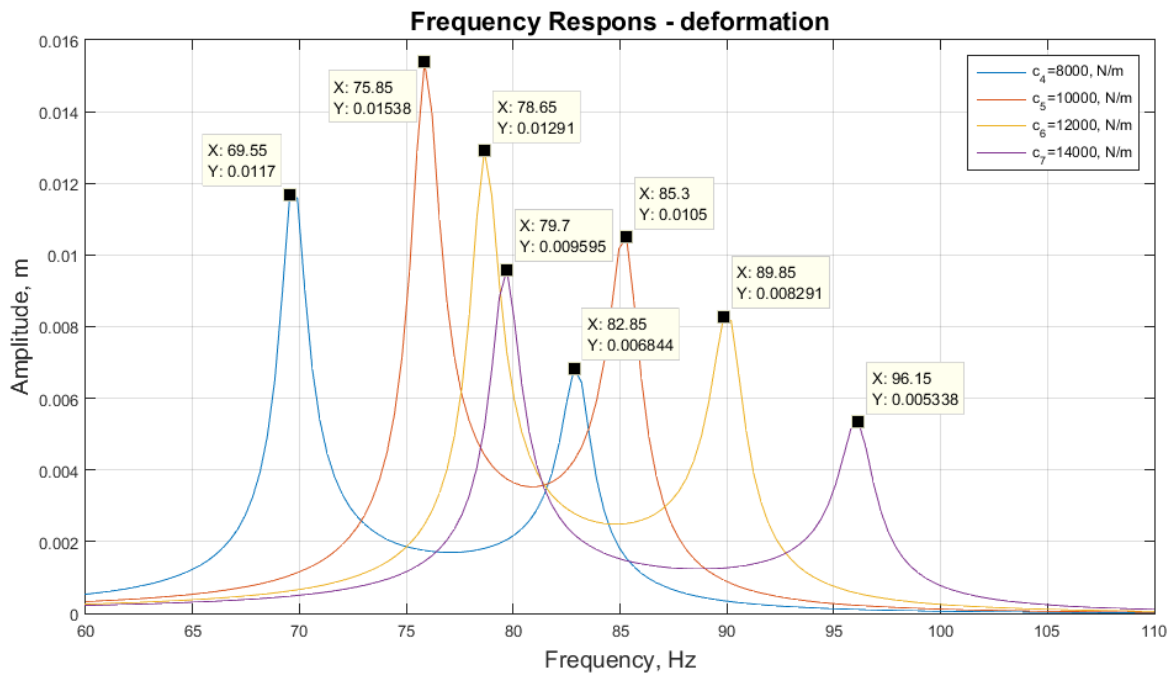


Figure 86 – Frequency response of the deformation of the free end of the cantilever for different spring constants (from 8000 N/m to 14000 N/m)

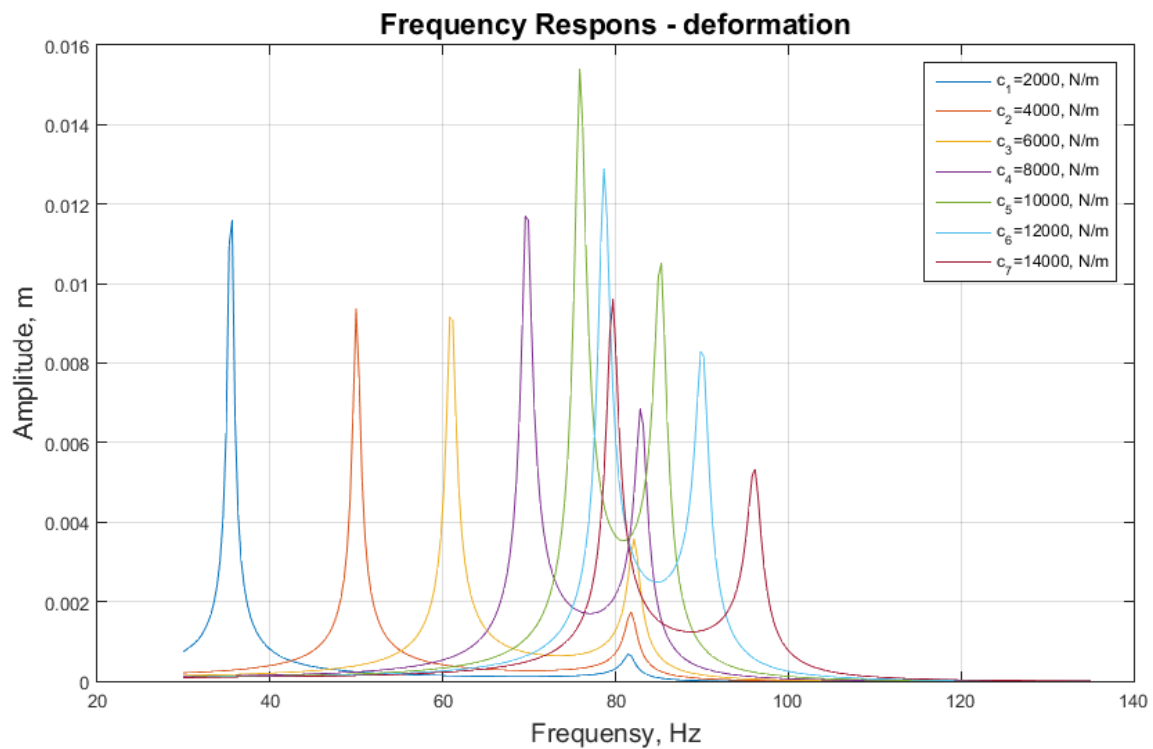


Figure 87 – Frequency response of the deformation of the free end of the cantilever for different spring constants (from 2000 N/m to 14000 N/m)

6. ANALISYS OF THE RESULTS

6.1. EXPERIMENTAL RESULTS

Figures 56, 57 and 58 show that the generated power grows when the voltage augments until it reaches a maximum for a certain voltage, after which, it decreases when the voltage grows. It is also possible to see that the power generated (absolute, per square centimetre and per cubic centimetre) increases when the acceleration of the forced oscillation in the cantilever also grows. Considering the point of the maximum power of the three figures, an increment of 1.3 times on acceleration means an increment of about 1.25 times on the power generated, so it can be said that the acceleration influences in a direct ratio to the generated power.

Figure 59 also show that the generated power is bigger for the biggest acceleration as well as the previous graphics do. Besides, it shows that the generated power has its maximum for a certain value of the electrical active load. This value is approximately 40 k Ω .

From figure 60 it is possible to prove that the voltage increases when the electric active load does so. However, growth is really pronounced at the beginning and almost disappears at the last points.

Finally, Figure 61 exhibits that the electric current decreases when the active load augments. As well as in Figure 53, this trend is really pronounced in the beginning.

6.2. ANSYS RESULTS

6.2.1. BASE MODEL

From the table that shows the results for the Base Model in ANSYS, it is possible to see that the output voltage increases from the first frequency (60 Hz) until it reaches its maximum on the resonant frequency (81.376 Hz). After that, the output voltage decreases. The two different accelerations show the same behaviour. For example, for an acceleration of 2 m/s², the output voltage at 60 Hz has a value of 0.104 V, then increases until it reaches a maximum of 2.5859 V for the resonant frequency, and then decreases it last value of 0.074937 V for a frequency of 100 Hz.

On the other hand, an increment on the acceleration for a concrete frequency means also that the output voltage increases. For example, for the resonant frequency (81.376 Hz), the output voltage is 2.859 V when the acceleration is 2 m/s², and it reaches a value of 12.93 V at 10 m/s². Therefore, an increment of 5 times in the acceleration means an increment of about 4.5 times in the output voltage.

6.2.2. MODEL WITH SPRING

In this case, there is a different table for each value of the spring constant, as the device presents two different resonant frequencies according to this parameter. However, all of the tables show similar behaviour.

The output voltage has an upward trend as the frequency increases, until it reaches its first maximum at the first resonant frequency. Then it decreases until a minimum, and after that it increases again until it gets the second resonant frequency where there is the other maximum. Finally, it has a downward trend.

For example, for a spring constant of 2000 N/m, the output voltage has a value of 0.80193 V when the frequency is 30 Hz, then goes up until it reaches a maximum of 14.678 V at its first resonant frequency (35.445 Hz). After that it decreases until a minimum of about 0.22 V at approximately 60 Hz. Then it enhances and gets a maximum of 2.3441 V with a frequency of 81.606 Hz, and it finally decreases. The last value of the study for this spring constant is of 0.18884 V at 88 Hz.

On the other hand, it can be analysed how the output voltage changes when the spring constant is varied. The results show that the maximum value of the voltage grows when the spring constant increases from its first value of 2000 N/m until 10000 N/m. After that it reduces when the spring constant grows. Therefore, the optimum value of this constant for the device is 10000 N/m.

7. CONCLUSIONS

1. The highest effectiveness of the vibration energy harvesting device of power is achieved at the regime of resonance frequency of these devices.
2. The acceleration influences in a direct ratio of the generated power/voltage.
3. The change of the acceleration leads to change of the voltage at which a maximum of the power is obtained.
4. The suggested numeric model in ANSYS showed good accordance with the experimental results.

8. REFERENCES

- [1]. Kaźmierski T. and Beeby S., *Energy Harvesting Systems: Principles, Modeling and Applications*, Springer, 2011.
- [2]. Kheng Tan Y., *Sustainable Energy Harvesting Technologies- Past, Present and Future*, 2011.
- [3]. Erturk A. and Inman D. J., *Piezoelectric Energy Harvesting*, Willey, 2011.
- [4]. http://e2e.ti.com/blogs_/b/fullycharged/archive/2013/11/18/energy-harvesting-is-there-no-free-lunch
- [5]. <http://www.morgantechnicalceramics.com/products/product-groups/piezo-ceramic-components/piezoelectric-ceramics-prop-apps>
- [6]. <http://www.piceramic.com>, *Piezoelectric Ceramic Products: Fundamentals, Characteristics and Applications*.
- [7]. <http://inhabitat.com/green-a-go-go-at-londons-first-eco-disco/>
- [8]. <http://inhabitat.com/sustainable-dance-club-opens-in-rotterdam/>
- [9]. http://content.time.com/time/specials/packages/article/0,28804,1852747_1854195_1854172,00.html
- [10]. <http://www.proetex.org/final%20proetex%20learning/power.htm>
- [11]. <http://www.energyharvestingjournal.com/articles/1589/energy-harvesting-roads-in-israel>
- [12]. <http://inhabitat.com/new-piezoelectric-railways-harvest-energy-from-passing-trains/>
- [13]. <http://www.treehugger.com/renewable-energy/japan-producing-electricity-from-train-station-ticket-gates.html>
- [14]. <http://classroom.materials.ac.uk/casePiez.php>
- [15]. <http://highlowtech.org/?p=1592>

- [16]. US 4,467,236 patent – Piezoelectric acousto-electric generator
- [17]. US 6,407,484 patent – Piezoelectric energy harvester and method
- [18]. US 6,858,970 patent – Multi-frequency piezoelectric energy harvester
- [19]. US 7,439,657 patent – Broadband energy harvester apparatus and method
- [20]. US 7,446,459 patent – Hybrid piezoelectric energy harvesting transducer system
- [21]. US 7,649,305 patent – Piezoelectric energy harvester
- [22]. US 7,812,508 patent – Power harvesting from railway: apparatus, system and method
- [23]. US 7,839,058 patent – Wideband vibration energy harvester
- [24]. US 2014/0285067 patent – Piezoelectric energy harvesting device or actuator
- [25]. US 2014/0159542 patent – Piezoelectric energy harvesting device and method of fabricating the same
- [26]. US 2013/0313946 patent – Piezoelectric energy harvesting array and method of manufacturing the same
- [27]. US 2012/0049694 patent – Micromachined piezoelectric energy harvester with polymer beam
- [28]. US 2010/0317978 patent – Implantable medical device housing modified for piezoelectric energy harvesting
- [29]. US 2007/0125176 patent – Energy harvesting device and methods
- [30]. US 2005/0134149 patent – Piezoelectric vibration energy harvesting device
- [31]. US 2006/0021261 patent – Footwear incorporating piezoelectric energy harvesting system
- [32]. US 8,723,398 patent – Piezoelectric energy harvesting apparatus
- [33]. US 8,581,475 patent – Generating device using piezoelectric energy harvester

- [34]. <https://wikicourses.wikispaces.com/piezo+electric+materials>
- [35]. <http://www.morgantechnicalceramics.com/products/product-groups/piezo-ceramic-components/piezoelectric-ceramics-prop-apps>